	Wang, Jian; Vertex Pharmaceuticals, Inc., Wang, Tiansheng; Vertex Pharmaceuticals, Inc., Wannamaker, M; Vertex Pharmaceuticals, Inc., Winquist, Raymond; Vertex Pharmaceuticals, Inc., Zuccola, Harmon; Vertex Pharmaceuticals, Inc.,

Discovery of VX-509 (Decernotinib): A Potent and Selective Janus kinase (JAK) 3 Inhibitor for the Treatment of Autoimmune Diseases

Luc Farmer[*τ], Mark W. Ledeboer[*], Thomas Hoock, Michael J. Arnost, Randy S. Bethiel, Youssef L. Bennani[τ], James J. Black, Christopher L. Brummel[υ], Ananthsrinivas Chakilam, Warren A. Dorsch, Bin Fan[ε], John E. Cochran, Summer Halas, Edmund M. Harrington, James K. Hogan, David Howe[Ψ], Hui Huang, Dylan H. Jacobs, Leena M. Laitinen, Shengkai Liao, Sudipta Mahajan, Valerie Marone, Gabriel Martinez-Botella[γ], Pamela McCarthy, David Messersmith, Mark Namchuk[ν], Luke Oh[κ], Albert C. Pierce, Scott A. Raybuck, Arthur Rugg, Francesco G. Salituro[γ], Kumkum Saxena, Dean Shannon[ϕ], Dina Shlyakter, Lora Swenson, Shi-Kai Tian[ξ], Christopher Town, Jian Wang, Tiansheng Wang, M. Woods Wannamaker, Raymond J. Winquist, and Harmon J. Zuccola

[*] To whom correspondence should be addressed:

(LF) Telephone: (450) 680-4656. Fax: 450 978-7972. E-mail: luc_farmer@vrtx.com;

(ML) Telephone: (617) 341-6309. Fax: (617) 444-7825. E-mail: mark_ledeboer@vrtx.com.

Vertex Pharmaceuticals Incorporated, 50 Northern Avenue, Boston, Massachusetts 02210, United States; [τ] Vertex Pharmaceuticals (Canada) Incorporated, 275 Armand-Frappier, Laval, Québec H7V 4A7, Canada

[γ] Present address: Sage Therapeutics, 215 First St, Cambridge, Massachusetts 02141, United States

[υ] Present address: RxDiscovery LLC, 38 Sidney Street, Marlborough, MA 01752, United States

[ε] Present address: Agios Pharmaceuticals, Inc., 38 Sidney Street, Cambridge, MA 02139, United States

[] Present address: Novartis, 250 Massachusetts Avenue, Cambridge, MA 02139, United States

[ϕ] Present address: DE Synthetics, 30 Dineen Drive, Fredericton, NB, E3B 5A3, Canada

[ν] Present address: Alkermes, 852 Winter Street, Waltham, MA 02451, United States

[κ] Present address: Mallinkrodt Pharmaceuticals, 6011 University blvd 260, Ellicott City, MD, USA 21043, United States

[Ψ] Present address: LuminaCare Solutions, Inc, 100 Trade Center, Suite G-700, Woburn, MA 01801, United States

[ξ] Present address: Department of Chemistry, University of Science and Technology of China, Hefei, Anhui 230026, China

Keywords. VX-509, Janus kinase, JAK3, JAK2, autoimmune diseases, immunosuppression, rheumatoid Arthritis, Inflammation, transplant rejection

Abstract. While several therapeutic options exist, the need for more effective, safe and convenient treatment for a variety of autoimmune diseases persists. Targeting the Janus tyrosine kinases (JAKs), which play essential roles in cell signaling responses and can contribute to aberrant immune function associated with disease, has emerged as a novel and attractive approach for the development of new autoimmune disease therapies. We screened our compound library against JAK3, a key signaling kinase in immune cells, and identified multiple scaffolds showing good inhibitory activity for this kinase. A

particular scaffold of interest, the 1*H*-pyrrolo[2,3-*b*]pyridine series (7-Azaindoles), was selected for further optimization based in part on binding affinity (K_i) as well as on cellular potency. Optimization of this chemical series led to the identification of **VX-509** (decernotinib), a novel, potent and selective JAK3 inhibitor, which demonstrates good efficacy in vivo in the rat host versus graft model (HvG). Based on these findings, it appears that **VX-509** offers potential for the treatment of a variety of autoimmune diseases.

Introduction

The Janus kinase family of protein kinases consists of four members: JAK1, JAK2, JAK3 and TYK2. JAK3 expression is largely restricted to lymphocytes, which are cells central to the uncontrolled immune response associated with many diseases, including rheumatoid arthritis (RA).[1, 2, 3] In these cells, JAK3 is constrained physically and functionally to only the common gamma (γ) chain, which is shared by receptors for interleukin (IL-2, IL-4, IL-7, IL-9, IL-15 and IL-21).[4, 5, 6, 7] Observations from genetic studies of mice and humans with loss of JAK3 function demonstrate that JAK3 is essential component of cell signaling that underlies immune response/function (Figure 1**)**.[8, 9, 10, 11] Conversely, while JAK3 expression and function is restricted to the immune system, the other JAKs are much more broadly expressed and utilized in a variety of cells and organs. Therefore, a potent and selective JAK3 inhibitor would be an attractive candidate molecule for the treatment of a variety of autoimmune diseases.[12, 13] Inhibition of other JAK isoforms could potentially increase the chances of unwanted safety and tolerability issues without adding any additional activity for controlling immune-mediated disease.[14, 15, 16, 17, 18, 19, 20]

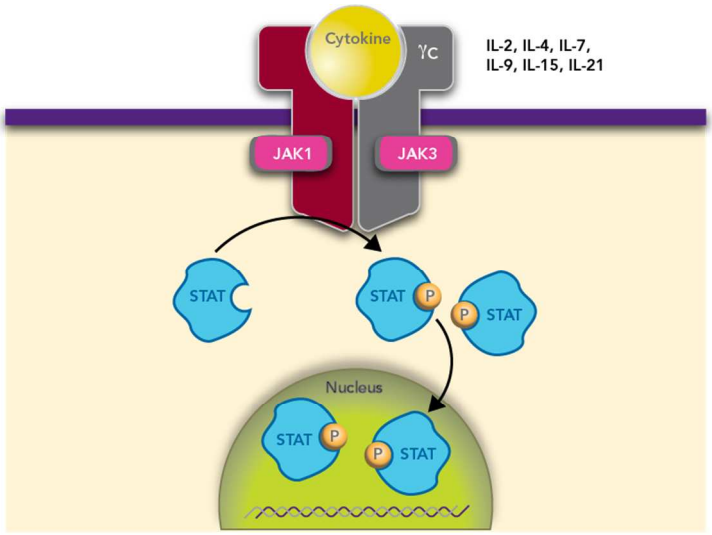

Figure 1. JAK-STAT signaling

Thus, over the last decade there have been extensive efforts to identify and design novel transformative small molecules JAK inhibitors with varied profiles of subtype selectivity in order to address unmet medical needs such as transplant rejection, rheumatoid arthritis (RA), cancers and other autoimmune diseases (Figure 2).[21, 22] Flanagan et al. have reported on tofacitinib (Xeljanz) as the first orally available JAK1/JAK3 inhibitor to be clinically approved for rheumatoid arthritis (RA).[23] Ruxolitinib, a JAK1/JAK2 sub-type selective inhibitor, was first to be approved for the treatment of myelofibrosis under the trade name Jakafi.[24] Baricitinib, a JAK1/2 inhibitor, and filgotinib, a JAK1 selective inhibitor, are currently in clinical trials for RA.[25, 26]

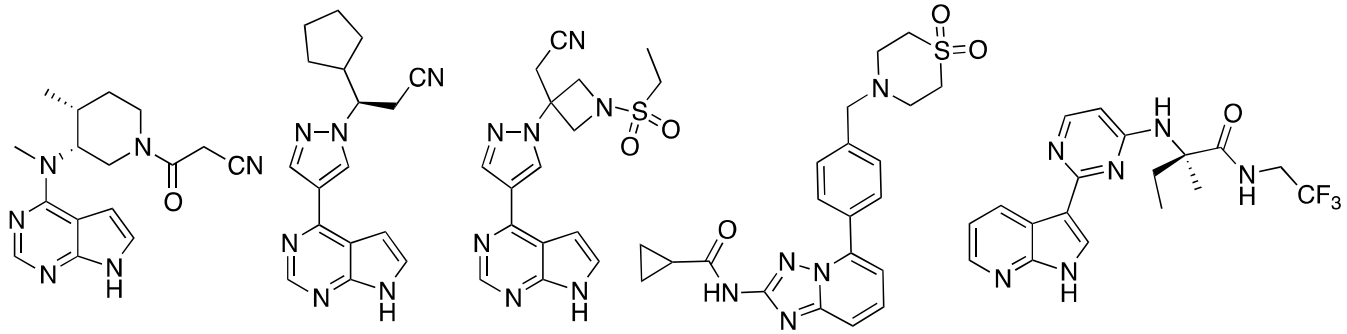

Tofacitinib **Ruxolitinib** **Baricitinib** **Filgotinib** **Decernotinib (VX-509)**

Figure 2. Selected Clinically Approved or Experimental JAK inhibitors

In this paper we report on the lead optimization process that led to the identification of decernotinib (**VX-509)**, an orally available, selective inhibitor of JAK3 for the treatment of autoimmune diseases.[27, 28] To date, this is the only selective JAK3 inhibitor that has been evaluated in clinical studies of RA and data from this clinical program has demonstrated that selective inhibition of JAK3 is sufficient for significant clinical response.

Results & Discussion

In our effort to discover potent and selective small-molecule JAK3 inhibitors, we conducted a high throughput screen of our in-house compound collections for their affinities to bind JAK3. Compounds with confirmed JAK3 inhibitory activity were then screened for selectivity against a small panel of kinases. Our JAK kinase assays were performed using a truncated form of the protein including only the active kinase domain. This was done primarily because the full-length protein was difficult to produce and does not remain stable in solution making its' utility as an enzyme screening reagent limited. It is clear from our assays and published work that the isolated kinase domains of the various JAK isotypes does not accurately measure the relative potency and selectivity of small molecule inhibitors in cells.[29, 30] The context of other JAK protein domains and the microenvironment at the sub-plasma membrane in the cell significantly affect these relative data. To assess JAK isoform selectivity we extended our enzymatic data set on isolated JAK kinase domains with a number of cell-based assays to provide data points from more biologically relevant systems.[31] We first investigated the ability of our compounds to inhibit STAT-5 phosphorylation by blocking the JAK3/1 - STAT5 cascade in IL-2 stimulated HT-2 cells. Likewise, the ability to block the JAK2 mediated phosphorylation of STAT5 was assessed in GMCSF-stimulated TF-1 cells. This provided a measure of selectivity for inhibition of JAK3/1 vs JAK2 mediated signaling in cells.[32] Further, assaying IFN-α mediated STAT2 translocation to the nucleus in

HeLa cells, which is dependent on JAK1 and TYK2, provides useful counter-screening data to establish each compounds specificity against these additional JAK isoforms.

One of the more promising classes of compounds resulting from our JAK3 screen was the diaminotriazole class represented by **1**. While optimizing this class of compounds, a parallel screening effort was maintained to identify additional structurally diverse inhibitors of JAK3 from other ongoing kinase inhibitor programs including SYK, FLT3 and AURA. As part of this latter strategy, a variety of known kinase inhibitor structures were compared with the crystal structure of **1** (Figure 3). From this approach a different chemotype (**2**) was identified based on the 1*H*-pyrrolo[2,3-*b*]pyridine (7-azaindole). The superposition of the crystal co-complexes of JAK2-**1** and ERK2-**2** showed that the *exo*-primary amino group of the triazole and the NH of the 1*H*-pyrrolo[2,3-*b*]pyridine core are closely aligned, as are the nitrogen hydrogen bond acceptors of the 1*H*-pyrrolo[2,3-*b*]pyridine and triazole. This overlay provided a basis for replacement of the anilino-aminotriazole hinge binding element of **1** with a smaller 1*H*-pyrrolo[2,3-*b*]pyridine hinge-binding element. Although the vectors from the triazole and 1*H*-pyrrolo[2,3-*b*]pyridine do not overlay perfectly, they are similar enough to suggest that the anilinopyrimidine of **1** might form a similar set of interactions on the 1*H*-pyrrolo[2,3-*b*]pyridine core. JAK2 was used as a surrogate for JAK3 because of difficulty in handling this protein and due to the close sequence homology of the ATP binding sites of JAK2 and 3. As such, the JAK2 co-complex should provide a reasonable approximation for binding of these compounds with the JAK3 isoform.

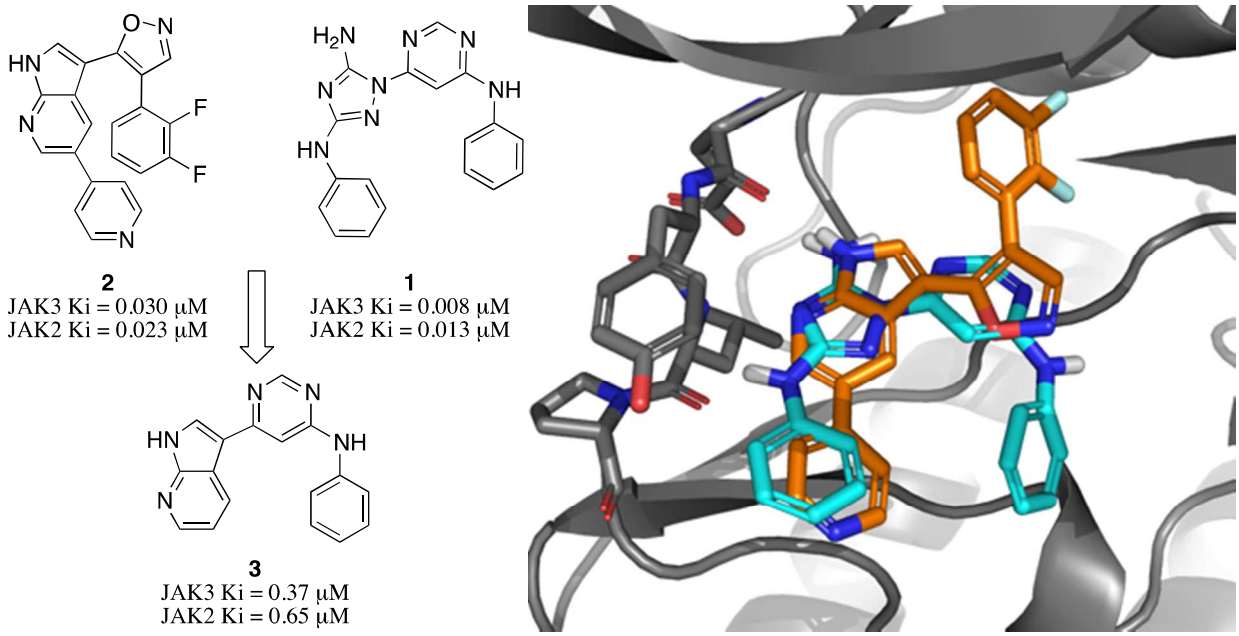

Figure 3. Compounds **1** and **2** overlaid in the JAK2 structure. Superposition created by overlaying the hinge regions of the ERK2 and JAK2 crystal structures

Our overlay also suggested that a 1,3-disubstitution pattern in the central core pyrimidine ring of **1** would position the phenyl group more optimally. The resulting 1*H*-pyrrolo[2,3-*b*]pyridine based hybrid compound **3** was prepared and exhibited moderate potency. Compound **3** became the starting point for further exploration of this class of JAK3 inhibitors. With a minimal survey to explore the amine- linked side chain we identified benzylamine-derived 1*H*-pyrrolo[2,3-*b*]pyridine **4** with good affinity for JAK3 and a K_i of 14 nM. From the outset we desired compounds with a clean selectivity profile against the kinome to avoid unwanted side effects. In particular, we needed to avoid binding to additional kinases with potential for undesirable pharmacologic activity. Despite its potent FLT3 inhibition, compound **4** was used as the prototype for the central ring variations with the goal to further improve potency as well as selectivity against FLT3, SYK and AURA. Changing the 4,6-pyrimidinyl moiety to 2,6- and 2,4-pyrimidinyl led to a decrease in affinity for JAK3, as exemplified by compounds **5** and **6** respectively. However, 2,4-pyrimidinyl regioisomer **6** exhibited the best selectivity against FLT3 (Table 1). The

addition of a 5-chloro atom on the 1*H*-pyrrolo[2,3-*b*]pyridine ring led to an overall improvement in potency for JAK3 as seen for **7** and **8**. The replacement of pyrimidine central core for a pyridine ring in compound **9** led to a similar activity profile as for analog **5**. Replacing the central heteroaryl ring with a phenyl ring gave a significant drop in affinity for JAK3 as exemplified with analog **10**.

Table 1. Central Core Ring Variations[33]

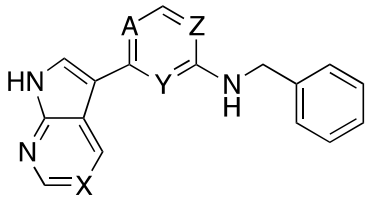

Compound	X	A	Y	Z	JAK3 Ki (μM)	JAK2 Ki (μM)	SYK Ki (μM)	FLT3 Ki (μM)	AURA Ki (μM)	HT-2-IL2 IC50 (μM)
4	CH	N	CH	N	0.014	0.035	2.9	< 0.06	> 0.8	9.85
5	CH	CH	N	N	0.096	0.11	> 3.33	< 0.06	0.38	> 20
6	CH	N	N	CH	0.38	0.35	> 3.33	0.7	0.8	N.A.
7	CCl	N	CH	N	0.003	0.006	0.2	< 0.06	0.062	5.4
8	CCl	CH	N	N	0.043	0.033	> 3.33	< 0.06	0.02	> 20
9	CCl	CH	N	CH	0.055	0.07	> 3.33	0.09	0.049	> 20
10	CCl	CH	CH	CH	0.15	0.22	1.9	0.078	N.A.	N.A.

Most of the compounds exhibited FLT3 activity and had limited or poor cellular activity in the JAK3/1 HT-2 assay. Compound **6** was the least potent inhibitor of JAK3 in this set, yet it exhibited only modest potency for FLT3, and poor affinity for both SYK and AURA. As a result, compound **6** was the only regioisomer considered for further exploration. To follow up on compound **6**, we identified additional potent analogs with a small set of compounds containing N-linked small branched or cyclic alkyl groups. Several examples containing hydrogen bond donor and acceptor groups were also examined. These results are presented in Table 2.

Table 2. Side Chain Variations

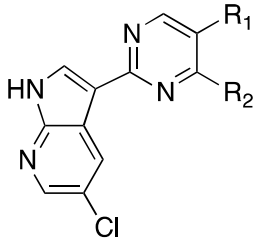

Compound	R1	R2	JAK3 Ki (μM)	JAK2 Ki (μM)	SYK Ki (μM)	FLT3 Ki (μM)	AURA Ki (μM)	HT-2-IL2 IC50 (μM)
11	F		0.005	0.005	0.39	0.33	0.030	> 20
12	F		0.011	0.012	0.43	0.05	N.A	N.A.
13	F	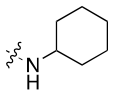	0.016	0.023	1.1	0.078	0.007	N.A.
14	H	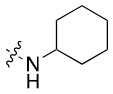	0.022	0.022	0.67	0.29	N.A.	N.A.
15	F	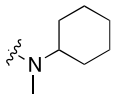	0.14	0.22	> 4	0.08	N.A.	N.A.
16	F	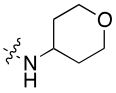	0.004	0.009	0.15	0.009	0.023	> 20
17	F	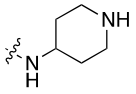	0.029	0.045	0.108	0.006	0.086	N.A.
18	F	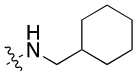	0.068	0.077	3.2	0.19	0.004	N.A.
19	F	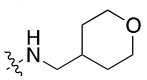	0.005	0.011	0.2	0.032	0.019	> 20
20	F	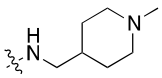	0.14	N.A.	3.6	0.045	0.27	N.A
21	H	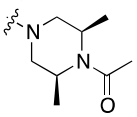	0.006	0.008	1.1	0.032	0.13	2.1

In general, derivatives with small, branched alkyl groups (**11**), and cycloalkyl groups (**12**) were well tolerated as these compounds exhibited good affinity for JAK3, yet in most cases they lacked adequate selectivity versus FLT3 (Table 2). Alkylation of the amine nitrogen on compound **13**, as shown in **15** led to a 10-fold decrease in JAK3 inhibition. From the X-ray structural data for related JAK3 inhibitors,

it appears unlikely that the aniline NH acts as a hydrogen bond donor to the protein. The introduction of the N-methyl in combination with the adjacent F causes the alkyl substituent to twist out of plane relative to the pyrimidine ring, leading to what we believe to be a modestly less favorable binding conformation. Incorporation of polar atoms was well tolerated and led to improved potency in some cases (**16** and **19**). However, addition of strongly basic amines as in compounds **17** and **20** did not provide the same enhancements in affinity. Among these analogs, piperazine amide derivative **21** was the most potent example in our HT-2 cellular assay, with an IC_{50} of 2.1 μM and exhibited a modest 21-fold selectivity vs AURA. Most examples showed reasonable selectivity against SYK and in the case of **21,** AURA as well (>20 fold). Finally, in this exercise no appreciable selectivity was achieved versus FLT3 for any of the compounds while also retaining potency in the cell.

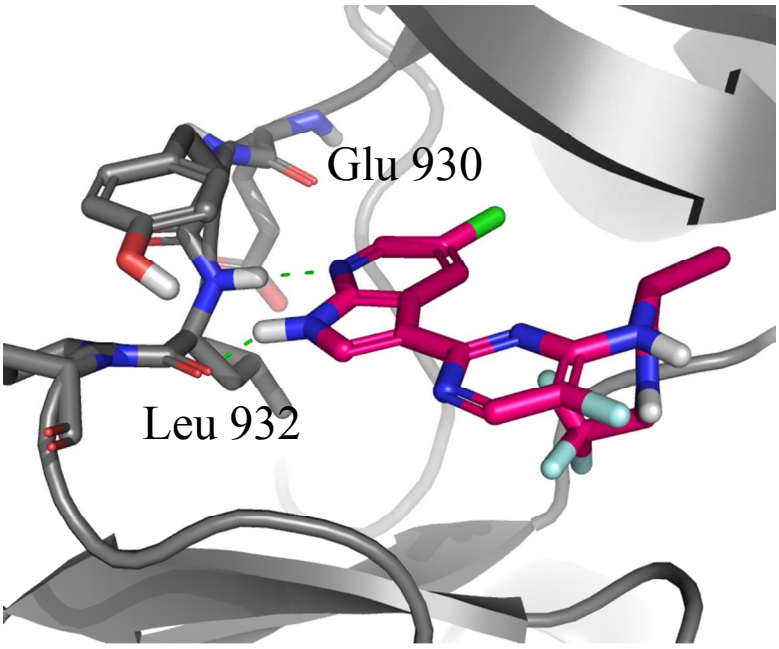

Figure 4. Crystal structure co-complex of **22** in JAK2. Hinge hydrogen bonds to Leu 932 highlighted in green.

N-Acetyl piperazine based compound **21** was the most active in our HT2 cell assay and it contained an amide moiety in the side chain. We found that a related compound (**22)** from our AURA program,

bearing an amide containing side chain with our preferred core, also exhibited good binding affinity for JAK3 (K_i = 2 nM). More importantly, in our IL2 driven HT-2 cell assay (Table 3), compound **22** exhibited an IC_{50} of 0.074 μM. To understand the binding of this compound, analysis of the x-ray co-complex of **22** and JAK2, indicated a different orientation of the 1*H*-pyrrolo[2,3-*b*]pyridine at the hinge than was anticipated in the original design concept from Figure 3 (see Figure 4 also). While both orientations would accept a hydrogen bond from the backbone NH of Leu 932, the orientation of **22** anticipated from the ERK2 structure would have the 1*H*-pyrrolo[2,3-*b*]pyridine NH donating a hydrogen bond to the backbone carbonyl of Glu 930. Instead, the 1*H*-pyrrolo[2,3-*b*]pyridine NH of **22** is donating a hydrogen bond to the carbonyl oxygen of Leu 932 (Figure 4). While unexpected, this difference in binding modes is not too surprising given the significant structural differences between compounds **2** and **22** and given that the compounds are complexed to different kinases. Interestingly, the amide of **22** does not appear to be involved in H bonding to the JAK2 protein.

Relative to earlier 1*H*-pyrrolo[2,3-*b*]pyridine derivatives, **22** exhibited excellent selectivity against SYK (Ki > 4 μM) and provided a good selectivity window against FLT3 as well as JAK2 as reflected by the more relevant cellular endpoints (HT2 vs TF1). In order to minimize potential off-target activity of our JAK3 inhibitors, further improvements in selectivity were still desired, particularly AURA, while maintaining the promising selectivity profile exhibited by **22**. Thus, a series of amino-acid containing analogs, capped with a trifluoroethyl amide, were prepared and the results are summarized in Table 3. Examples containing amides capped with -NHMe, -NEt or -NMeEt were also assessed, but these were all less selective for FLT3 and often accompanied by significant loss of cell potency (data not shown). As such, we chose to focus on amides containing the trifluoroethyl group.

Many natural and unnatural amino acid-based analogs were explored. As demonstrated by compounds **23**, **24** and **27**, smaller and larger amino acids such as glycine, norvaline, as well as methionine, were all tolerated and maintained good enzyme affinity for JAK3 with retention of selectivity for SYK. However, SAR with respect to cellular potency for these compounds was quite sensitive to variation of the side chain.

Table 3. 5-Substituted 1*H*-pyrrolo[2,3-*b*]pyridine with Aminoacid Side Chain Variations*

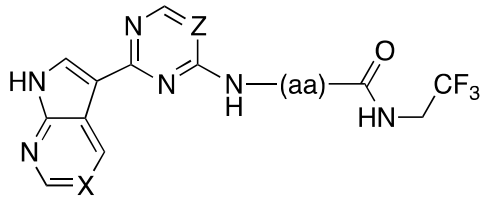

Cmpd	X	Z	(aa)	JAK3 Ki (μM)	JAK2 Ki (μM)	HT-2-IL2 IC50 (μM)	TF-1 GM-CSF IC50 (μM)	FLT3 Ki (μM)	AURA IC50 (μM)	RLM %
22	CCl	CF	(S)-Ala	0.002	0.007	0.074	2.67	0.55	0.004	95
23	CCl	CH	Gly	0.001	0.005	0.16	2.9	0.29	0.007	75
24	CCl	CF	(S)-Nva	0.002	0.023	0.75	3.6	1.3	< 0.025	65
25	CCl	CH	(S)-Ser	0.006	0.037	1.5	20	0.093	0.05	n/a
26	CCl	CH	(S)-SerOMe	0.013	0.069	8.3	n/a	0.49	0.26	n/a
27	CCl	CH	(S)-Met	0.04	0.03	2.9	n/a	0.39	0.02	n/a
28	CCl	CF	(S)-Pro	0.009	0.026	2.5	11	1.603	0.024	63
29	CCl	CF	(S)-aminobutanoic acid	0.045	0.12	11.4	n/a	0.31	0.15	n/a
30	CCl	CF	(R)-Ala	0.002	0.011	1.3	>20	>4	0.063	n/a
31	CCl	CH	(R)-Ala	0.001	0.005	0.11	14.3	0.61	0.027	96
32	CCl	CH	(R)-Nva	0.002	0.01	0.22	2.1	0.41	0.23	47
33	CCl	CH	(R)-Propargyl glycine	0.002	0.011	0.51	5.1	0.37	0.032	44
34	CCl	CH	(R)-Val	0.002	0.001	0.11	2.93	0.56	0.16	78
35	CCl	CH	(R)-Leu	0.004	0.023	1.7	10.3	1.5	0.405	n/a
36	CCl	CH	(R)-Phe	0.006	0.058	2.8	> 20	1.6	< 0.025	n/a
37	CCl	CF	(R)-His	0.018	0.081	2.6	2.3	1	0.15	n/a
38	CF	CF	(S)-Ala	0.007	0.042	5.5	n/a	>3.7	0.049	n/a
39	CH	CF	(S)-Ala	0.031	0.15	6.1	n/a	>4.0	0.21	n/a
40	COMe	CF	(S)-Ala	0.006	0.034	1.5	2.2	0.48	0.033	91
41	COMe	CF	(R)-Ala	0.007	0.038	1.3	n/a	0.61	0.21	79
42	N	CF	(R)-Ala	0.019	0.33	>20	n/a	>4.0	>0.8	n/a
43	CCl	CH		0.001	0.001	0.058	0.41	0.18	0.10	30
44	CCl	CF		0.001	0.002	0.081	0.96	0.325	0.082	88
45	CCl	CH		0.003	0.002	0.081	0.65	0.2	0.62	52
46	N	CH		0.003	0.006	0.52	3	1.3	> 0.8	100
VX-509	CH	CH		0.002	0.013	0.099	2.59	1.04	> 0.8	70
47	CCl	CH		0.002	0.028	0.9	7.9	0.29	0.070	n/a
48	CH	CH		0.003	0.004	0.072	1.65	0.54	> 0.8	63
49	CH	N		0.003	0.024	0.33	3.7	1.39	0.49	97

*All compound showed Ki > 4 uM for SYK

In the natural (*S*)-configuration, the amino acid variations largely failed to significantly reduce AURA affinity. Only methyl serine derived **26** showed modestly improved selectivity against AURA (20-fold),

but because of its very weak potency in our HT-2 cell assay, this compound did not meet the requirements for further investigation. The rigid proline-based analog **28** exhibited favorable selectivity against both SYK and FLT3, but no improvement in selectivity against AURA was observed. A homologated version of **22** containing a beta-alanine group as in **29** exhibited poorer JAK3 affinity as well as 150-fold reduction of cellular potency. Inversion of the absolute stereochemistry of *S*-**22**, (compound *R*-**30**), did not show any significant improvement in the overall profile relative to its enantiomer while an 18-fold loss of cellular potency was observed. Interestingly, the des-fluoropyrimidyl analog **31** with the same *R* configuration exhibited a similar selectivity profile as **30** and improved cellular potency (HT-2 IC_{50} 1.3 μM *vs.* 0.11 μM). Compounds bearing unnatural amino acids with sp and sp2 character such as analogs **33**, **36** and **37** did not show selectivity against AURA. These compounds also exhibited weak cellular activities. Fortunately, incorporation of bigger unnatural hydrophobic amino acid side chains, such as (*R*)-norvaline **32**, (*R*)-valine **34** and (*R*)-leucine **35**, led to a significant improvement in selectivity versus AURA. Several of these compounds, **34** and **32**, also retained good discrimination against SYK and FLT3 and displayed potent JAK3 mediated cellular activity in our HT2 assay with IC_{50} of 0.11 and 0.22 μM respectively. It is interesting to note that differences in enzyme affinity do not always translate to potent cellular activity. This may be attributed to subtle differences in the affinity of our compounds for the truncated JAK kinase enzyme domains versus full-length enzymes present in the cells.

A brief survey of substituents at the C-5 position of the *R*/*S*-alanine based 1*H*-pyrrolo[2,3-*b*]pyridine indicated that smaller substituents such as H, F or OMe (compounds **38** to **41**) were all tolerated for JAK3 binding activity with good selectivity, but lacked the potency that the 5-chloro analog **22** displayed in the HT-2 cellular assay. Incorporation of larger C-5 substituents such as carbamates, or

amides provided compounds with modest enzyme activity and cellular potency at best (data not shown) and compounds of this type were not pursued further. Changing the 1*H*-pyrrolo[2,3-*b*]pyridine (azaindole) core to a deazapurine core (CH → N) led to a complete or partial loss of potency in the HT-2 assay for compound **42** and diminished activity for compound **46**. Taken together, these results suggest that polar groups with available lone pairs at this C-5 position are less optimal for potency.

With the hope that we could retain the positive aspect of compounds **22** and **31** (HT-2 cell potency) as well as **30** (AURA selectivity) we prepared a series of compounds with germinal substitution, as exemplified by **43** to **49**. Both **43** and **44** retained the cellular activity as was seen for both the (*S*)- and (*R*)-alanine derivatives **22** and **31**, with *des*-fluoro pyrimidine **43** being the most potent (HT-2 IC_{50} = 0.058 μM). However, the selectivity with respect to AURA was modest overall.

Since the addition of a methyl group on the glycine side chain of **23** with the *R* stereochemistry, as in (*R*)-**31**, improved selectivity vs AURA (**23** vs **31**) we employed a similar strategy to follow up on **43** by increasing steric bulk of the germinal *R* substituent. Thus, the (*R*)-2-amino-2-methylbutanoic acid based compound (*R*)-**45** was prepared and tested for its affinity in our kinase panel and cellular assays. A similar level of cellular potency (HT-2 IC_{50} = 0.081 μM) was observed for (*R*)-**45**, but more importantly, a dramatic increase in selectivity against AURA (K_i = 0.620 μM) was achieved. As expected from previous results, its enantiomer, (*S*)-**47,** was 10-fold less selective for AURA (K_i = 0.070 μM). Furthermore, optimization at the 5 position of the 1*H*-pyrrolo[2,3-*b*]pyridine core, as shown for compounds, **VX-509** and **48** led to the most kinase-selective analogs of the series with excellent cellular potencies (HT-2 IC_{50} < 0.1 μM).

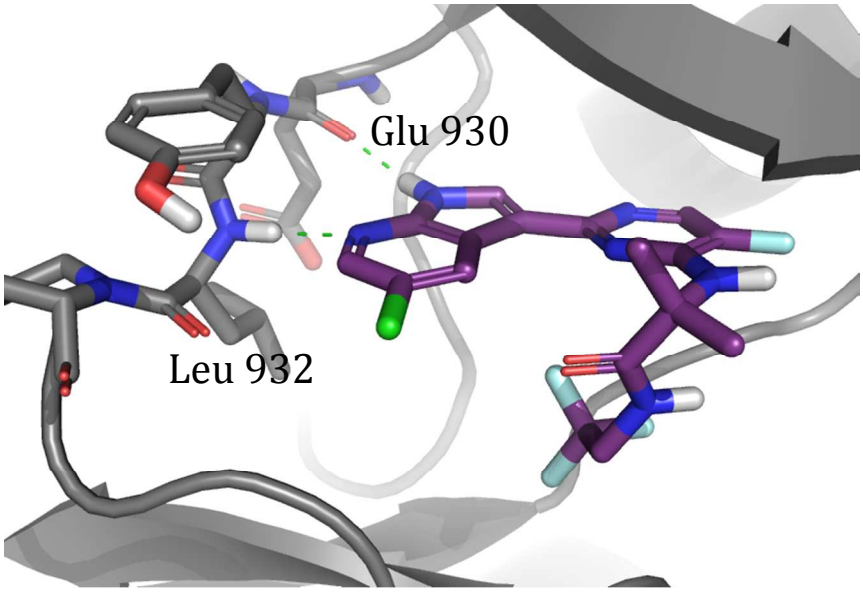

Figure 5. Crystal structure of **44** in JAK2. Hinge hydrogen bonds to Leu 932 and Glu 930 highlighted in green.

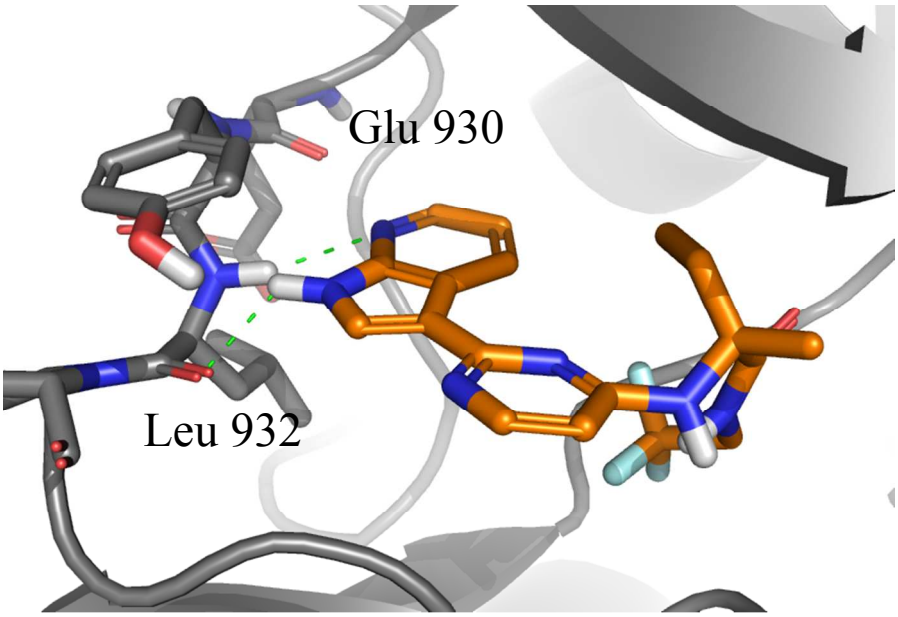

Figure 6. Crystal structure of **VX-509** in JAK2. Hinge hydrogen bonds to Leu 932 highlighted in green.

Interestingly, a crystal structure of **44** revealed that the orientation of the 1*H*-pyrrolo[2,3-*b*]pyridine hinge-binding element was flipped relative to **22** to give the same orientation as **2** (Figure 5). Given the relatively modest structural differences between **44** and **22**, this significant change in binding mode was

unexpected. However, as shown in the structure of **VX-509**, these significant binding mode changes between structurally very similar compounds were fairly common with this compound class (Figure 6). This phenomenon of flipping binding modes for closely related compounds obviously complicated the interpretation of SAR. Given the interesting binding behavior of these compounds in JAK2, a separate manuscript is in preparation to address the topic.[34]

With promising candidates in hand we decided to investigate JAK isotype selectivity further. At the outset of our efforts we were concerned about mitigating JAK2-mediated pharmacological effects.[35] Significant hematopoietic consequences were expected (e.g. anemia) with potent JAK2 inhibition. Therefore, we sought to optimize JAK isotypes selectivity, with a particular emphasis on JAK3 versus JAK2. In our enzyme binding studies using isolated active kinase domains, selectivity for JAK3 versus JAK2, was typically less than 10-fold for most of the compounds made in this optimization process. Given the high degree of structural similarity in the ATP binding pockets of JAK2 and JAK3 (identical except for JAK3 Cys 909 vs JAK2 Ser 936 and JAK3 Ala 966 vs JAK2 Gly 993), our observations are consistent with the expectation that the potential for JAK3 vs JAK2 selectivity would be limited. Furthermore, it is known that other domains of the JAK kinases have some degree of regulatory function for the kinase, and we had indications from cellular data sets that the selectivity window between JAK3 and JAK2 was greater in cellular assays.[36] Thus, this limited JAK3/JAK2 enzymatic selectivity might be explained by the fact that truncated isolated protein kinase domains were used for K_i determinations. This does not fully account for the subtle structural differences in the full-length proteins, particularly in the context of their natural microenvironment, when bound to the gamma chain of the IL-2 family of cytokine receptors in cells. Thus, we chose to emphasize JAK isotypes selectivity characterization in the more physiologically relevant biologic systems with the hope of minimizing off-target JAK2 inhibition.

Comparison of inhibition of the JAK3/1- or JAK2-mediated phosphorylation of STAT5 in HT-2 or TF-1 cells following brief stimulation with IL-2 or GMCSF, respectively, provided a useful selectivity ratio for the compounds. Further, assessment of selectivity against JAK1/TYK2 was obtained by counter-screening our compounds in HeLa cells stimulated with IFN-α and measuring inhibition of STAT2 translocation to the nucleus. Results from the HeLa assays show that **VX-509** has an IC50 of >10 μM, demonstrating a high degree of selectivity against these additional JAK isoforms. However, a more relevant predictor of in vivo selectivity was also needed. To confirm and expand upon these findings, primary human and mouse cell assays were used. Specifically, T-cell proliferative response in mixed lymphocyte reactions (MLR), IL-2-stimulated T-cell blast assays from isolated peripheral blood mononuclear cells (PBMCs), and erythroid colony formation assays (CFU-E) from human bone marrow after stimulation with erythropoietin (a JAK2 dependent signaling pathway) were used to assess JAK isotype selectivity ratios in a more physiologically relevant manner (Table 4).

Table 4. Enzyme (K_i nM ± SD, n), Cell-Based Potency (IC_{50} nM ± SD, n) & Selectivity (ratio)

Assay	JAK isoform Involved	**VX-509**	**44**	**34**	**43**	**45**	tofacitinib
JAK3	JAK3	2 ± 0.7, 5	1 ± 0.07, 10	1 ± 0.09, 5	1 ± 0.3, 10	3 ± 2, 3	0.5 ± 0.07, 7
JAK1	JAK1	11 ± 0, 1	3 ± 0, 1	N.A.	2 ± 0, 1	N.A.	3 ± 0.4, 2
JAK2	JAK2	13 ± 0, 4	2 ± 0.5, 12	4 ± 009, 6	1 ± 0.5, 12	2 ± 1, 5	1 ± 0.9, 5
TYK2	TYK2	11 ± 2, 2	10 ± 0, 1	N.A.	11 ± 0, 1	N.A.	11 ± 0, 1
HT-2/IL-2/P-STAT5	JAK3/1	99 ± 50, 4	90 ± 30, 10	112 ± 70, 5	58 ± 40, 5	81 ± 70, 2	30 ± 20, 72
TF-1/ GMCSF/P-STAT5	JAK2	2600 ± 1664, 4	1060 ± 600, 9	2927 ± 1350, 7	409 ± 142, 6	651 ± 13, 2	190 ± 137, 35
Mouse 2-Way MLR	JAK3/1	170 ± 100, 4	160 ± 110, 3	280, 1	170 ± 70, 2	N.A.	60, 1
1° Human IL-2 T-cell Blast	JAK3/1	240 ± 180, 2	N.A.	N.A.	N.A.	N.A.	130 ± 28, 2
Human CFU-E 3 U/ml EPO	JAK2	7700 ± 6100, 2	6100 ± 3400, 2	5400 ± 2000, 2	2500 ± 2200, 2	N.A.	380 ± 160, 10
Human CFU-E 0.3 U/ml EPO	JAK2	5300 ± 740, 2	3600 ± 1200, 2	3000 ± 1000, 2	1700 ± 325, 2	N.A.	320 ± 150, 10
HeLa IFN-a STAT2	JAK1/ TYK2	11900 ± 3650, 3	>20000, 1	N. A.	N.A.	N.A.	2800 ± 2000, 11
CFU-E / MLR (3 U/ml EPO)		45.3	38.1	22.1	10.6	N.A.	6.7
CFU-E / MLR (0.3 U/ml EPO)		31.3	22.5	14.2	7.6	N.A.	5.7
TF-1/HT-2 ratio		26	12	26	7	8	6

The selectivity ratios of JAK3-versus JAK2-mediated endpoints (TF-1 / HT-2) were superior to that of binding selectivity for all the above compounds tested, ranging from 7- to 26-fold. The three most selective compounds, **44** and **VX-509** and **34,** were further evaluated for their functional activity in primary human cell-based assays dependent on either JAK3 or JAK2, namely the MLR and CFU-E assays. Analogs **44** and **VX-509** exhibited robust selectivity windows between JAK3- and JAK2-dependent cell assays, with 38-fold and 45-fold selectivity, respectively, in favor of JAK3 (CFU- E / MLR). As a clinical benchmark reference tofacitinib was similarly evaluated for selectivity in our

assays. Tofacitinib proved to be generally less selective in this assessment with a selectivity ratios of 6- and 7-fold (TF-1 / HT-2) and (CFU-E / MLR) respectively. In these assays, the superior selectivity for compound **VX-509** with respect to tofacitinib was consistent with the results obtained for the TF-1 / HT-2 ratios. Furthermore, **VX-509** was evaluated along with tofacitinib in a primary human IL-2 T-cell blast proliferation assay, which provided an additional functional measure of the ability of compounds to inhibit JAK3 activity. Both compounds showed similar potency with IC50s at 0.14 μM and 0.15 μM respectively.

Table 5. Pharmacokinetic parameter determinations in Sprague-Dawley rats (single IV bolus dose)

Compound	Dose (mg/kg)	DN-AUC_{inf}[a] (hr*μg/ml)	CL (mL/min/kg)	$T_{1/2}$ (h)	V_{dss} (L/kg)
34	1.0	0.46	36.2	2.6	6.1
44	1.9	1.76	9.45	2.2	1.5
43	2.0	0.42	39.7	1.2	1.3
45	1.7	0.60	41.1	4.6	4.1
VX-509	0.98	0.74	24.3	5.57	4.98

[a]The AUC_{INF} values are normalized to a 1 mg/kg dose

During our lead optimization process we routinely determined the pharmacokinetic parameters for potent and selective compounds following a single IV bolus dose to Sprague-Dawley (SD) rats. The results for the most promising analogs are summarized in Table 5. While compound **44** exhibited the lowest clearance coupled with an acceptable $T_{1/2}$, **VX-509** also demonstrated reasonable exposure, with a moderate clearance and extended $T_{1/2}$ of 5.1 hr. In addition, **VX-509** had a superior kinase selectivity profile (particularly against JAK2 and AURA) relative to **44**. Based on these promising results, **VX-509** was selected for further evaluation.

In vitro profiling indicated that **VX-509** was moderately to extensively metabolized in liver microsomes and S9 fractions in the mouse, rat, dog, monkey, and human (Table 6 and 7). This suggested that the contributions to drug clearance from non-CYP mediated metabolic pathways was minimal.

Table 6. Mean $T_{1/2}$ and Predicted Hepatic Clearance for **VX-509** at an Initial Concentration of 1 μM in Liver Microsomes After Incubation at 37°C

Species	Mean $T_{1/2}$ (SD) and Mean Predicted Hepatic Clearances (SD)	
	$T_{1/2}$ (min)	Predicted Hepatic Clearance (mL/min/kg)
Mouse	19 ± 7.9	69 ± 6.4
Rat	21 ± 1.6	38 ± 0.9
Dog	34 ± 2.4	24 ± 0.4
Monkey	7 ± 0.4	38 ± 0.3
Human	19 ± 1.2	17 ± 0.2

Table 7. Mean $T_{1/2}$ and Predicted Hepatic Clearance for **VX-509** at an Initial Concentration of 1 μM in Liver S9 After Incubation at 37°C

Species	Mean $T_{1/2}$ (SD) and Mean Predicted Hepatic Clearances (SD)	
	$T_{1/2}$ (min)	Predicted Hepatic Clearance (mL/min/kg)
Mouse	9 ± 1.01	78 ± 1.2
Rat	21 ± 1.6	37 ± 0.9
Dog	36 ± 3.4	23 ± 0.6
Monkey	6 ± 0.3	39 ± 0.09
Human	20 ± 5.4	17 ± 0.9

Other properties that favored selection of **VX-509** included its high permeability in human colon carcinoma (Caco-2) cell monolayer assays, indicating potential for good oral absorption, and demonstration that it was a weak efflux pump protein substrate to P-glycoprotein (P-gp) and breast cancer resistance protein (BCRP) with efflux ratios ranging between 2 and 3. Although, the efflux ratios

were small for P-gp and BCRP, more than 50% reduction of these efflux ratios in the presence of standard inhibitors was used to classify them as weak substrates. In addition, the hERG IC_{50} value for **VX-509** was determined to be 51.9 μM and its solubility was found to be 6.38 μg/mL in water.

Preclinical pharmacokinetics (Table 8A) of **VX-509** was investigated in multiple species. Following a nominal 1 mg/kg intravenous dose to rats and monkeys, plasma clearances were moderate at 24.3 mL/min/kg and 21.7 mL/min/kg, respectively; volume of distribution at steady-state (Vdss) ranged from 1.7-5.0 L/kg. In dogs, the clearance and Vdss values were significantly lower at 4.17 mL/min/kg and 0.4 L/kg, respectively. These lower values in dogs might be explained, at least in part, by differences in aldehyde oxidase mediated metabolism in that species (results to be published elsewhere). The percentage of **VX-509** (1 μM) bound to plasma proteins was 89, 93, 99, 80, and 81% in mouse, rat, dog, monkey, and human plasma, respectively. Consistent with its high permeability and low to moderate clearance, **VX-509** exhibited high oral bioavailability in both rats and dogs (Table 8B).

Table 8. Mean Pharmacokinetic Parameters for **VX-509**

A) Single IV bolus dose

Species	Dose (mg/kg)	DN-AUC_{inf}[a] (hr*μg/ml)	CL (ml/min/kg)	V_{dss} (L/kg)	$T_{1/2}$ (hr)
Rat	0.98	0.74	24.3	4.98	5.57
Dog	0.88	4.06	4.17	0.39	1.58
Monkey	0.88	0.79	21.7	1.65	1.28

[a]The AUC_{INF} values are normalized to a 1 mg/kg dose

B) Single oral dose

Species	Dose (mg/kg)	DN-AUC_{inf}[a] (hr*μg/ml)	C_{max} (μg/mg)	T_{max} (hr)	$T_{1/2}$ (hr)	F %
Rat	10.7	6.75	1.73	1.50	5.87	91.8
Dog	9.65	44.6	7.46	1.00	5.82	100

[a]The AUC_{INF} values are normalized to a 10 mg/kg dose

Comparison of the estimated hepatic clearance values from liver microsomes in rats, dogs, and monkeys (Table 6: 38, 24, and 38 mL/min/kg, respectively) with clearance values obtained in vivo (Table 8: 24.3, 4.2, and 21.7 mL/min/kg, respectively) showed that clearance was overestimated based on in vitro data and suggested that **VX-509** might exhibit acceptable clearance in humans. Due to its favorable potency, selectivity and pharmacokinetic profile, **VX-509** was selected for assessment of its potential for in vivo efficacy in JAK3 mediated models of disease. Thus, **VX-509** efficacy was evaluated in vivo in the rat host versus graft (HvG) model (Figure 7). HvG response was elicited by the injection of allogeneic cells isolated from Dark Agouti rat spleen into the footpad of the host Lewis rat. The HvG reaction is primarily a T-cell-mediated response, in which host T cells recognize major histocompatibility complex (MHC) antigens presented by the antigen presenting cells on the graft cells. The graft cells migrate to the host local popletial lymph node (PLN) and induce an immune response leading to hyperplasia of the lymph node. The enlargement of host PLN peaks at Day 4, and the weight difference (delta) between contralateral (non-grafted) and ipsilateral (grafted) PLNs was the efficacy assessment. Concomitantly, *ex vivo* analysis of T cell activation of CD25 in whole blood from dosed animals was also evaluated as a biomarker of JAK3 activity.

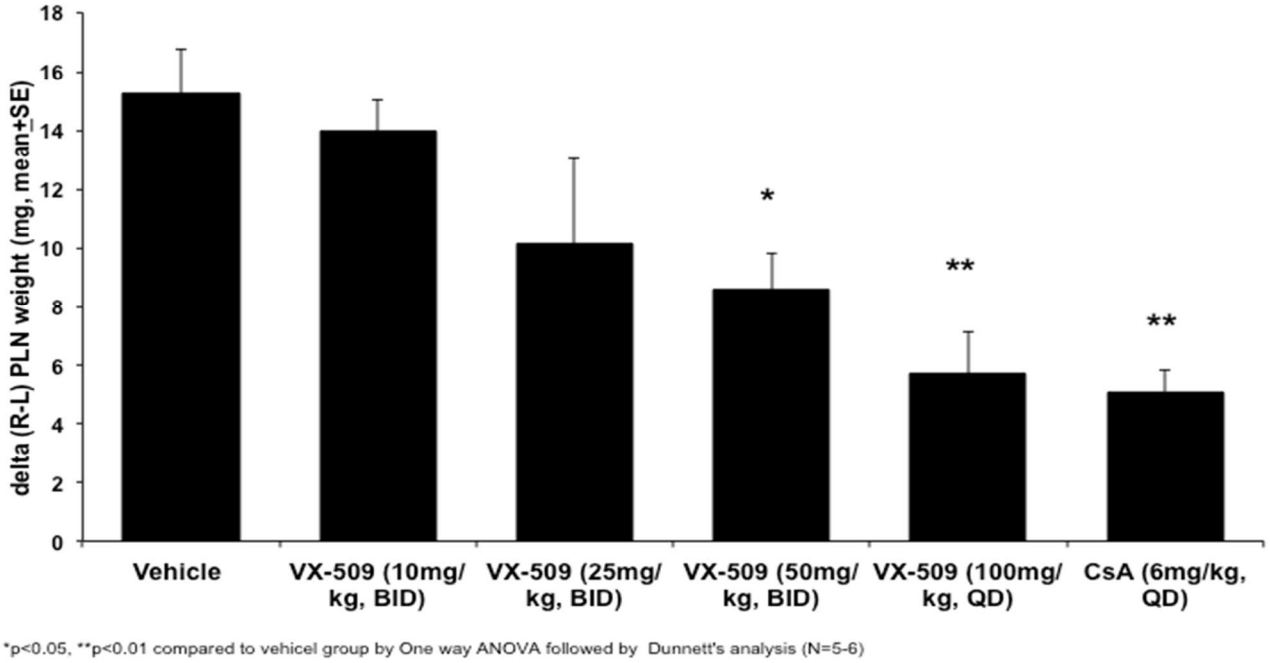

Figure 7. Dose dependent inhibition of popletial lymph node (PLN) hyperplasia by **VX-509** in Rat HvG Model.

VX-509 was evaluated at oral doses of 10 mg/kg BID, 25 mg/kg BID, 50 mg/kg BID, or 100 mg/kg QD. Cyclosporine A was administered orally as a reference compound at a dose of 6 mg/kg QD. Popliteal LNs were collected at termination. For *ex vivo* CD25 biomarker analysis, terminal blood samples at 1 and 14 hours (trough) post dose were used. **VX-509** demonstrated statistically significant, dose-dependent inhibition on PLN hyperplasia as determined by delta measurement, which is the weight difference between the grafted and non-grafted PLNs. As illustrated in Figure 7, **VX-509** 50 mg/kg BID or 100mg/kg QD were significantly efficacious, inhibiting 66% ($p = 0.019$) and 94 % ($p<0.01$) of the PLN hyperplasia, respectively relative to CyclosporinA (CsA). There was a partial but non-significant inhibition (50%, $p = 0.101$) at 25 mg/kg BID group relative to CsA. Tofacitnib, when evaluated in the HvG model, also demonstrated statistically significant inhibition of PLN hyperplasia. The compound

inhibited the PLN hyperplasia by 87% at 20 mg/kg TID, 88% at 20 mg/kg BID or 100% at 60 mg/kg BID as compared to CsA (100%). (supplementary Figure 13). There was significant reduction of the CD25 expression by tofacitinib at 1 hour post dose in all groups tested. (supplementary Figure 14)

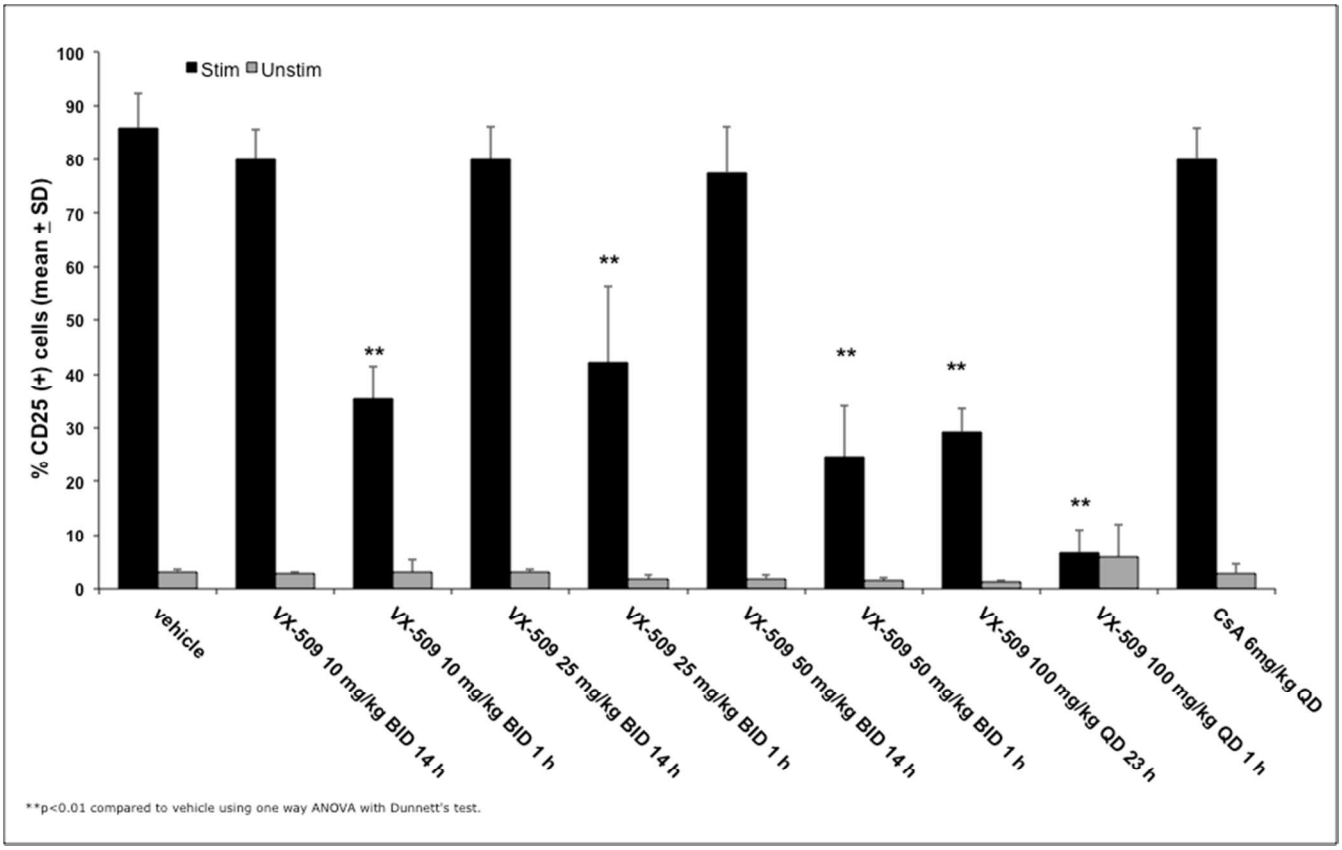

Figure 8. Dose dependent decrease in ex vivo stimulated biomarker CD25 by **VX-509** in Rat HvG model.

Terminal whole blood samples at 1 and 14 hours post-dose were analyzed using *ex vivo* 4 beta-phorbol 12-myristate 13-acetate (PMA) and anti-CD28 antibody-stimulated CD25 expression. In the absence of stimulation with PMA and anti-CD28 antibody, CD25 expression in CD3 (+) T cells was below 5%, whereas CD25 expression reached approximately 85% within 24 hours after stimulation. There was significant reduction of CD25 expression by **VX-509** at 1 hour post-dose in all of the dose groups tested: 59 % (P<0.01) inhibition at 10 mg/kg BID, 51 % (P<0.01) at 25 mg/kg BID, 71% (P<0.01) at 50 mg/kg

BID, and 92% (P<0.01) was observed at 100 mg/kg QD. There was also significant reduction (66 %, p<0.01) in CD25 expression in the 100 mg/kg QD group at trough (23 hours post dose)(Figure 8), supporting the potential for a QD dosing regimen in clinical studies. In this study, **VX-509** exhibited significant dose-dependent immunosuppressive activity. Ex vivo whole blood analysis of CD25 expression demonstrates that **VX-509** effectively attenuated T-cell activation at 1 hour post-dose.

Given the potency, its unique selectivity profile favoring JAK3 as determined using cellular assays, the pharmacokinetic profile and its efficacy in pre-clinical pharmacologic models of aberrant immune function, **VX-509** appears to have potential clinical utility for treatment of a variety of immune-based diseases and results from clinical studies will be reported in due course.

Synthesis

Synthesis of final compounds relied on ready access to common 1*H*-pyrrolo[2,3-*b*]pyridine and deazapurine boronates **50**. These key intermediates were all similarly prepared according to the general route outlined in Scheme 1.

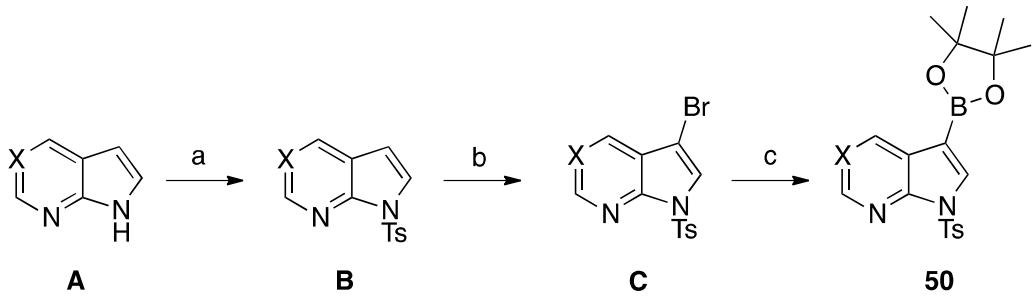

A **B** **C** **50**

a: X = CH, **b:** X = CCl, **c:** x = CF, **d:** X = $COCH_3$, or **e**: X = N

Scheme 1. Conditions: a) NaH, TsCl, THF; b) Br_2, CH_2Cl_2; c) bis(pinacolato)diboron, $Pd(PPh_3)_4$, KOAc, 1,4-dioxane.

N-Tosyl protection starting from known intermediates **A**, followed by bromination at C-3 enabled efficient preparation of the 3-bromo-1*H*-pyrrolo[2,3-*b*]pyridine or deazapurines **C**. Treatment with bis(pinacolato)diboron and palladium tetrakis(triphenylphosphine) provided the desired Suzuki coupling partners, intermediates **50a-e**.

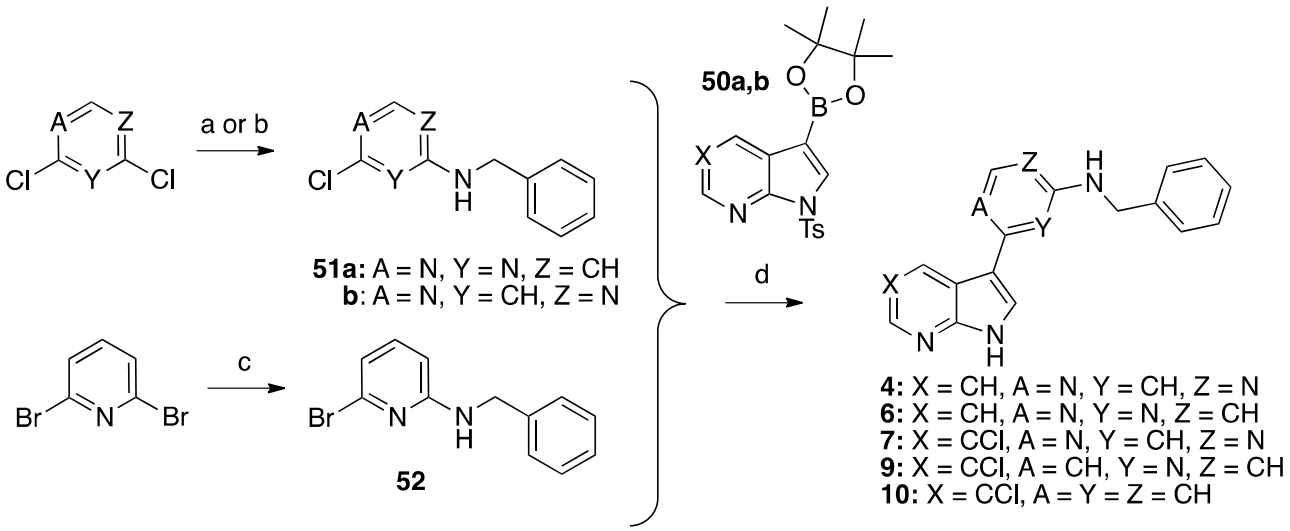

Scheme 2a. Conditions: a) $PhCH_2NH_2$, DIPEA, THF, reflux, 1-2h or IPA, 90 °C, (54-79%); b) $PhCH_2NH_2$, neat, (79%); c) $PhCH_2NH_2$, 150 °C (μW) (40-55%) d) i: $Pd(PPh_3)_4$, DME, 2 M Na_2CO_3, reflux ii: NaO*t*Bu, 130-160 °C, 10-20 min (μW) (25-89%)

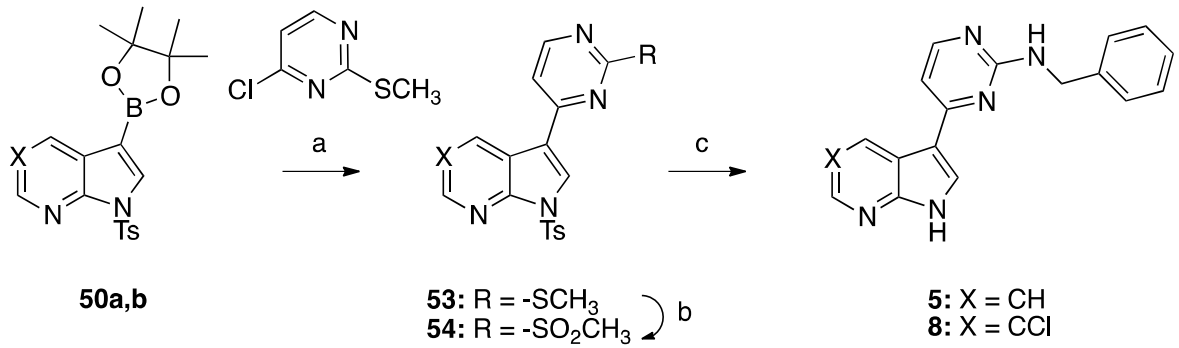

Scheme 2b. Conditions: a) $Pd(PPh_3)_4$, DME, 2M Na_2CO_3, reflux (51%; X = CCl); b) Oxone, CH_3OH-H_2O (1:1) (32%; X = CCl); c) i: $PhCH_2NH_2$, EtOH, reflux, 16 h (94%; X = CCl), ii: 3N NaOH, CH_3OH (75%; X = CCl) or NaO*t*Bu, 130-160 °C, 10-20 min (μW)

The syntheses of analogs containing the benzylamine group and with central core ring variations in Table 1 were achieved *via* the general route described in Scheme 2. The sequence involved Suzuki coupling of protected boronates **50a,b** with suitably substituted aryl halides followed by deprotection as shown in scheme 2a. Thus, SnAr displacement of suitable dihalopyrimidine regioisomers with benzylamine, provided halo-coupling partners **51a,b** and **52** in moderate to good yields. Suzuki coupling under standard conditions was followed by removal of the tosyl group under basic conditions to provide compounds **4**, **6** and **7**, as well as pyridine derived analogs **9**. The corresponding phenyl analog **10** was accessed using commercial *N*-benzyl-3-bromoaniline following the same sequence. Compounds **11**−**21** were prepared most conveniently by the same sequence starting from either 2,4-dichloropyrimidine or 2,4-dichloro-5-fluoropyrimidine and the corresponding amines. Thus, chloride displacement followed by Suzuki coupling and tosyl deprotection delivered compounds **11-21.**

Scheme 2b describes the chemistry to gain access to compounds **5** and **8**. Interemediates **53** and **54** were prepared in moderate yield *via* Suzuki coupling of boronic esters **50a** and **50b** with 4-chloro-2-methylthiopyrimidine followed by oxidation of **53** to provide the corresponding sulfones **54**. This sequence allowed for facile SnAr displacement with benzylamine to obtain, after de-tosylation, the desired analogs **5** and **8**.

The syntheses of amino acid-based compounds **22**−**49** depicted in Table 3 were accomplished in a 5-step protocol from commercially available N-Boc amino acids **M** (Scheme 3). The requisite amide cap was installed *via* the coupling of **M** with trifluoroethyl amine hydrochloride under standard conditions using either HATU or EDC/HOBt to furnish, after Boc deprotection with CH_2Cl_2-TFA, the corresponding amides **N** in good overall yield. N-arylation with the either 2,4-dichloropyrimidine, 2,4-dichloro-5-fluoropyrimidine or 2,4-dichlorotriazine provided the desired coupling partners **Q** for assembly of the

final compounds. Finally, Pd mediated Suzuki coupling of **Q** with **50a-e** delivered, after removal of the tosyl protecting group using basic conditions, the desired analogs **22-49** in moderate to good yield.

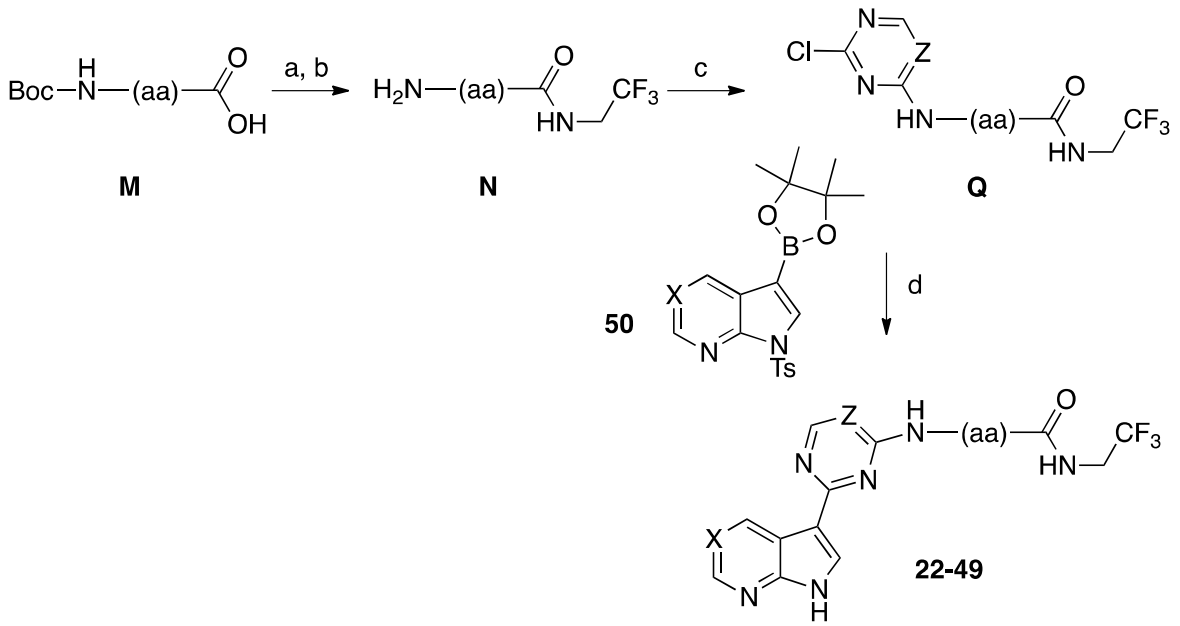

Scheme 3. a) HATU or EDC, HOBt, DIEA, DMF, $CF_3CH_2NH_2$-HCl, rt (60-92%); b) 1:1 TFA- CH_2Cl_2 or 2 M HCl, Et_2O-CH_3OH (quant.); c) DIEA, IPA or THF (29-80%); d) *i*) **50a-e**, 2 M Na_2CO_3, $Pd(PPh_3)_4$, DME, 150 °C, 10 min. (μW) or reflux; 16h; ii) LiOH, THF, H_2O, rt or CH_3OH, 25% $NaOCH_3$ in CH_3OH, 60 °C,1h (30-65% 2-steps)

Experimental Section

Protein preparation. Human JAK3 kinase domain (A815-E1124) was cloned by PCR from a previously isolated full-length JAK3 cDNA (GenBank accession number AAD22741) and inserted into pBEV10 (a custom shuttle vector for insect cell expression via the baculovirus polyhedrin promoter). The expressed protein contains a thrombin-cleavable N-terminal hexahistidine tag. For production, Sf9 insect cells grown to 2×10^6 cell/ml in Excell-405 medium (JRH Bioscience, KS, US) were infected with virus at a multiplicity of infection (MOI) of 2.5 and incubated for 72-96 h at 27 ˚C. Frozen cell paste was thawed in 5-10 volumes of Buffer A (50 mM HEPES pH 8.0, 500 mM NaCl, 20% (v/v) glycerol, 0.2% Tween 20 (v/v), 0.05% (v/v) mM β-mercaptoethanol, 5 mM imidazole) containing 1 mM PMSF, 5 mg/ml leupeptin, 3 mM benzamidine, and 625 units/L Benzonase (EMD Millipore, Bellerica, MA) and mechanically lysed in a microfluidizer (Microfluidics, Newton, MA). The lysate was clarified by centrifugation at 54,000 × *g* for 1 h, and JAK3 was purified by nickel metal affinity resin (Sigma-Aldrich, St. Louis, MO) followed by sizing in Buffer B (50 mM HEPES pH 8.0, 500 mM NaCl, 20% (v/v) glycerol, 0.05% (w/v) β-octylglucopyranoside and 5 mM DTT) using an HR 16/60 Superdex-75 size exclusion column (GE Healthsciences, Piscataway, NJ). The final protein concentration was quantified using molar extinction coefficient of 39440 $Lmol^{-1}cm^{-1}$ calculated from the protein sequence. Purified JAK3 protein was stored at -80 ˚C in small aliquots until further use.

Human JAK2 kinase domain (T842-G1132) (SwissProt entry O60674) and SYK full-length protein (Genbank accession number L28824) were cloned, expressed and purified in a similar manner to JAK3 kinase domain. For JAK2, the final purified material was activated at 0.5-1 mg/ml using 5 mM ATP and 20 mM MgCl2 for 1 h at 25 ˚C followed by a desalting step in Buffer B. A molar extinction coefficient

of 38975 $Lmol^{-1}cm^{-1}$ was used for determining protein concentration. For SYK, the activation step was performed at 0.1 mg/ml for 16 hours at 4 ˚C. A molar extinction coefficient of 111,660 $Lmol^{-1}cm^{-1}$ was used for determining protein concentration of the SYK. For crystallography, JAK2 protein was prepared as previously described.[32]

Human FLT3 kinase domain (H564-V958) was expressed and purified as previously described.[37] The protein was activated at 0.1 mg/ml using 2.5 mM ATP and 5 mM MgCl2 for 16 h at 4 ˚C followed by a desalting step and protein concentration was determined using a molar extinction coefficient of 66280 $Lmol^{-1}cm^{-1}$.

Recombinant AURA (1-403) was expressed as N-terminal, His6-tagged fusion proteins using a baculovirus expression system (FastBac, Gibco BRL). The protein was purified by using affinity chromatography using Ni-NTA agarose, followed by size exclusion using a Superdex 200 26/60 column (Amersham Biosciences).[38]

Kinase inhibition assay. Inhibition of kinase activity was assessed using a standard enzyme-coupled system or a radiometric, phosphocellulose-peptide capture assay as previously described.[39]

Crystallization and Structure Determination.

Crystals of JAK2 were obtained as described previously[32]. Briefly the kinase domain of JAK2 was concentrated to 10 mg/mL. Crystals were grown by hanging-drop vapor diffusion in 24-well plates using repeated seeding. The reservoir contained 0.5 mL of 1.7 to 2.1 M DL-malic acid, pH 7.0 and 2 mM

dithiothreitol. The crystallization drop contained 0.5 µL protein containing 1 mM of compound dissolved in DMSO + 0.5 µL resevoir solution + 0.5 µL water. The crystals were transferred to a drop containing crystallization buffer that was 25% glycerol, and then flash frozen in liquid nitrogen. Data were collected at the Advanced Light Source. Images were processed with autoPROC[40]. The structure was solved by difference Fourier methods using a previously determined structure, and refinement and model building were performed with BUSTER[41] and COOT[42], respectively (see supplemental data for data collection and refinement statistics.

HT-2-IL-2 Assay (JAK3 mediated cell assay): HT-2 cells were deprived of growth factors for 4 hours at 37°C. Cells were plated in 96-well plates at a density of 2.5 x 10^5 cells per well (50 µl of a 5 x 10^6 cells/mL stock). **VX-509** solution was plated in triplicate, in columns, at a final concentration ranging from 10 µM to 4.5 nM. Two columns of cells were plated with DMSO as the proliferation control. The cells were incubated at 37 °C for 1 hour, after which cells in the **VX-509** columns and in one of the control columns were stimulated with IL-2 for 20 min at 37 °C. The second column of control cells was not stimulated and served as the negative control. Plates were centrifuged at 500 × g for 5 minutes and the supernatant was aspirated. Cells were fixed with 4% formaldehyde for 10 minutes at room temperature. Plates were centrifuged and the supernatant was aspirated. Cells were then permeabilized by incubation in 90% methanol for 30 minutes at 4°C. Plates were centrifuged at 500 × g for 5 minutes and the supernatant was aspirated. Plates were washed by adding phosphate buffered saline (PBS) and immediately centrifuging at 500 × g for 5 minutes, after which the supernatant was aspirated. Cells were stained with a 1:10 dilution of anti-phospho-STAT5 PE antibody for 45 minutes on a shaker at room temperature. Cells were then washed by adding PBS, centrifuging plates for 5 minutes at 500 × g, and aspirating the supernatant. Cells were re-suspended in PBS and STAT-5 phosphorylation was quantified

on a Guava PCA 96 FACS reader (Millipore, City, State). The half-maximal inhibitory concentration (IC_{50}) of **VX-509** was determined using Softmax pro software.

TF-1GM-CSF (JAK2 mediated cell assay): TF-1 cells were deprived of growth factors for 4 hours at 37°C. Cells were plated in 96-well plates at a density of 2.5 x 10^5 cells per well (50 µl of a 5 x 10^6 cells/mL stock). **VX-509** solution was plated in triplicate, in columns, at a final concentration ranging from 10 µM to 4.5 nM. Two columns of cells were plated with DMSO as the proliferation control. The cells were incubated at 37°C for 1 hour, after which cells in the **VX-509** columns and in one of the control columns were stimulated with GM-CSF for 15 min, at 37°C. The second column of control cells was not stimulated and served as the negative control. Plates were centrifuged at 500 × g for 5 minutes and the supernatant was aspirated. Cells were fixed with 4% formaldehyde for 10 minutes at room temperature. Plates were centrifuged and the supernatant was aspirated. Cells were then permeabilized by incubation in 90% methanol for 30 minutes at 4°C. Plates were centrifuged at 500 × g for 5 minutes and the supernatant was aspirated. Plates were washed by adding PBS and immediately centrifuging at 500 × g for 5 minutes, after which the supernatant was aspirated. Cells were stained with a 1:10 dilution of anti-phospho-STAT-5 PE antibody for 45 minutes on a shaker at room temperature. Cells were then washed by adding PBS, centrifuging plates for 5 minutes at 500 × g, and aspirating the supernatant. Cells were resuspended in PBS and STAT-5 phosphorylation was quantified on a Guava PCA 96 FACS reader (Millipore, City, State). The half-maximal inhibitory concentration (IC_{50}) of **VX-509** was determined using Softmax pro software.

Mouse 2-Way MLR from Table 6: Spleens from 8- to 10-week-old female mice (CBA and BALB/c, Jackson Labs) were used to isolate splenocytes. The splenocytes from each strain of mouse were plated

at a density of 1.8 x 10^5 cells per well in 96-well plates, in total 3.6 x 10^5 cells per well. The **VX-509** dilutions were added to the wells; two rows were plated with DMSO alone and served as the proliferation controls for the assay. The plates were incubated at 37°C in a CO_2 incubator for 4 days. On day 5, 20 μCi/mL methyl-^{3}H-thymidine was added to each well. After 7 hours, cells were harvested onto Betaplate double filters using a TOMTEC Harvester 96. Filters were dried for 1 hour and then 20 ml scintillation fluid was added per filter. Filters were were analyzed for radioactive counts on a PerkinElmer-Wallace beta-counter (1205 Betaplate Beta Liquid Scintillation Counter). Data were analyzed to generate an IC_{50} value using Softmax pro software.

STAT-2 Nuclear Translocation Assay: HeLa cells were plated in a 96-well plate at a density of 5 x 10^3 cells/well. The plates were incubated at 37° C for 18 hours (overnight) in a CO_2 incubator. **VX-509** was added to plates at a final concentration ranging from 4.5 nM to 10 μM, which were placed in a CO_2 incubator at 37°C for 1 h. Cells were then stimulated with IFN α and incubated for 45 min at 37°C in a CO_2 incubator (medium only for negative control plates). Plates were processed according to the protocol from the Cellomics STAT2 activation HitKit and screened using the ArrayScan II HCS System (Beckman Coulter, Fullerton, CA). Data were analyzed using Softmax pro software to generate an IC_{50} value for **VX-509**.

IL-2-Stimulated Human T-cell Blast Proliferation Assay: Whole blood samples from healthy volunteers were used to collect PBMCs, which were plated in T75 tissue culture flasks at a density of 1 x 10^6/ml. Cells were stimulated with 10 μg/ml of PHA at 37^{o}C for 72 hours. After 72 h, cells were detached from the flask by scraping, washed, and plated at a density of 1x10^5/well in a 96-well plate. **VX-509** (9.7 nM to 10 μM) was added and plates were incubated for 30 min at 37 $^\circ$ C followed by

stimulation with human IL-2. In two rows, only DMSO was added; one row was not stimulated with IL-2, and one row was stimulated with IL-2 to serve as the proliferation control. Plates were incubated at 37 °C for 2 days. On day 2, cells were pulsed with 20 μCi/mL methyl-^{3}H-thymidine for 18-24 hours and harvested onto filters for radiographic determination using a Perkin Elmer-Wallace beta counter (1205 Betaplate Beta Liquid Scintillation Counter). Data were analyzed to generate an IC_{50} value using Softmax pro software.

Colony Forming Unit-erythroid (CFU-E) Assay: CFU-E assays were performed by StemCell Technologies (Vancouver, BC, Canada). Briefly, clonogenic progenitors from normal human bone marrow of the erythroid, myeloid, and multi-potential lineages were plated in methylcellulose-based media formulations containing 50 ng/ml SCF, 10 ng/ml GM-CSF, 10 ng/ml IL-3 and either 3.0 or 0.3 U/ml Epo. **VX-509** was added to produce final concentrations between 0.01 μM and 10 μM. Solvent control cultures, as well as standard controls, were also made for each media formulation. The cultures were performed in triplicate at 1 x 10^4 cells per culture. Following 14 days in culture, the colonies were assessed and classified based on size, and cell and colony morphology.

Liver Microsome and S9 Fraction Stability Assays. In the liver microsomal stability experiments, 1 μM or 10 μM of **VX-509** was incubated with liver microsomes from either the mouse, rat, dog, monkey, or human at a final protein concentration of 0.5 mg/mL and 50 μg of alamethicin/mg microsomal protein. The reactions were initiated upon the addition of cofactors, either nicotinamide adenine dinucleotide phosphate (NADPH, 2 mM final concentration) to evaluate the role of NADPH-dependent metabolic pathways or NADPH (2 mM final concentration) and uridine diphosphate glucuronic acid (UDPGA, 5 mM final concentration) to evaluate the role of glucuronidation in the metabolism of **VX-**

509 across species. No cofactors were added to the control reactions. The liver microsomal incubations were performed in triplicate. The reactions were terminated by protein precipitation using acetonitrile containing the analytical standard N-(1H-indazol-3-yl)-2-[2-(trifluoromethyl)phenyl]quinazolin-4-amine as the quenching reagent at 0, 5, 15 and 30 minutes (min). The samples were analyzed using liquid chromatography/tandem mass spectrometry (LC-MS/MS) and the percentage of **VX-509** remaining based on the zero time point was determined.

In the liver S9 stability experiments, 1 μM or 10 μM of **VX-509** was incubated with liver S9 from the mouse, rat, dog, monkey, or human at a final protein concentration of 3.0 mg/mL. The reactions were initiated upon the addition of nicotinamide adenine dinucleotide phosphate (NADPH, 2 mM final concentration) to evaluate the role of NADPH-dependent metabolic pathways. No cofactors were added to the control reactions. The liver S9 incubations were performed in triplicate. The reactions were terminated by protein precipitation using acetonitrile containing the analytical standard N-(1H-indazol-3-yl)-2-[2-(trifluoromethyl)phenyl]quinazolin-4-amine as the quenching reagent at 0, 5, 15 and 30 minutes (min). The samples were analyzed using liquid chromatography/tandem mass spectrometry (LC-MS/MS) and the percentage of **VX-509** remaining based on the zero time point was determined.

In Vivo Pharmacokinetic Studies. Rat IV/PO studies: Male Sprague-Dawley rat intravenous bolus/oral administration studies were conducted in house and Beagle dog intravenous bolus/oral administration studies were conducted at Huntingdon Life sciences, Eastmillstone, NJ. Male Sprague-Dawley rats (n=3 per dose group) received single nominal intravenous doses of 1 mg/kg of **VX-509** solutions formulated in DMI-D5W-PG-EtOH (dimethylisosorbide (DMI), 5% dextrose in water (D5W), propylene glycol (PG), and ethanol (EtOH) in a ratio of 10:40:35:15). Blood samples (approximately 0.25 mL each) were

collected via a carotid artery catheter pre-dose and at 0.08, 0.17, 0.25, 0.50, 1.00, 2.00, 4.00, 6.00, 8.00, 12.00 and 24.00 hours post-dose.

Rat IV/PO studies. Male Sprague-Dawley rats (n=3 per dose group) were administered single nominal oral doses of 10, mg/kg of **VX-509** by gavage as suspension formulated in 10% VitE TPGS (Vitamin E d-α-tocopheryl polyethylene glycol 1000 succinate). Blood samples were collected via carotid artery catheter prior to dosing and at 0.25, 0.50, 1.00, 1.50, 2.00, 3.00, 4.00, 6.00, 8.00, 12.00, 24.00 and 48.00 hours post-dose.

Dog IV/PO studies. One group of male beagle dogs (n=3) was administered a single nominal intravenous dose of 1 mg/kg of **VX-509** as solution formulated in propylene glycol 400 (PEG 400) and 5% dextrose in water (10:90, v:v) (PEG 400/D5W (10/90)). Blood samples (approximately 0.25 mL each) were collected via jugular, cephalic or saphenous venipuncture at 0 (pre-dose), 0.08, 0.17, 0.25, 0.50, 1.00, 1.50, 2.00, 3.00, 4.00, 6.00, 8.00, 24.00 and 48.00 hours post-dose.

Male beagle dogs (n=3 per dose group) were administered single nominal oral doses of 10 mg/kg of **VX-509** by gavage as suspension formulated in 10% Vitamin E d-α-tocopheryl polyethylene glycol 1000 succinate (10% VitE TPGS). Blood samples were collected via jugular, cephalic or saphenous venipuncture prior to dosing (pre-dose) and at 0.25, 0.50, 1.00, 1.50, 2.00, 3.00, 4.00, 6.00, 8.00, 24.00 and 48.00 hours post-dose.

Blood Sample Collection and Plasma Sample Analysis. Blood samples for the rat and dog pharmacokinetic studies were collected in tubes containing dipotassium EDTA and kept at approximately 4°C. Plasma was separated and stored at approximately -70°C until analysis. Plasma samples were analyzed using LC-MS/MS to determine **VX-509** concentrations, with a lower limit of quantitation (LLOQ) of 1 ng/mL. The linear range of the assay was from 1 to 5000 ng/mL. **VX-509** and the internal standard N-(1H-indazol-3-yl)-2-[2-(trifluoromethyl)phenyl]quinazolin-4-amine were extracted from plasma, 100 μL each, by direct protein precipitation with acetonitrile (1:4 ratio of plasma/acetonitrile). After centrifugation, the supernatant extract (10 μL) was injected into the LC-MS/MS system. The HPLC portion of the system included a Waters Xterra MS C18 column (5 micron, 2.1 mm diameter x 50 mm long) eluted with a gradient mobile phase containing 10 mM ammonium acetate in water and acetonitrile. The analytes were detected by MS/MS with Atmospheric Pressure Chemical Ionization (APCI) in the mode of multiple reaction monitoring (MRM). Plasma concentration vs. time data were subjected to noncompartmental pharmacokinetic (PK) analysis using WinNonlin® Professional Edition software, Version 5.1.1 (Pharsight Corporation, Mountain View, CA).

Rat Host versus Graft (HvG) Model. Male Lewis and Dark Agouti (DA) rats weighing 200-250 g (Harlan, Indianapolis, IN) were allowed to acclimate to the animal facility for 6 days, during which time they had ad libitum access to food and water. Spleen cells isolated from four DA male rats were pooled and gamma-irradiated at 3000cGy. A total of 40 male Lewis rats received injections into the right foot pad of 20 x 10^6 irradiated allogeneic spleen cells suspended in 100 μL PBS. All treatments were initiated on day 0, one hour prior to the injection of graft cells. All groups were terminated on day 4. **VX-509** was solubilized at 10 mg/kg, 25 mg/kg, 50 mg/kg and 100 mg/kg as an aqueous solution in 10% Vitamin E D-alpha-tocophenyl polyethylene glycol 1000 succinate (VitE TPGS) and 1% hydroxypropyl

methylcellulose acetyl succinate (HPMC-AS). **VX-509** was administered by oral gavage (PO) once a day (QD) at 100 mg/kg or twice a day (BID, on a 10/14 hr dosing schedule) at 10 mg/kg/day, 25 mg/kg/day, or 50 mg/kg/day for 4 days. Cyclosporine A (CsA), an immunosuppressive drug used clinically, was used as a reference compound and was dosed at 6 mg/kg PO, QD. **VX-509** and CsA were administered in a dosing volume of 10 mL/kg. At study termination on day 4, animals were sacrificed by CO_2 asphyxiation, and the popliteal lymph nodes were excised and weighed. The delta weight difference between ipsilateral (right, grafted) and contralateral (left, non-grafted) popliteal lymph nodes was calculated and compared to the delta values of vehicle control and CsA-treated groups. Whole blood samples were collected via cardiac puncture and used for the ex vivo whole blood biomarker assay.

Ex-vivo Whole Blood Biomarker Assay: Whole blood was collected from Lewis rats via cardiac puncture in tubes containing lithium heparin (Vacutainer, BD, Franklin, NJ). Blood samples were plated at a volume of 100 μL (final concentration of whole blood in assay is 50%) in 96-well cluster tubes. Three wells per animal were stimulated with 4 beta-phorbol 12-myristate 13-acetate (PMA) at 100 ng/mL and rat anti-CD28 at a concentration of 10 μg/mL. Control medium was added to the other three wells (unstimulated). The final volume of the cluster tubes was 200 μL. The cluster tubes were incubated overnight at 37°C in a CO_2 incubator. After 18 to 24 hours of incubation, cells were stained with anti-CD3 PE and anti-CD28 FITC for 30 min at room temperature. Lysis buffer (800 μL of 1X RBC, Sigma) was added to the plate and incubated at room temperature for 10 minutes. The cluster plate was centrifuged and the supernatant was aspirated. Lysis buffer (300 μL of 1X) was added and plates were centrifuged. Once the supernatant was aspirated, cell pellet was resuspended in 300 μL PBS

containing 1% formaldehyde. Samples were read on the FACS Calibur HTS reader. Data was analyzed using Flow Jo and Excel.

Compound Preparation and Characterization. All commercially available reagents and anhydrous solvents were used without further purification. Purity assessment for final compounds based on analytical HPLC: column, 4.6mm_50mmWaters YMC Pro-C18 column, 5 μm, 120A. Mobile phases are as follows: A, H_2O with 0.2% formic acid; B, acetonitrile with 0.2% formic acid; gradient, 10_90% B in 3 min with 5 min run time. The flow rate is 1.5 mL/min. Unless specified otherwise, all compounds were $\geq$ 95% purity. Mass samples were analyzed on a Micro Mass ZQ, ZMD, Quattro LC, or Quatro II mass spectrometer operated in a single MS mode with electrospray ionization. Samples were introduced into the mass spectrometer using flow injection (FIA) or chromatography. The mobile phase for all mass analysis consisted of acetonitrile-water mixtures with either 0.2% formic acid or ammonium formate. ^1H NMR spectra were recorded either using a Bruker Avance 400 (400 MHz) or a Bruker Avance II-300 (300 MHz) instrument. The column chromatography was performed using Teledyne ISCO RediSep Normal Phase (35-70 microns) or RediSep Gold Normal Phase (25-40 microns) silica flash columns using a Teledyne ISCO Combiflash Companion or Combiflash Rf purification system. Preparative reversed phase chromatography was carried out using a Gilson 215 liquid handler coupled to a UV-VIS 156 Gilson detector, an Agilent Zorbax SB-C18 column, 21.2 mm × 100 mm, a linear gradient from 10 to 90% CH_3CN in H_2O over 10 min (0.1% trifluoroacetic acid); the flow rate was 20 mL/min.

High-resolution mass spectrometry data was collected on a Thermo Scientfic QExactive mass spectrometer coupled to a Waters Acquity UPLC system. Samples were analyzed from a 100 μM DMSO solution with 3 μL injection volumes. The chromatographic column was a Waters Acquity CSH C18, 2.1 × 50 mm, 1.7 μm particle size. Gradient elution was employed using 0.1% formic acid in water

as mobile phase A and 0.1% formic acid as mobile phase B. The gradient began at 10% B, increased to 60% B over 0.8 minutes, to 100% B over the next 0.2 minutes, and was followed by a 0.5 minute re-equilibration at initial conditions. The mass spectrometer was run in full-MS mode, positive polarity, with resolution set to 35,000. A heated electrospray source was used with settings of 3.5 kV and 400 °C.

(Scheme 1) Preparation of 1*H*-Pyrrolo[2,3-*b*]pyridine**s Intermediates**

5-Chloro-1-tosyl-1H-pyrrolo[2,3-b]pyridine (B: X = CCl**).** A 22-L, four-necked, round-bottomed flask equipped with an overhead stirrer, dropping funnel, and thermocouple was charged with 3 L of anhydrous THF followed by 131.6 g (3.29 mol) of NaH and 582.8 g (3.06 mol) of p-toluenesulfonyl chloride. A solution of 467.5 g (3.06 mol) of **4** in 2 L of THF was added to the mixture via the dropping funnel. A significant exotherm was observed that was controlled by the rate of addition. The mixture was stirred at room temperature overnight, quenched with water, and extracted with EtOAc. The organic extract was dried ($MgSO_4$) and evaporated in vacuo. The crude product was dissolved in CH_2Cl_2 and filtered over a plug of silica gel. The plug was eluted with CH_2Cl_2 and the filtrate was evaporated in vacuo to afford 917 g (98%) of **5** as a light yellow solid. ^{1}H NMR (500 MHz, $CDCl_3$) δ 12.21 (s, 1H), 8.67 (s,1H), 8.32 (t, 1H) 8.26 (dd, 2H), 8.0 (s, 1H), 7.47 (s, 1H), 3.78 (m, 2H), 1.59 (s, 6H).

3-Bromo-5-chloro-1-tosyl-1H-pyrrolo[2,3-b]pyridine (C: X = CCl**).** A 22-L, four-necked, round-bottomed flask equipped with an overhead stirrer, dropping funnel and thermocouple was charged with 855.6 g (2.79 mol) of **5** and 5 L of CH_2Cl_2. Bromine (290 mL, 5.64 mol) was added via the dropping funnel. An exotherm was observed during the addition and an orange solid precipitated. The mixture was stirred overnight and washed with aqueous $NaHSO_3$. The organic solution was dried ($MgSO_4$), and

filtered over a plug of silica gel. The plug was eluted with CH_2Cl_2 and the filtrate was evaporated in vacuo to afford 1047 g (97%) of **6** as an off-white solid. ^{1}H NMR (500 MHz, $CDCl_3$) δ 8.38 (d, 1H), 8.08 (d, 2H), 7.76 (d, 1H), 7.28 (d, 2H), 2.39 (s, 3H).

5-Chloro-3-(4,,4,5,5-tetramethyl-1,3,2-dioxaborolan-2-yl)-1-tosyl-1H-pyrrolo[2,3-b]pyridine (50b: X = CCl**).** A 22-L, four-necked, round-bottomed flask equipped with an overhead stirrer and thermocouple was charged with 1074 g (2.79 mol) of **6** and 6L of 1,4-dioxane. Bis-pinacol diboron (1030 g, 4.06 mol) was added along with 812 g (8.27 mol) of KOAc. The mixture was deoxygenated for two hours with a stream of nitrogen and 185 g (160 mmol) of $Pd(PPh_3)_4$ was added along with 200 mL of distilled water. The mixture was heated to 95°C overnight. The reaction was cooled and filtered over celite. The celite was washed with EtOAc and the filtrate was evaporated in vacuo. The crude product mixture was dissolved in EtOAc and filtered over a plug of florisil. The plug was eluted with EtOAc and the filtrate was evaporated in vacuo. The solid was slurried with hexane and filtered. The filter cake was washed with hexane and dried to afford 984 g (82%) of **50b** as a grey solid. ^{1}H NMR (500 MHz, $CDCl_3$) δ 8.31 (d, 1H), 8.13 (m, 2H), 8.05 (d, 2H), 2.38 (s, 3H), 1.38 (s, 12H).

3-(4,4,5,5-tetramethyl-1,3,2-dioxaborolan-2-yl)-1-tosyl-1*H*-pyrrolo[2,3-*b*]pyridine (50a: X = CH**):** ^{1}H NMR (400 MHz, $CDCl_3$) δ 8.39 (dd, *J* = 4.8, 1.6 Hz, 1H), 8.17 (dd, *J* = 7.8, 1.6 Hz, 1H), 8.12 (s, 1H), 8.10 – 8.04 (d, J = 8.1 Hz, 2H), 7.24 (d, *J* = 8.1 Hz, 2H), 7.17 (dd, *J* = 7.8, 4.8 Hz, 1H), 2.34 (s, 3H), 1.34 (s, 12H).

5-fluoro-3-(4,4,5,5-tetramethyl-1,3,2-dioxaborolan-2-yl)-1-tosyl-1*H*-pyrrolo[2,3-*b*]pyridine (50c: X = CF**):** ^{1}H NMR (400 MHz, DMSO-d6) δ 8.38 (dd, J = 2.7, 1.3 Hz, 1H), 8.11 (s, 1H), 8.02 (d, J = 8.4 Hz, 2H), 7.81 (dd, J = 8.4, 2.7 Hz, 2H), 7.40 (d, J = 8.4 Hz, 2H), 2.32 (s, 3H), 1.29 (s, 12H)

5-methoxy-3-(4,4,5,5-tetramethyl-1,3,2-dioxaborolan-2-yl)-1-tosyl-1*H*-pyrrolo[2,3-*b*]pyridine (50d: X = $COCH_3$**):** ^{1}H NMR (400 MHz, $CDCl_3$) δ 8.13 (d, *J* = 2.8 Hz, 1H), 8.08 (s, 1H), 8.06 – 8.00 (d, J = 8.0 Hz , 2H), 7.63 (d, *J* = 2.8 Hz, 1H), 7.28 – 7.20 (d, J = 8.0 Hz, 2H), 3.86 (s, 3H), 2.34 (s, 3H), 1.33 (s, 12H).

5-(4,4,5,5-tetramethyl-1,3,2-dioxaborolan-2-yl)-7-tosyl-7*H*-pyrrolo[2,3-*d*]pyrimidine (50e: X = N**):** ^{1}H NMR (500 MHz, DMSO-d6) δ 9.07 (s, 1H), 8.96 (s, 1H), 8.10 (s, 1H), 8.07 (d, J = 8.5 Hz, 2H), 7.43 (d, J = 8.0 hZ, 2H), 2.33 (s, 3H), 1.30 (s, 12H).

(Scheme 2a) Compounds from Table 1.

Benzyl-(2-chloro-pyridin-4-yl) amine (51a). To a solution of 2,4-dichloropyrimidine (0.15 g, 1.0 mmol), benzylamine (0.109 mL, 1.0 mmol) in THF, was added DIPEA (0.526 mL, 3.0 mmol) and the reaction mixture was heated at reflux for 2 hours resulting in the formation of a 4:1 mixture of regioisomers (desired vs undesired) by TLC (5% CH_3OH- CH_2Cl_2). The reaction was concentrated in vacuo to an oil that was then subjected to flash chromatography (2% CH_3OH in CH_2Cl_2 to provide 120 mg (54%) of the desired product **51a**. ^{1}H NMR (300 MHz, CD_3OD) δ 4.95 (bs, 2H), 6.6 (d, 1H), 7.2 (m, 1H), 7.3-7.5 (m, 5H), 8.0 (d, 1H), 8.3 (d, 1H), 8.4 (s, 1H), 8.55 (d, 1H). LCMS $[M + H]^+$= 220.

Benzyl-[2-(1H-pyrrolo[2,3-b]pyridine-3-yl)-pyrimidin-4-yl]-amine (6). A solution of **50a** (0.36 g, 0.09 mmol), **51a** (0.028 g, 0.108 mmol), 2 M Na_2CO_3 (0.108 mL, 0.271 mmol) and catalytic $PdCl_2$ in 1 mL of DMSO was heated in the microwave at 160°C for 5 minutes, resulting in conversion to the tosylated intermediate product. NaOtBu (0.026 g, 0.271 mmol) was added and the reaction mixture was heated in the microwave for 5 minutes at 160 °C, resulting in complete conversion to product. The reaction was filtered and purified by preparative HPLC giving 0.0032g of **6** as a white solid in 11% yield. ^{1}H NMR (300 MHz, CD_3OD) δ 4.95 (bs, 2H), 6.6 (d, lH), 7.2 (, lH), 7.3-7.5 (m, 5H), 8.0 (d, lH), 8.3 (d, lH), 8.4 (s, lH), 8.55 (d, lH). LCMS $[M + H]^+$ = 302.0. HRMS $[M + H]^+$ calculated for (C18H15N5 + H^+): 302.1400221, found: 302.13962 with a deviation of only 1.33 ppm.

Benzyl-(6-chloro-pyrimidin-4-yl)-amine (51b). Benzyl amine (0.697 ml, 6.76 mmol) was added to 4,6-dichloropyrimidine (l.0g, 6.76 mmol) neat causing a vigorous reaction and color change. The reaction was slowly diluted with methylene chloride resulting in a white precipitate. Triethyl amine (1 mL) was added and TLC indicated conversion to product (5% CH_3OH-CH_2Cl_2). The reaction was loaded directly onto silica and purified (2% CH_3OH-CH_2Cl_2), giving 1.17g (5.32 mmol) of **51b** as a yellow wax in 79% yield.

***N*-benzyl-6-(1*H*-pyrrolo[2,3-*b*]pyridin-3-yl)pyrimidin-4-amine (4).** Final product **4** was formed as described for **6,** giving 0.012 g of a white solid. ^{1}H NMR (300 MHz, CD_3OD) δ 4.8 (s, 2H), 7.05 (s, lH), 7.2-7.6 (m, 6H), 8.2 (s, lH), 8.4 (m, 2H), 8.55 (s, lH). LCMS $[M + H]^+$ = 302. HRMS $[M + H]^+$ calculated for (C18H15N5 + H^+): 302.14002, found: 302.13956 with a deviation of only 1.53 ppm.

***N*-benzyl-6-(5-chloro-1*H*-pyrrolo[2,3-*b*]pyridin-3-yl)pyrimidin-4-amine (7).** Final product **7** was

formed as described for **6** giving 0.010g of a white solid. ^{1}H NMR (300 MHz, $CDCl_3$) δ 8.7 (bs, 2H); 8.4 (bs, 2H); 8.3 (s, 1H); 7.4 (m, 5H); 4.8 (s, 2H). LCMS $[M + H]^+$ = 335.9; rt = 2.4 min (10-90% CH_3CN-water with 0.1% TFA.

N-Benzyl-6-bromopyridin-2-amine (52). This compound is commercially available from several sources. However, the compound was conveniently prepared as described here. A microwave vial was charged with benzylamine (700 mg; 5 mmol) and 2,6-dibromopyridine (238 mg, 1 mmol). The reaction mixture was stirred in the microwave at 150°C for three times for ten minutes each. The reaction mixture was diluted with diethyl ether (50 ml), washed with 10% aqueous citric acid, saturated aqueous sodium bicarbonate and brine. The organic phase was dried over magnesium sulfate and, after filtration, concentrated in vacuo to afford the title compound (300 mg, 100% yield) as an oil, which was used without further characterization. LCMS $[M + H]^+$ = 264.

***N*-benzyl-6-(5-chloro-1*H*-pyrrolo[2,3-*b*]pyridin-3-yl)pyridin-2-amine (9).** A microwave vial was charged with N-benzyl-6-bromopyridin-2-amine (300 mg, 1 mmol), 5 chloro-3-(4,4,5,5-tetramethyl-[l,3,2]dioxaborolan-2-yl)-l-(toluene-4-sulfonyl-lH-[2,3-b]pyridine (**50b**) (215 mg, 0.5 mmol), tetrakis(triphenylphosphine) palladium (60mg, 0.05 mmol), 2 M sodium hydroxide (0.75 ml) and dimethoxyethane (5 ml). The suspension was degassed with nitrogen. The reaction mixture was stirred in the microwave at 130°C for ten minutes. It was then diluted with ethyl acetate (60 ml), washed with brine twice, dried over magnesium sulfate and, after filtration, concentrated in vacuo. The compound was purified by flash chromatography (eluent: petroleum ether/ ethyl acetate 60/40) to afford 50 mg of the tosyl protected title compound. This residue was taken up in a mixture of methanol and tetrahydrofuran (1:3) and 1 M sodium hydroxide solution (1ml) was added to the reaction mixture,

which was then stirred at room temperature for three hours. The reaction mixture was then concentrated *in vacuo* and the residue was triturated with methanol. The suspension was filtered to afford the title compound (35mg, 10%). ^{1}H NMR (300 MHz, CD_3CN) δ 10.55 (s, 1H), 8.38 (m, 1H), 8.30 (m, 2H), 7.89 (t, 1H), 7.41 (m, 4H), 7.34 (m, 1H), 7.12 (d, 1H), 6.73 (d, 1H), 4.7-5.7 (s, 4H) 4.60 (s, 2H). LCMS $[M + H]^+$ = 335; rt = 4.1 min (10-90% CH_3CN-water with 0.1% TFA). HRMS $[M + H]^+$ calculated for (C19H15ClN4 + H^+): 335.10580, found: 335.10515 with a deviation of only 1.94 ppm.

***N*-benzyl-3-(5-chloro-1*H*-pyrrolo[2,3-*b*]pyridin-3-yl)aniline (10).** Final product **10** was formed as described for **6** starting from commercially available *N*-benzyl-3-bromoaniline (160 mg, 73%). ^{1}H NMR (400 MHz, DMSO-d6) δ 12.04 (s, 1H), 8.23 (d, J = 2.3 Hz, 1H), 8.06 (d, J = 2.3 Hz, 1H), 7.81 (d, J = 2.6 Hz, 1H), 7.41 (d, J = 7.0 Hz, 2H), 7.35 (dd, J = 10.3, 4.8 Hz, 2H), 7.24 (t, J = 7.3 Hz, 1H), 7.10 (t, J = 7.8 Hz, 1H), 6.90 (t, J = 1.8 Hz, 1H), 6.84 (d, J = 7.7 Hz, 1H), 6.51 (dd, J = 8.1, 1.6 Hz, 1H), 6.33 (t, J = 6.0 Hz, 1H), 4.34 (d, J = 5 .9 Hz, 2H) LCMS $[M + H]^+$ = 333.8; rt = 2.4 min (10-90% CH_3CN-water with 0.1% TFA).

(Scheme 2b) Compounds from Table 1.

3-(2-Methylthio-pyrimidin-4-yl)-1-(toluene-4-sulfonyl)-H-pyrrolo[2,3b] pyridine (53a: X = CH**).** A mixture of boronic ester **50a** (900 mg, 0.0023 mmol), 4-chloro-2-thiomethyl pyridine (341 mg, 0.0068 mmol) in 20 mL of DME was refluxed under nitrogen for 18 hours. Diluted with ethyl acetate and the organic layer was washed with water, brine, dried (Na_2SO_4) and concentrated in vacuo. The residue was subjected to flash chromatography (40% EtOAc in hexanes) to give 460 mg (51%) of the desired

product **53a**. ^{1}H NMR (300 MHz, $CDCl_3$) δ 8.8 (d, 1H), 8.7 (d, 2H), 8.4 (s, 1H), 8.1 (d, 2H); 7.2 (m, 4H); 2.6 (s, 3H); 2.3 (s, 3H).

3-(2-Methanesulfonyl-pyrimidin-4-yl)-1-(toluene-4-sulfonyl)-H-pyrrolo[2,3b] pyridine (54a). The above pyrimidine **53a** (460 mg, 0.0012 mmol) was dissolved in 20 mL of methanol-water (1:1), then oxone (2.14 g, 0.0035 mmol) was added and the reaction was refluxed for 18 hours. The methanol was removed in vacuo and the aqueous was extracted with ethyl acetate. The organic phase was washed with water, brine and then dried (Na_2SO_4) and concentrated in vacuo. The residue was subjected to flash chromatography (40% EtOAc in hexanes) to give 160 mg (32%) of the desired product **54a**, which was used without further purification. LCMS $[M + H]^+ = 428.9$

Benzyl-[4-(1H-pyrrolo[2,3-b]pyridine-3-yl)-pyrimidin-2-yl]-amine (5). A solution of **54a** (20 mg, 0.047 mmol) and benzylamine (0.007 mL, 0.061 mmol) in 1 mL of ethanol was heated in a seal tube at 80°C for 18 hours. The solvent was removed in vacuo and the crude product was purified by preparative TLC (50% EtOAc/ 50% hexanes) to give 20 mg of intermediate product, which was deprotected with 2 mL of 3N NaOH in methanol for 4 hours. To evaporate to dryness, 2 mL of 3N HCl was added. Reverse phase HPLC (20-70% CH_3CN-water with 0.1% TFA (20 ml/min) gave 10 mg (75%) of desired product **5**. ^{1}H NMR (300 MHz, DMSO-d6) δ 8.7 (bs, 1H), 8.4 (bs, 1H), 8.25 (d, 1H), 8.1 (d, 1H), 7.4 (m, 2H), 7.25 (m, 3H), 7.2 (bs, 1H), 7.15 (bs, 1H), 4.7 (bs, 2H); LCMS $[M + H]^+ = 302.14$

***N*-benzyl-4-(5-chloro-1*H*-pyrrolo[2,3-*b*]pyridin-3-yl)pyrimidin-2-amine (8).** The compound was prepared according to the above procedure for compound **5**. *N*-benzyl-4-(5-chloro-1H-pyrrolo[5,4-b]pyridin-3-yl)pyrimidin-2-amine (trifluoroacetic acid (1)) (51 mg, 0.1097 mmol, 49.14%) ^{1}H NMR

(400 MHz, CD_3OD) δ 8.62 (br s, 1H), 8.60 (s, 1H), 8.29 (d, J = 2.2 Hz, 1H), 8.07 (d, J = 6.5 Hz, 1H), 7.47 (d, J = 7.6 Hz, 2H), 7.43 - 7.32 (m , 3H), 7.29 (t, J = 7.1 Hz, 1H), 4.83 (s, 2H). LCMS $[M + H]^+$ = 335.9; rt = 2.6 min (10-90% CH_3CN-water with 0.1% TFA). HRMS $[M + H]^+$ calculated for (C18H14ClN5 + H^+): 336.10104, found: 336.10051 with a deviation of only 1.61 ppm.

(Scheme 2a) Compound from table 2.

2-(5-chloro-1*H*-pyrrolo[2,3-*b*]pyridin-3-yl)-5-fluoro-*N*-isopropylpyrimidin-4-amine (11). A solution of 2-isopropylamine (0.27 mL, 3.12 mmol) and 2,4-dichloro-5-fluoropyrimidine (518 mg, 3.12 mmol) and DIPEA (0.790 mL, 4.6 mmol) in 2 mL of isopropanol was heated at 90°C in a sealed tube overnight. Allowed to cool and the volatile removed *in vacuo*. The residue was dissolved in ethyl acetate and washed twice with water, dried (Na_2SO_4) and concentrated *in vacuo* to provide a brown oil that was used directly for the next step.

A microwave vial was charged with 2-chloro-5-fluoro-*N*-isopropylpyrimidin-4-amine (85 mg, 0.45 mmol) from previous step, 5-chloro-3-(4,4,5,5-tetramethyl-[l,3,2]dioxaborolan-2-yl)-l-(toluene-4-sulfonyl-lH-[2,3-b]pyridine (**50b**) (146 mg, 0.347 mmol), tetrakis(triphenylphosphine)palladium (39 mg, 0.035 mmol), 2 M K_2CO_3 (0.52ml) and dimethoxyethane (4 ml). The suspension was degassed with nitrogen. The reaction mixture was stirred in the microwave at 130°C for 15 minutes. The compound was purified by flash chromatography (0 to 45% ethyl acetate / hexanes) to afford the tosyl protected title compound. This residue was taken up in a mixture (5 mL) of methanol and tetrahydrofuran (1:3)

and 2 M sodium hydroxide solution (1ml) was added to the reaction mixture, which was then stirred at room temperature for two hours. Trituration from TFA/acetonitrile provided after filtration 30 mg (28%; 2-steps) of desired product **11** as a white solid. ^{1}H NMR (400 MHz, DMSO-d6) δ 12.79 – 12.42 (m, 1H), 8.63 (d, J = 2.4 Hz, 1H), 8.45 – 8.09 (m, 3H), 4.43 (dq, J = 13.4, 6.6 Hz, 1H), 1.29 (d, J = 6.6 Hz, 6H). ^{13}C NMR (400 MHz, DMSO-d6) δ 148.04, 142.35, 131.89, 129.04, 124.61, 119.27, 43.36, 22.49. LCMS $[M + H]^+$ = 306.46; rt = 4.8 min (1-99% CH_3CN-water with 0.1% TFA). HRMS $[M + H]^+$ calculated for (C14H13ClFN5 + H^+): 306.091628, found: 306.09043 with a deviation of only 3.91 ppm.

2-(5-chloro-1*H*-pyrrolo[2,3-*b*]pyridin-3-yl)-*N*-cyclopropyl-5-fluoropyrimidin-4-amine (12). Title compound was prepared according to the procedure detailed for **11**, using cyclopropylamine as starting material, to provide 50 mg of an off white solid. ^{1}H NMR (400 MHz, $CDCl_3$) δ 9.16 (s, exchanged with D_2O, 1H), 9.07 (d , J = 2.0Hz, 1H), 8.30 (d, J=2.4 Hz, 1H), 8.17 (d, J=2.4 Hz, addition of D_2O changed to s, 1H), 8.07 (d, J=3.6 Hz, 1H), 5.28 (s, exchanged with D_2O, 1H), 2.98-2.95 (m, 1H), 1.05-1.00 (q, 2H), 0.75-0.71 (m, 2H). HRMS $[M + H]^+$ calculated for (C14H11ClFN5 + H^+): 335.1058008, found: 335.10515 with a deviation of only 1.94 ppm.

2-(5-chloro-1*H*-pyrrolo[2,3-*b*]pyridin-3-yl)-*N*-cyclohexyl-5-fluoropyrimidin-4-amine (13). Title compound was prepared according to the procedure detailed for **11**, using cyclohexylamine as starting material, to provide 30 mg (25%; 2-steps) of the desired product **13**. ^{1}H NMR (400 MHz, DMSO-d6) δ 0.85 (1H, m), 1.48 (4H, m), 1.68 (1H, d), 1.81 (2H, m), 2.04 (2H, m), 4.03 (1H, m), 7.49 (1H, d), 8.13 (1H, s), 8.19 (1H, s), 8.29 (1H, s), 8.73 (1H, s), 12.21 (1H, s). LCMS $[M + H]^+$ = 346.43; rt = 5.25 min (10-100% CH_3CN-water with 0.1% TFA).

2-(5-chloro-1*H*-pyrrolo[2,3-*b*]pyridin-3-yl)-*N*-cyclohexylpyrimidin-4-amine (14). Title compound was prepared according to the procedure detailed for **11**, using cyclohexylamine as starting material, to provide 18.4 mg of a white solid. ^{1}H NMR (300 MHz, CDCl3) δ 10.84 (s, 1 H), 8.91 (d, J = 2.2 Hz, 1 H), 8.29 - 8.14 (m, 3 H), 6.13 (d, J = 5.9 Hz, 1 H), 4.96 (s, 1 H), 3.86 (s, 1 H), 2.15 -1.48 (m, 10 H). LCMS $[M + H]^+$ = 328.2; rt = 2.07 min (10-90% CH_3CN-water with 0.1% TFA). HRMS $[M + H]^+$ calculated for (C17H18ClN5 + H^+): 328.13235, found: 328.13112 with a deviation of only 3.75 ppm.

2-(5-chloro-1*H*-pyrrolo[2,3-*b*]pyridin-3-yl)-*N*-cyclohexyl-5-fluoro-*N*-methylpyrimidin-4-amine (15). Title compound was prepared according to the procedure detailed for **11**, using N-Me cyclohexylamine as starting material, to provide 18.4 mg of a white solid. ^{1}H NMR (300 MHz, CDCl3) δ 10.02 (br s, 1H), 8.81 (d, 1H), 8.31 (d, 1H), 8.29 (br s, 1H), 8.07 (d, 1H), 4.58 (m, 1H), 3.17 (d, 3H), 1.94-1.51 (m, 10 H). LCMS $[M + H]^+$ = 360.2; rt = 3.18 min (10-90% CH_3CN-water with 0.1% TFA).

2-(5-chloro-1*H*-pyrrolo[2,3-*b*]pyridin-3-yl)-5-fluoro-*N*-(tetrahydro-2*H*-pyran-4-yl)pyrimidin-4-amine (16). Title compound was prepared according to the procedure detailed for **11**, using tetrahydro-2*H*-pyran-4-amine as starting material, to provide, after chromatography of final product (0 to 100% ethyl acetate/hexanes), 55 mg (27%; 2-steps) of the desired product **16** as an off white solid. ^{1}H NMR (400 MHz, DMSO-d6) δ 12.79 – 12.42 (m, 1H), 8.63 (d, J = 2.4 Hz, 1H), 8.45 – 8.09 (m, 3H), 4.43 (dq, J = 13.4, 6.6 Hz, 1H), 1.29 (d, J = 6.6 Hz, 6H). ES^+ = 348.68; rt = 4.42 min (10-100% CH_3CN-water with 0.1% TFA). HRMS $[M + H]^+$ calculated for (C16H15ClFN5O + H^+): 348.102193, found: 348.10078 with a deviation of only 4.06 ppm.

2-(5-chloro-1*H*-pyrrolo[2,3-*b*]pyridin-3-yl)-5-fluoro-*N*-(piperidin-4-yl)pyrimidin-4-amine (17).

Title compound was prepared according to the procedure detailed for **11**, using *tert*-butyl 4-aminopiperidine-1-carboxylate as starting material, to provide, after the removal of the Boc with TFA/ CH_2Cl_2 at rt for 2h, the crude desired product. Reverse phase preparative chromatography (10-80% CH_3CN-water with 0.1% TFA) purification of final product, gave 20 mg (36%; 2-steps) of the desired product **17** as an off white solid. ^{1}H NMR (400 MHz, DMSO-d6) δ 1.67 (2H, m), 1.96 (2H, d), 3.49 (2H, t), 3.96 (2H, d), 4.30 (1H, m), 7.62 (1H, d), 8.18 (1H, s), 8.22 (1H, s), 8.29 (1H, s), 8.72 (1H, s), 12.36 (1H, s). LCMS $[M + H]^+$ = 347.4; rt = 3.5 min (10-100% CH_3CN-water with 0.1% TFA). HRMS $[M + H]^+$ calculated for (C16H16ClFN6 + H^+): 347.118177, found: 347.11708 with a deviation of only 3.16 ppm.

2-(5-chloro-1*H*-pyrrolo[2,3-*b*]pyridin-3-yl)-*N*-(cyclohexylmethyl)-5-fluoropyrimidin-4-amine (18). Title compound was prepared according to the procedure detailed for **11**, using cyclohexylmethanamine as starting material, to provide, after chromatography of final product (0 to 100% EtOAc-hexanes), 60 mg (29%; 2-steps) of the desired product **18** as an off white solid. ^{1}H NMR (400 MHz, DMSO-d6) δ 12.81 – 12.50 (m, 1H), 8.66 (d, J = 2.6 Hz, 1H), 8.45 – 8.25 (m, 3H), 3.39 (t, J = 6.5 Hz, 2H), 2.0 –1.41 (m, 6H), 1.30– 0.82 (m, 5H). ^{13}C NMR (400 MHz, DMSO-d6) δ 147.72, 142.38, 128.91, 124.88, 119.44, 42.20, 37.11, 31.37, 26.72, 26.01. LCMS $[M + H]^+$ = 360.46; rt = 5.39 min (10-100% CH_3CN-water with 0.1% TFA). HRMS $[M + H]^+$ calculated for (C18H19ClFN5 + H^+): 360.138578, found: 360.13722 with a deviation of only 3.77 ppm.

2-(5-chloro-1*H*-pyrrolo[2,3-*b*]pyridin-3-yl)-5-fluoro-*N*-((tetrahydro-2*H*-pyran-4-yl)methyl) pyrimidin-4-amine (19). Title compound was prepared according to the procedure detailed for **11**, using (tetrahydro-2*H*-pyran-4-yl)methanamine as starting material, to provide, after chromatography of

final product (0 to 100% EtOAc-hexanes), 19 mg (14%; 2-steps) of the desired product **19** as a yellow solid. ^{1}H NMR (400 MHz, DMSO-d6) δ 12.31 (d, J = 2.2 Hz, 1H), 8.70 (dd, J = 2.4, 1.0 Hz, 1H), 8.25 (dd, J = 2.5, 1.0 Hz, 1H), 8.18 (d, J = 2.4 Hz, 1H), 8.11 (dd, J = 4.0, 0.9 Hz, 1H), 7.78 (t, J = 5.8 Hz, 1H), 3.84 (d, J = 9.5 Hz, 2H), 3.38 (t, J = 6.5 Hz, 2H), 3.23 (d, J = 11.1 Hz, 2H), 1.69 (d, J = 12.5 Hz, 2H), 1.25 (dd, J = 12.6, 4.4 Hz, 2H). LCMS $[M + H]^+$ = 361.0; rt = 4.5 min (10-100% CH_3CN-water with 0.1% TFA). HRMS $[M + H]^+$ calculated for (C17H17ClFN5O + H^+): 362.117843, found: 362.11669 with a deviation of only 3.18 ppm.

2-(5-chloro-1*H*-pyrrolo[2,3-*b*]pyridin-3-yl)-5-fluoro-*N*-((1-methylpiperidin-4-yl)methyl)pyrimidin-4-amine (20). Title compound was prepared according to the procedure detailed for **11**, using (1-methylpiperidin-4-yl) methanamine as starting material, to provide, after chromatography of final product (0 to 100% ethyl acetate/hexanes), 10 mg (10%; 2-steps) of the desired product **20** as a yellow solid. ^{1}H NMR (400 MHz, DMSO-d6) δ 1.14 - 1.24 (2H, m), 1.75 - 1.80 (5H, m), 2.11 (3H, s), 2.75 (2H, d), 3.40 (2H, t), 7.80 (1H, t), 8.13 (1H, d), 8.20 (1H, s), 8.28 (1H, d), 8.73 (1H, d), 12.35 (1H, s). LCMS $[M + H]^+$ = 375.0; rt = 3.95 min (10-100% CH_3CN-water with 0.1% TFA). HRMS $[M + H]^+$ calculated for (C18H20ClFN6 + H^+): 375.149477, found: 375.14795 with a deviation of only 4.07 ppm.

2-((2-(5-chloro-1*H*-pyrrolo[2,3-*b*]pyridin-3-yl)-5-fluoropyrimidin-4-yl)amino)-2-methylpropan-1-ol (21). A solution of (2*S*,6*R*)-2,6-dimethylpiperazine (1.2g, 10 mmol) and 2,4-dichloropyrimidine (1.49g, 10 mmol) and DIPEA (3.5 mL) in 3.5 mL of isopropanol was heated to reflux for 3 hours. Allowed to cool and the volatile removed *in vacuo*. The residue was suspended in ethyl acetate (100 mL) and heated with 10 mL of acetic anhydride and 3 mL of N-methyl morpholine and stirred overnight at room temperature. The reaction mixture was washed with satd' $NaHCO_3$, then brine and the organic

phase dried with Na_2SO_4. Concentrated *in vacuo* to give 2.3 g of a crude gummy solid that was subjected to chromatography (5% CH_3OH-CH_2Cl_2) providing 0.58 g of desired intermediate that was used directly for the next step.

A microwave vial was charged with 1-((2*S*,6*R*)-4-(2-chloropyrimidin-4-yl)-2,6-dimethylpiperazin-1-yl)ethan-1-one (32 mg, 0.13 mmol) from previous step, 5-chloro-3-(4,4,5,5-tetramethyl-[l,3,2]dioxaborolan-2-yl)-l-(toluene-4-sulfonyl-lH-[2,3-b]pyridine (**50b**) (43 mg, 0.10 mmol), tetrakis(triphenylphosphine)palladium (20 mg, 0.025 mmol), 2 M K_2CO_3 (0.5ml) and dimethoxyethane (4 ml). The suspension was degassed with nitrogen. The reaction mixture was stirred in the microwave at 140°C for 20 minutes. The compound was filtered over celite and concentrated to afford the tosyl protected title compound. This residue was dissolved in a mixture 3 mL of THF and 1 mL of 1 M lithium hydroxide solution, which was then microwaved at 150°C for 5 minutes. Chromatography (30 to 100% ethyl acetate/hexanes) provided 12 mg (30%; 2-steps) of desired product **21** as a white solid. ^{1}H NMR (500 MHz, CD_3OD) δ 8.68 (d, J = 2.2 Hz, 1H), 8.50 (s, 1H), 8.40 (d, J = 2.3 Hz, 1H), 8.17 (d, J = 7.6 Hz, 1H), 7.08 (d, J = 7.5 Hz, 1H), 3.58 (bs, 4H), 2.22 (s, 3H), 1.36 (bs, 6H). ES^+ = 385.1; rt = 1.6 min (10-90% CH_3CN-water with 0.1% TFA). HRMS $[M + H]^+$ calculated for (C19H21ClN6O + H^+): 385.153814, found: 385.15248 with a deviation of only 3.46 ppm.

(Scheme 3) Compound from table 3.

Representative procedures for synthesis of compounds in Table 3

Synthesis of 2-((2-(5-chloro-1*H*-pyrrolo[2,3-*b*]pyridin-3-yl)-5-fluoropyrimidin-4-yl)amino)-2-methyl-*N*-(2,2,2-trifluoroethyl)propanamide (44).

***tert*-butyl 2-(2,2,2-trifluoroethylcarbamoyl)propan-2-ylcarbamate**. Boc-N-2-methylpropanoic acid **M** (aa = $C(CH_3)_2$) (14.6 g, 72.1 mmol), HATU (27.4 g, 72.1 mmol), diisopropylethylamine (18.8 mL, 108.1 mmol) and trifluoroethylamine hydrochloride (14.6 g, 108.1 mmol) were dissolved in 100mL of DMF and stirred at rt for 16 h. The reaction mixture was poured into water (1 L) and the pH was adjusted to 4 with 1N HCl. The aqueous phase was extracted with MBTE (2X 1L) and the combined organic phases was washed with satd' $NaHCO_3$, water and brine. The organic layer was dried Na_2SO_4 and concentrated in vacuo to provide 15.11g (78%) a white solid that was used directly for the next step. ^{1}H NMR (400 MHz, CD_3OD) δ 3.90 - 3.80 (m, 2H), 1.41 (s, 9H), 1.40 (s, 6H).

2-amino-*N*-(2,2,2-trifluoroethyl)-2-methylpropanamide (**N**).

The white solid Boc-amide (15.11g) was dissolved in 75 mL of CH_2Cl_2. 37 mL of TFA was slowly added and the reaction mixture was stirred for 1h at rt. The reaction mixture was concentrated *in vacuo* to an oil that was diluted with 100 mL of ether and evaporated to dryness to remove the residual TFA. Two more dissolution/evaporation cycles were necessary to remove excess TFA and provided the desired amine peptide **N** quantitatively as the TFA salt. This intermediate was used directly for the next step. ^{1}H NMR (400 MHz, CD_3OD) δ 3.96 (q, J = 9.3 Hz, 2H), 1.58 (s, 6H).

2-(2-chloro-5-fluoropyrimidin-4-ylamino)-*N*-(2,2,2-trifluoroethyl)-2-methylpropanamide (**Q:** Z = CF).

Amine **N** (12.37 g, 44 mmol) and DIEA (38 mL, 220 mmol) were dissolved in 125 mL of DMF. 5-Fluoro-2,4-dichloropyrimidine (7.4 g, 44 mmol) was then added and the reaction mixture was stirred at rt for 8 h. The reaction mixture was poured into water (600 mL) and extracted with MBTE (2 x 200 mL)

after adjusting the pH to 4-5 with 1N HCl. The combined organics were washed with water, brine, dried and filtered. And concentrated in vacuo to a crude solid. The residue was subjected to chromatography on the ISCO (120g column; grad 0%-80% EtOAc in Hexanes) to provide 4.38 g (32%) of the desired product **Q** (Z = CF**)**. H NMR (400 MHz, CD_3OD) δ 7.97 (d, J = 3.4 Hz, 1H), 3.83 (q, J = 9.3 Hz, 2H), 1.60 (s, 6H). LCMS $[M + H]^+$ = 315.07; rt = 0.65 min (10-90% CH_3CN-water with 0.1% TFA).

2-(2-(5-Chloro-1-tosyl-1H-pyrrolo[2,3-b]pyridin-3-yl)-5-fluoropyrimidin-4-ylamino)-2-methyl-N-(2,2,2-trifluoroethyl)propanamide. A 1-L, four-necked, round-bottomed flask was charged with 11.86 g (27.4 mmol) of **50b**, 8.54 g (27.1 mmol) of 2-(2-chloro-5-fluoropyrimidin-4-ylamino)-2-methyl-N-(2,2,2-trifluoroethyl)propanamide (**Q:** Z = CF), 200 mL of DME, 100 mL of 2 M Na_2CO_3. The mixture was degassed with a stream of nitrogen gas for 20 minutes and 2.19 g (1.89 mmol) of $Pd(PPh_3)_4$ was added. The mixture was heated to reflux overnight, cooled, diluted with water and extracted with EtOAc. The organic extract was dried ($MgSO_4$), and evaporated in vacuo. The crude product was triturated with MBTE to afford 10.48 g (66%) of the desired coupled product as an off-white solid. ^{1}H NMR (500 MHz, $CDCl_3$) δ 8.69 (d, 1H), 8.42 (s, 1H), 8.37 (d, 1H), 8.18 (d, 1H) 8.08 (d, 2H), 6.57 (br t, 1H), 5.40 (s, 1H), 3.95 (m, 1H), 2.38 (s, 3H), 1.73 (s, 6H).

2-(2-(5-Chloro-1H-pyrrolo[2,3-b]pyridin-3-yl)-5-fluoropyrimidin-4-ylamino)-2-methyl-N-(2,2,2-trifluoroethyl)propanamide (44). A 5L four-necked, round-bottomed flask equipped with an overhead stirrer was charged with 350.1 g (598 mmol) of 2-(2-(5-Chloro-1-tosyl-1H-pyrrolo[2,3-b]pyridin-3-yl)-5-fluoropyrimidin-4-ylamino)-2-methyl-N-(2,2,2-trifluoroethyl)propanamide, 2L of THF and then 1L of water. To this mixture was added 130.3 g (3.10 mol) of LiOH. The mixture was stirred at room temperature overnight, acidified with 1N HCl, and extracted with EtOAc. The extract was washed with

sat. aq. $NaHCO_3$, dried ($MgSO_4$), and filtered over a plug of silica gel. The plug was eluted with 25% EtOAc/CH_2Cl_2 and the filtrate was evaporated in vacuo to afford 199.6 g (77%) of **9** as a white solid. ^{1}H NMR (400 MHz, DMSO-d6) δ 12.29 (d, J = 2.8 Hz, 1H), 8.65 (dd, J = 2.4, 0.5 Hz, 1H), 8.36 (t, J = 6.4 Hz, 1H), 8.30 – 8.15 (m, 2H), 8.02 (d, J = 2.8 Hz, 1H), 7.62 (s, 1H), 3.79 – 3.67 (m, 2H), 1.53 (s, 6H). ^{13}C NMR (400 MHz, DMSO-d6) δ 175.56, 150.88, 147.69, 141.73, 131.26, 129.39, 124.33, 119.27, 57.29, 25.61. LCMS $[M + H]^+$ = 441.2; rt = 2.46 min (10-90% CH_3CN-water with 0.1% TFA).

(S)-2-((2-(5-chloro-1H-pyrrolo[2,3-b]pyridin-3-yl)-5-fluoropyrimidin-4-yl)amino)-N-(2,2,2-trifluoroethyl)propanamide (22). To a stirred solution of Boc-alanine **M** (aa = L-Ala; 3.8 g, 0.02 mol), EDC (4.63 g, 0.024 mol), HOBt (4.0 g, 0.026 mol), DIEA (10.5 mL, 0.06 mol) in 100 mL of CH_2Cl_2 is added trifluoroethylamine HCl (2.92 g, 0.022 mol). The reaction mixture is stirred for 16 h. It is concentrated to dryness and redissolved in EtOAc, washed successively with 0.5N HC1, saturated aqueous solution of $NaHCO_3$ and brine. The organic layer is dried (Na_2SO_4) and concentrated *in vacuo* to give 5.4g (98%) of a white solid, which was used directly for the next step.

The white solid (5.32 g, 0.0197 mol) was treated with a 1:1 mixture of CH_2Cl_2/TFA at rt for 45 min. Concentration to dryness gives the intermediate amine **N** as the TFA salt, which was used directly in the next step without further purification. A mixture of 5-fluoro-2,4-dichloropyrimidine (3.28 g, 0.0197 mol), the crude amine **N** (5.25 g, 0.0197 mol) and DIEA (10.27 mL, 0.059 mol) are stirred in isopropanol at rt for 16 h. The reaction mixture is concentrated *in vacuo* and redissolved in EtOAc, washed successively with 0.5N HCl, saturated aqueous solution of $NaHCO_3$ and brine. The organic layer is dried (Na_2SO_4) and concentrated *in vacuo* to give a crude oil that is subjected to chromatography (50% EtOAc / 50% hexanes) to yield the desired compound **Q** (Z = CF) which is used directly for the

next step.

A mixture of 1*H*-pyrrolo[2,3-*b*]pyridine boronate **50b** (X = CCl) (150 mg, 0.33 mmol, **Q** (Z = CF, 150 mg, 0.5 mmol), $Pd(Ph_3P)_4$ (30 mg, 0.026 mmol) and sodium carbonate 2 M (600 uL) in 4 mL of DME is microwaved at 140°C for 30 minutes. The reaction mixture is filtered through a short pad of silica gel with 30% EtOAc-70% hexanes as eluent to provide, after concentration to dryness, the crude intermediate that is used directly for the next step.

The crude intermediate is dissolved in 5 mL of dry methanol and 1 mL of sodium methoxide in methanol 25% was added. The reaction mixture is stirred at 60°C for 1 h and quenched with 6N HC1 (800 uL). The mixture was concentrated *in vacuo* and purified by reverse phase HPLC (10-60 CH_3CN/ water w/0.5% TFA) to provide 40 mg (27%; from **50b**) of **22**. DMSO d6 12.4 (bs, 1H); 8.8 (t, 1H); 8.7 (s, 1H); 8.3 (s, 2H); 8.2 (s, 1H); 7.9 (bs, 1H); 4.7 (q, 1H); 4.0 (m, 2H); 1.3 (d, 3H). LCMS $[M + H]^+$ = 416.19; rt = 2.3 min (10-90% CH_3CN-water with 0.1% TFA). HRMS $[M + H]^+$ calculated for (C16H13ClF4N6O + H^+): 417.084826, found: 417.08344 with a deviation of only 3.32 ppm.

2-((2-(5-chloro-1H-pyrrolo[2,3-b]pyridin-3-yl)pyrimidin-4-yl)amino)-N-(2,2,2-trifluoroethyl)acetamide (23). This compound was prepared from Boc-glycine **M** (aa = Gly) as for compound **44** using chloropyrimidine **Q** (Z = CH) and 5-chloro-1*H*-pyrrolo[2,3-*b*]pyridine **50a** (X = CCl) to provide 5.8 mg of **23** as a white solid. ^{1}H NMR (500 MHz, DMSO-d6) δ 12.97 (s, 1H), 9.30 (bs, 1H), 8.92 (s, 1H), 8.61 (s, 1H), 8.56 (s, 1H), 8.40 (d, J = 2.3 Hz, 1H), 8.19 (d, J = 2.1 Hz, 1H), 6.71 (s, 1H), 4.32 (s, 2H), 4.01 - 3.94 (m, 2H). LCMS $[M + H]^+$ = 385.1; rt = 1.6 min (10-90% CH_3CN-water with 0.1% TFA).

(S)-2-((2-(5-chloro-1H-pyrrolo[2,3-b]pyridin-3-yl)-5-fluoropyrimidin-4-yl)amino)-N-(2,2,2-trifluoroethyl)pentanamide (24). This compound was prepared from Boc-norvaline **M** (aa = (S)-Nor) as for compound **44** using chloropyrimidine **Q** (Z = CF) and 5-chloro-1*H*-pyrrolo[2,3-*b*]pyridine **50b** (X = CCl) to provide 17.4 mg of **24** as a white solid. ^{1}H NMR (500 MHz, CD_3OD) δ 12.4 ppm (s, 1H), 8.8 (t, 1H), 8.7 (s, 1H), 8.3 (m, 3H), 7.8 (bs, 1H), 4.6 (q, 1H), 3.8-4.0 (m, 2H), 1.8 (m, 2H), 1.3-1.5 (m, 2H), 0.9 (t, 3H). LCMS $[M + H]^+$ = 445.1; rt = 2.7 min (10-90% CH_3CN-water with 0.1% TFA). HRMS $[M + H]^+$ calculated for (C18H17ClF4N6O + H^+): 445.1161262, found: 445.1149 with a deviation of only 2.75 ppm.

(S)-2-((2-(5-chloro-1H-pyrrolo[2,3-b]pyridin-3-yl)pyrimidin-4-yl)amino)-3-hydroxy-N-(2,2,2-trifluoroethyl)propanamide (25). This compound was prepared from Boc-serine **M** (aa = (S)-Ser) as for compound **44** using chloropyrimidine **Q** (Z = CH) and 5-chloro-1*H*-pyrrolo[2,3-*b*]pyridine **50b** (where X = CCl) to provide 3.0 mg of **25** as a white solid. ^{1}H NMR (500 MHz, CD_3OD) δ 8.85 and 8.80 (2s, 1H), 8.25-8.13 (m, 3 H), 7.12 (d, 1H), 4.63 (dd, 1H), 3.98 (d, 2H), 3.96-3.34 (m, 2H). LCMS $[M + H]^+$ = 414.7; rt = 1.7 min (10-90% CH_3CN-water with 0.1% TFA). HRMS $[M + H]^+$ calculated for (C16H14ClF3N6O2 + H^+): 415.0891625, found: 415.08823 with a deviation of only 2.25 ppm.

(S)-2-((2-(5-chloro-1H-pyrrolo[2,3-b]pyridin-3-yl)pyrimidin-4-yl)amino)-3-methoxy-N-(2,2,2-trifluoroethyl)propanamide (26). This compound was prepared from Boc-Methoxy serine **M** (aa = (S)-C(H)CH_2OCH_3) as for compound **44** using chloropyrimidine **Q** (Z = CH) and 5-chloro-1*H*-pyrrolo[2,3-*b*]pyridine **50b** (where X = CCl) to provide 4.5 mg of **26** as a white solid. ^{1}H NMR (500 MHz, CD_3OD) δ 3.41 (s, 3H), 3.73-4.01 (m, 4H), 5.01 (s, br., 1H), 7.32 (s, br, 1H), 8.29 (s, 1H), 8.40 (d, 1H), 8.45 (d,

1H), 8.65 (d, 1H). LCMS $[M + H]^+$ = 429.1; rt = 1.9 min (10-90% CH_3CN-water with 0.1% TFA). HRMS $[M + H]^+$ calculated for (C17H16ClF3N6O2 + H^+): 429.1048126, found: 429.10387 with a deviation of only 2.20 ppm.

(*R*)-2-((2-(5-chloro-1*H*-pyrrolo[2,3-*b*]pyridin-3-yl)pyrimidin-4-yl)amino)-3-(methylthio)-*N*-(2,2,2-trifluoroethyl)propanamide (27). This compound was prepared from Boc-Methyl cysteine **M** (aa = (S)-C(H)CH_2SCH_3) as for compound **44** using chloropyrimidine **Q** (Z = CH) and 5-chloro-1*H*-pyrrolo[2,3-*b*]pyridine **50b** (X = CCl) to provide 12 mg of **27** as a white solid. ^{1}H NMR (400 MHz, DMSO-d6) δ 12.8(br m,1H), 8.85(m,1H), 8.8(m,1H), 8.65 (s,1H), 8.3(d,1H), 8.25(1H), 7.75(br m,1H), 7.3(d,1H), 4.85(m,1H), 3.9(m,2H), 3.0(d ,2H), 2.2(s,3H). LCMS $[M + H]^+$ = 449.9; rt = 2.2 min (10-90% CH_3CN-water with 0.1% TFA). HRMS $[M + H]^+$ calculated for (C17H16ClF3N6OS + H^+): 445.08196, found: 445.08093 with a deviation of only 2.23 ppm.

(*S*)-1-(2-(5-chloro-1*H*-pyrrolo[2,3-*b*]pyridin-3-yl)-5-fluoropyrimidin-4-yl)-*N*-(2,2,2-trifluoroethyl)pyrrolidine-2-carboxamide (28). This compound was prepared from Boc-L-Proline **M** (aa = (S)-Pro) as for compound **44** using chloropyrimidine **Q** (Z = CF) and 5-chloro-1*H*-pyrrolo[2,3-*b*]pyridine **50b** (X = CCl) to provide 12.3 mg of **28** as a white solid. ^{1}H NMR (400 MHz, DMSO-d6) δ 12.4 (br s, 1H); 8.7 (dd, 1H); 8.65 (s, 1H); 8.25 (m, 2H); 8.2 (m, 1H); 4.8 (d, 1H); 4.0-3.8 (m, 4H); 2.3 (m, 1H); 2.05-1.9 (m, 3H). LCMS $[M + H]^+$ = 442.9; rt = 2.2 min (10-90% CH_3CN-water with 0.1% TFA). HRMS $[M + H]^+$ calculated for (C18H15ClF4N6O + H^+): 443.10047, found: 443.09942 with a deviation of only 2.38 ppm.

(*S*)-3-((2-(5-chloro-1*H*-pyrrolo[2,3-*b*]pyridin-3-yl)-5-fluoropyrimidin-4-yl)amino)-*N*-(2,2,2-trifluoroethyl)butanamide (29). This compound was prepared from Boc-(S)-aminobutanoic acid **M** (aa = (S)-C(H)MeCH$_2$) as for compound **44** using chloropyrimidine **Q** (Z = CF) and 5-chloro-1*H*-pyrrolo[2,3-*b*]pyridine **50b** (X = CCl) to provide 1.5 mg of **29** as a white solid. ^{1}H NMR (400 MHz, DMSO-d6) δ 12.5 (bs, 1H); 8.8 (s, 1H); 8.7 (t, 1H); 8.3 (s, 1H); 8.2 (m, 1H); 4.8 (sept, 1H); 3.9 (m, 2H); 2.7 (dd, 2H); 1.25 (d, 3H). LCMS $[M + H]^+$ = 430.9; rt = 2.0 min (10-90% CH$_3$CN-water with 0.1% TFA). HRMS $[M + H]^+$ calculated for (C17H15ClF4N6O + H$^+$): 431.1004762, found: 431.09945 with a deviation of only 2.38 ppm.

(*R*)-2-((2-(5-chloro-1*H*-pyrrolo[2,3-*b*]pyridin-3-yl)-5-fluoropyrimidin-4-yl)amino)-*N*-(2,2,2-trifluoroethyl)propanamide (30). This compound was prepared from unnatural Boc-R-alanine **M** (aa = (R)-C(H)Me) as for compound **44** using chloropyrimidine **Q** (Z = CF) and 5-chloro-1*H*-pyrrolo[2,3-*b*]pyridine **50b** (X = Cl) to provide 15 mg of **30** as a white solid. ^{1}H NMR (400 MHz, DMSO-d6) δ 8.70 (dd, 1H); 8.65 *s, 1H); 8.28 (m, 2H); 8.20 (m, 1H); 7.90 (m, 1H); 4.62 (m, 1H); 3.88 (m, 2H); 1.41 (d, 3H). LCMS $[M + H]^+$ = 417.0; rt = 2.4 min (10-90% CH$_3$CN-water with 0.1% TFA). HRMS $[M + H]^+$ calculated for (C16H13ClF4N6O + H$^+$): 417.0848261, found: 417.0838 with a deviation of only 2.46 ppm.

(*R*)-2-((2-(5-chloro-1*H*-pyrrolo[2,3-*b*]pyridin-3-yl)pyrimidin-4-yl)amino)-*N*-(2,2,2-trifluoroethyl)propanamide (31). This compound was prepared from unnatural Boc-R-alanine **M** (aa = (R)-C(H)Me) as for compound **44** using chloropyrimidine **Q** (Z = CH) and 5-chloro-1*H*-pyrrolo[2,3-*b*]pyridine **50b** (X = CCl) to provide 11 mg of **31** as a white solid. ^{1}H NMR (400 MHz, DMSO-d6) δ

8.92 (m , 1H); 8.60 (m, 2H); 8.32 (s, 1H); 8.18 (m, 1H); 6.65 (m, 1H); 6.72 (m, 1H); 4.80 (m, 1H); 4.00 (m, 2H); 1.42 (d, 3H). LCMS $[M + H]^+$ = 399.0; rt = 1.7 min (10-90% CH_3CN-water with 0.1% TFA). HRMS $[M + H]^+$ calculated for (C16H14ClF3N6O + H^+): 399.094248, found: 399.09351 with a deviation of only 1.85 ppm.

(*R*)-2-((2-(5-chloro-1*H*-pyrrolo[2,3-*b*]pyridin-3-yl)pyrimidin-4-yl)amino)-*N*-(2,2,2-trifluoroethyl)pentanamide (32). This compound was prepared from unnatural norvaline **M** (aa = (R)-C(H)*n*Pr) as for compound **44** using chloropyrimidine **Q** (Z = CH) and 5-chloro-1*H*-pyrrolo[2,3-*b*]pyridine **50b** (X = CCl) to provide 10.4 mg of **32** as a white solid. ^{1}H NMR (500 MHz, DMSO-d6) δ 13.0 ppm (bs, 1H), 9.0 (s, 1H), 8.6 (d, 2H), 8.4 (s, 1H), 8.2 (d, 1H), 6.7 (s, 1H), 4.8 (s, 1H), 3.8-4.2 (m, 3H), 1.9 (m, 2H), 1.4-1.5 (m, 2H), 0.9 (t, 3H). LCMS $[M + H]^+$ = 427.1; rt = 1.9 min (10-90% CH_3CN-water with 0.1% TFA). HRMS $[M + H]^+$ calculated for (C18H18ClF3N6O + H^+): 427.1255481, found: 427.12418 with a deviation of only 3.20 ppm.

(*R*)-2-((2-(5-chloro-1*H*-pyrrolo[2,3-*b*]pyridin-3-yl)pyrimidin-4-yl)amino)-*N*-(2,2,2-trifluoroethyl)pent-4-ynamide (33). This compound was prepared from (R)-Propagyl glycine **M** (aa = (R)-C(H)CH_2CHCH) as for compound **44** using chloropyrimidine **Q** (Z = CH) and 5-chloro-1*H*-pyrrolo[2,3-*b*]pyridine **50b** (Z = Cl) to provide 4.5 mg of **33** as a white solid. ^{1}H NMR (500 MHz, DMSO-d6) δ 12.95 (bs, 1H), 9.07 (s, 1H), 8.63 (s, 1H), 8.60 (s, 1H), 8.40 (d, J = 2.1 Hz, 1H), 8.20 (s, 1H), 6.75 (s, 1H), 4.99 (s, 1H), 4.05 - 3.83 (m, 2H), 2.98 (t, J = 2.4 Hz, 1H), 2.80 (d, J = 7.3 Hz, 2H). LCMS $[M + H]^+$ = 423.0; rt = 1.8 min (10-90% CH_3CN-water with 0.1% TFA). HRMS $[M + H]^+$ calculated for (C18H14ClF3N6O + H^+): 423.094248, found: 423.09315 with a deviation of only 2.60 ppm.

(S)-2-((5-fluoro-2-(5-fluoro-1H-pyrrolo[2,3-b]pyridin-3-yl)pyrimidin-4-yl)amino)-N-(2,2,2-trifluoroethyl)propanamide (38). This compound was prepared as for compound **44** using chloropyrimidine **Q** (Z = CF) and 5-fluoro-1*H*-pyrrolo[2,3-*b*]pyridine **50c** (X = CF) to provide 27 mg of **38** as a white amorphous solid. ^{1}H NMR (400 MHz, DMSO-d6) δ 12.5 (bs, 1H); 8.9 (t, 1H); 8.4 (d, 1H); 8.2 (m, 2H); 8.2 (bs, 1H); 4.8 (q, 1H); 4.0 (m, 2H); 1.5 (d, 3H). LCMS $[M + H]^+$ = 401.0; rt = 2.0 min (10-90% CH_3CN-water with 0.1% TFA). HRMS $[M + H]^+$ calculated for (C16H13F5N6O + H^+): 401.1143766, found: 401.11368 with a deviation of only 1.73 ppm.

(*S*)-2-((5-fluoro-2-(1*H*-pyrrolo[2,3-*b*]pyridin-3-yl)pyrimidin-4-yl)amino)-*N*-(2,2,2-trifluoroethyl)propanamide (39). This compound was prepared as for compound **44** using chloropyrimidine **Q** (Y = CF) and 1*H*-pyrrolo[2,3-*b*]pyridine **50a** (X = CH) to provide 8.1 mg (28%; 2-steps) of **39** as a white amorphous solid. ^{1}H NMR (500 MHz, DMSO-d6) δ 12.2 (bs, 1H); 8.8 dd, 1H); 8.65 (d, 1H); 8.3 (m, 2H); 8.2 (s, 1H); 8.15 (brs, 1H); 7.2 br s, 1H); 4.5 (m, 1H); 3.9 (m, 2H); 1.5 (d, 3H). LCMS $[M + H]^+$ = 383.0; rt = 1.6 min (10-90% CH_3CN-water with 0.1% TFA).

(S)-2-((5-fluoro-2-(5-methoxy-1H-pyrrolo[2,3-b]pyridin-3-yl)pyrimidin-4-yl)amino)-N-(2,2,2-trifluoroethyl)propanamide (40). This compound was prepared as for compound **44** using chloropyrimidine **Q** (Y = CF) and 5-methoxy-1*H*-pyrrolo[2,3-*b*]pyridine **50d** (X = COMe) to provide 31 mg of **40** as a white amorphous solid. ^{1}H NMR (400 MHz, DMSO-d6) δ 12.2 (bs, 1H); 8.7 (t, 1H); 8.4 (s, 1H); 8.2 (s, 1H); 8.1 (s, 1H); 8.0 (s, 1H); 4,8 (q, 1H); 3.9 (s, 3H); 3.85 (m, 2H); 1.15 (d, 3H). LCMS $[M + H]^+$ = 412.9; rt = 1.9 min (10-90% CH_3CN-water with 0.1% TFA). HRMS $[M + H]^+$ calculated for (C17H16F4N6O2 + H^+): 413.13436, found: 413.13331 with a deviation of only 2.55 ppm.

(R)-2-((5-fluoro-2-(5-methoxy-1H-pyrrolo[2,3-b]pyridin-3-yl)pyrimidin-4-yl)amino)-N-(2,2,2-trifluoroethyl)propanamide (41). This compound was prepared from unnatural Boc-R-alanine (where **M**; (aa) = (R)-Ala) as for compound **44** using chloropyrimidine **Q** (Z = CF) and 5-methoxy-1*H*-pyrrolo[2,3-*b*]pyridine **50d** (X = COMe) to provide 8 mg of **41** as a white solid. ^{1}H NMR (400 MHz, DMSO-d6) δ 8.66 (dd, 1H); 8.28 (m, 1H); 8.18 (s, 1H); 8.15 (m, 1H); 8.02 (m, 1H); 4.72 (m, 1H); 3.88 (s, 3H); 3.90 (m, 2H); 1.42 (d, 3H). LCMS $[M + H]^+$ = 412.9; rt = 1.8 min (10-90% CH_3CN-water with 0.1% TFA). HRMS $[M + H]^+$ calculated for (C17H16F4N6O2 + H^+): 413.1343631, found: 413.13332 with a deviation of only 2.52 ppm.

(R)-2-((5-fluoro-2-(7H-pyrrolo[2,3-d]pyrimidin-5-yl)pyrimidin-4-yl)amino)-N-(2,2,2-trifluoroethyl)propanamide (42). This compound was prepared from unnatural Boc-alanine **M** (aa = (R)-Ala) as for compound **44** using chloropyrimidine **Q** (Z = CF) and deazapurine **50e** (where X = N) to provide 35 mg of **42** as a white solid. ^{1}H NMR (400 MHz, DMSO-d6) δ 9.65 (s, 1H); 8.96 (s, 1H); 8.76 (dd, 1H); 8.35 (s, 1H); 8.30 (d, 1H); 7.92 (d, 1H); 4.63 (m, 1H); 3.88 (m, 2H); 1.45 (d, 3H). LCMS $[M + H]^+$ = 384; rt = 2.0 min (5-45% CH_3CN-water with 0.1% TFA). HRMS $[M + H]^+$ calculated for (C15H13F4N7O + H^+): 384.1190474, found: 384.11844 with a deviation of only 1.58 ppm.

Synthesis of (*R*)-2-((2-(5-chloro-1*H*-pyrrolo[2,3-*b*]pyridin-3-yl)pyrimidin-4-yl)amino)-3-methyl-*N*-(2,2,2-trifluoroethyl)butanamide (34).

***tert*-butyl (*R*)-1-(2,2,2-trifluoroethylcarbamoyl)-2-methylpropylcarbamate (N**). To a suspension of Boc-(R)-valine **M** (aa = (R)-C(H)CHMe_2, 25g, 0.115 mol), EDC (24.2 g, 0.127 mol), HOBT (4.65g,

0.034 mol) and trifluoroethylamine hydrochloride (17.14g, 0.127 mol) in 250 mL of THF at 0°C was added triethylamine (35.2 mL, 0.253 mol) maintaining the temperature below 25°C. The reaction mixture was stirred at rt for 16h. It was quenched with 250 mL of water and ethyl acetate (250 mL) was added followed by acidification to pH 4 with 1N HC. The layers were separated and the aqueous was back extracted with an additional 250 mL of EtOAc. The organics were combined and washed with satd' $NaHCO_3$, brine and then dried with Na_2SO_4. Filtered and concentrated *in vacuo* to provide 33.53g (98%) of monopeptide.

(*R*)-2-amino-*N*-(2,2,2-trifluoroethyl)-3-methylbutanamide)

Boc-(R)-valine amide **N** (33.53g, 0.112 mol) was dissolved in 250 mL of CH_2Cl_2. 30 mL of TFA was slowly added and the reaction mixture was stirred for 16h at rt. The reaction mixture was concentrated *in vacuo* to give an oil that was diluted with 300 mL of ether and evaporated to dryness to remove the residual TFA. Two more dissolution/evaporation cycles were necessary to remove most of the TFA and provided the desired amine peptide **N** quantitatively. This intermediate was used directly for the next step.

(*R*)-2-(2-chloropyrimidin-4-ylamino)-*N*-(2,2,2-trifluoroethyl)-3-methylbutanamide (**Q:** Z = CH).

Unprotected (R)-valine amide salt **N** (1.84g, 6 mmol) was dissolved in isopropanol (50 mL) and diisopropylethylamine (2.1 mL, 12.02 mmol). 2,4-Dichloropyrimidine (1.3 g, 6.01 mmol) was added and the reaction mixture was heated at 90°C for 16 h. Cooled to rt and the solvent was removed *in vacuo* to give a residue that was partitioned in a 1:1 mixture of EtOAc/ water (200mL). The pH was adjusted to 1 with 1 N HCl. Extracted with EtOAc. The organic layer was washed with water, brine, dried with Na_2SO_4, filtered and concentrated in vacuo. The oily solid was recrystallized in MBTE-CH_2Cl_2 mixture

to provide 1.09 g (60%) of the desired product **Q** (Z = CH). ^{1}H NMR (400 MHz, CD_3OD) δ 8.82 (t, J = 5.8 Hz, 1H), 7.90 (d, J = 5.8 Hz, 1H), 6.59 (d, J = 5.8 Hz, 1H), 4.42 (d, J = 6.4 Hz, 1H), 4.09 - 3.92 (m, 1H), 3.90 - 3.73 (m, 1H), 2.14 (dq, J = 13.6, 6.8 Hz, 1H), 1.02 (dd, J = 6.7, 5.2 Hz , 6H). LCMS [M + H]$^+$ = 310.95; rt = 0.64 min (0-95% CH_3CN-water with 0.1% TFA).

(*R*)-2-((2-(5-chloro-1*H*-pyrrolo[2,3-*b*]pyridin-3-yl)pyrimidin-4-yl)amino)-3-methyl-*N*-(2,2,2-trifluoroethyl)butanamide (34). This compound was prepared from boronic ester **50b** (X = CCl) and (*R*)-2-(2-chloropyrimidin-4-ylamino)-*N*-(2,2,2-trifluoroethyl)-3-methylbutanamide (**Q:** Z = CH) as for compound **44** to provide 297.6 mg of the desired product **34**. ^{1}H NMR (400 MHz, DMSO-d6) δ 12.30 (s, 1H), 8.78 (t, J = 6.3 Hz, 1H), 8.72 (s, 1H), 8.29 (s, 1H), 8.23 (d, J = 2.4 Hz, 1H), 8.08 (d, J = 5.9 Hz, 1H), 7.41 (d, J = 7.8 Hz, 1H), 6.45 (s, 1H), 4.52 (s, 1H), 3.99 (m, 1H), 3.90 – 3.70 (m, 1H), 2.08 (q, J = 6.8 Hz, 1H), 0.97 (d, J = 6.8 Hz, 6H). ^{13}C NMR (400 MHz, DMSO-d6) δ 173.00, 161.97, 141.38, 131.89, 129.39, 123.82, 119.89, 119.55, 30.67, 19.65. LCMS [M + H]$^+$ = 427.3; rt = 1.88 min (10-90% CH_3CN-water with 0.1% TFA). HRMS [M + H]$^+$ calculated for (C18H18ClF3N6O + H^+): 427.125548, found: 427.12388 with a deviation of only 3.90 ppm.

(*R*)-2-((2-(5-chloro-1*H*-pyrrolo[2,3-*b*]pyridin-3-yl)pyrimidin-4-yl)amino)-4-methyl-*N*-(2,2,2-trifluoroethyl)pentanamide (35). This compound was prepared from (R)-Isoleucine **M** (aa = (R)-C(H)CH_2iPr) as for compound **44** using chloropyrimidine **Q** (Z = CH) and 5-chloro-1*H*-pyrrolo[2,3-*b*]pyridine **50b** (X = CCl) to provide 13.7 mg of **35** as a white solid. ^{1}H NMR (400 MHz, DMSO-d6) δ 13.0 ppm (bs, 1H), 9.0 (t, 1H), 8.7 (s, 2H), 8.4 (s, 1H), 8.1 (d, 1H), 6.6 (d, 1H), 4.8 (t, 1H), 3.8-4.2 (m, 4H), 1.7 (bs, 2H), 1.0 (d, 3H), 0.9 (d, 3H). LCMS [M + H]$^+$ = 441.2; rt = 2.0 min (10-90% CH_3CN-water

with 0.1% TFA). HRMS [*M* + *H*]$^+$ calculated for (C19H20ClF3N6O + H$^+$): 441.1411981, found: 441.14025 with a deviation of only 2.15 ppm.

(*R*)-2-((2-(5-chloro-1*H*-pyrrolo[2,3-*b*]pyridin-3-yl)pyrimidin-4-yl)amino)-3-phenyl-*N*-(2,2,2-trifluoroethyl)propanamide (36). This compound was prepared from (R)-Phenylalanine **M** (aa = (R)-C(H)CH_2Ph) as for compound **44** using chloropyrimidine **Q** (Z = CH) and 5-chloro-1*H*-pyrrolo[2,3-*b*]pyridine **50b** (X = CCl) to provide 13.5 mg of **36** as a white solid. ^{1}H NMR (400 MHz, DMSO-d6) δ 13.0 ppm (bs, 1H), 9.2 ppm (t, 1H), 8.6 (s, 1H), 8.4 (s, 1H), 8.1 (d, 1H), 7.4 (d, 2H), 7.3 (t, 2H), 7.2 (d, 1H), 6.7 (d, 1H), 5.2 (t, 1H), 3.9-4.1 (m, 3H), 3.3 (m, 1H), 3.1 (t, 1H). LCMS [*M* + *H*]$^+$ = 475.23; rt = 2.0 min (10-90% CH_3CN-water with 0.1% TFA). HRMS [*M* + *H*]$^+$ calculated for (C22H18ClF3N6O + H$^+$): 475.12554, found: 475.12478 with a deviation of only 1.62 ppm.

(*R*)-2-((2-(5-chloro-1*H*-pyrrolo[2,3-*b*]pyridin-3-yl)-5-fluoropyrimidin-4-yl)amino)-3-(1*H*-imidazol-4-yl)-*N*-(2,2,2-trifluoroethyl)propanamide (37). This compound was prepared from (R)-Histidine **M** (aa = (R)-His) as for compound **44** using chloropyrimidine **Q** (Z = CF) and 5-chloro-1*H*-pyrrolo[2,3-*b*]pyridine **50b** (X = CCl) to provide 60 mg of **37** as a white solid. ^{1}H NMR (400 MHz, DMSO-d6) δ 12.0 (s, 1H), 10.7 (s, 1H), 8.57 (s, 1H), 8.42 (s, 2H), 8.39 (s, 1H), 8.28 (d, 1H), 7.90 (m, 1H), 7.75 (d, 1H), 7.28 (s, 1H), 5.22 (m, 1H), 3.96 (m, 2H), 3.61 (m, 1H), 3.41 (m, 1H) CD3CN. LCMS [*M* + *H*]$^+$ = 483.0; rt = 1.7 min (10-90% CH_3CN-water with 0.1% TFA). HRMS [*M* + *H*]$^+$ calculated for (C19H15ClF4N8O + H$^+$): 483.10662, found: 483.1059 with a deviation of only 1.50 ppm.

2-((2-(5-chloro-1*H*-pyrrolo[2,3-*b*]pyridin-3-yl)pyrimidin-4-yl)amino)-2-methyl-*N*-(2,2,2-trifluoroethyl)propanamide (43). This compound was prepared from Boc-N-2-methylpropanoic acid **M** (aa = $C(CH_3)_2$) as for compound **44** using chloropyrimidine **Q** (Z = CH) and 5-chloro-1*H*-pyrrolo[2,3-*b*]pyridine **50b** (X = CCl) to provide 3.54 g of **43** as a white solid. ^{1}H NMR (500 MHz, CD_3OD) δ 8.75 (d, J = 1.9 Hz, 1H), 8.55 (t, J = 5.9 Hz, 1H), 8.48 (s, 1H), 8.36 (d, J = 2.2 Hz, 1H), 8.06 (d, J = 7.2 Hz, 1H), 6.71 (d, J = 7.2 Hz, 1H), 3.85 (m, 2H), 1.75 (s, 6H) LCMS $[M + H]^+$ = 413.25; rt = 1.86 min (10-90% CH_3CN-water with 0.1% TFA). HRMS $[M + H]^+$ calculated for (C17H16ClF3N6O + H^+): 413.10989, found: 413.10834 with a deviation of only 3.77 ppm.

(*R*)-2-((2-(5-chloro-1*H*-pyrrolo[2,3-*b*]pyridin-3-yl)pyrimidin-4-yl)amino)-2-methyl-*N*-(2,2,2-trifluoroethyl)butanamide (45). This compound was prepared from (*R*)-2-((*tert*-butoxycarbonyl)amino)-2-methylbutanoic acid **M** (aa = (R)-$C(CH_3)CH_2CH_3$) as for compound **44** using chloropyrimidine **Q** (Z = CH) and 5-chloro-1*H*-pyrrolo[2,3-*b*]pyridine **50b** (X = Cl) to provide 13 mg of **45** as a white solid. ^{1}H NMR (500 MHz, DMSO-d6) δ 12.96 (s, 1H), 9.00 (s, 1H), 8.69 (s, 1H), 8.56 (s, 2H), 8.37 (d, J = 1.6 Hz, 1H), 8.18 (d, J = 6.7 Hz, 1H), 6.72 (s, 1H), 3.80 (dd, J = 9.8, 16.6 Hz, 2H), 2.12 - 1.93 (m, 2H), 1.59 (s, 3H), 0.87 (t, J = 7.5 Hz, 3H), 0.00 (TMS). LCMS $[M + H]^+$ = 427.1; rt = 1.8 min (10-90% CH_3CN-water with 0.1% TFA). HRMS $[M + H]^+$ calculated for (C18H18ClF3N6O + H^+): 427.12554, found: 427.12419 with a deviation of only 3.18 ppm.

(*R*)-2-((2-(7*H*-pyrrolo[2,3-*d*]pyrimidin-5-yl)pyrimidin-4-yl)amino)-2-methyl-*N*-(2,2,2-trifluoroethyl)butanamide (46). This compound was prepared from (*R*)-2-((*tert*-butoxycarbonyl)amino)-2-methylbutanoic acid **M** (aa = (R)-$C(CH_3)CH_2CH_3$) as for compound **44** using chloropyrimidine **Q** (Z = CH) and deazapurine **50e** (X = N) to provide 18 mg of **46** as a white solid. ^{1}H

NMR (500 MHz, DMSO-d6) δ 13.2 (bs, 1H), 9.57 (s, 1H), 8.98 (bs, 2H), 8.61 (bs, 2H), 8.23 (d, J = 6.8 Hz, 1H), 6.76 (s, 1H), 3.78 (bs, 2H), 2.13 - 2.07 (m, 1H), 1.97 - 1.93 (m, 1H), 1.59 (s, 3H), 0.88 (t, J = 7.5 Hz, 3H). LCMS $[M + H]^+$ = 394.2; rt = 1.2 min (10-90% CH_3CN-water with 0.1% TFA). HRMS $[M + H]^+$ calculated for (C17H18F3N7O + H^+): 394.15976, found: 394.15877 with a deviation of only 2.53 ppm.

(*R*)-2-((2-(1*H*-pyrrolo[2,3-*b*]pyridin-3-yl)pyrimidin-4-yl)amino)-2-methyl-*N*-(2,2,2-trifluoroethyl)butanamide (VX-509). This compound was prepared from (*R*)-2-((*tert*-butoxycarbonyl)amino)-2-methylbutanoic acid **M** (aa = (R)-$C(CH_3)CH_2CH_3$) as for compound **44** using chloropyrimidine **Q** (Z = CH) and 1*H*-pyrrolo[2,3-*b*]pyridine **50a** (X = H) to provide 8 g of **VX-509** as a white solid. ^{1}H NMR (400 MHz, DMSO-d6) δ 11.94 (d, J = 2.8 Hz, 1H), 8.68 (d, J = 7.8 Hz, 1H), 8.31 – 8.21 (m, 1H), 8.20 (dd, J = 4.7, 1.7 Hz, 1H), 8.09 (d, J = 5.9 Hz, 1H), 7.99 (d, J = 2.8 Hz, 1H), 7.26 (s, 1H), 7.10 (dd, J = 7.9, 4.7 Hz, 1H), 6.36 (s, 1H), 3.73 (ddd, J = 19.3, 9.6, 6.2 Hz, 1H), 2.04 (dd, J = 13.8, 7.3 Hz, 1H), 1.79 (dd, J = 13.8, 7.4 Hz, 1H), 0.78 (t, J = 7.5 Hz, 3H). ^{13}C NMR (400 MHz, DMSO-d6) δ 172.47, 160.76, 149.51, 143.33, 130.55, 129.36, 118.44, 116.91, 114.93, 59.83, 21.95, 8.9. LCMS $[M + H]^+$ = 393.3; rt = 1.6 min (10-90% CH_3CN-water with 0.1% TFA).

(*S*)-2-((2-(5-chloro-1*H*-pyrrolo[2,3-*b*]pyridin-3-yl)pyrimidin-4-yl)amino)-2-methyl-*N*-(2,2,2-trifluoroethyl)butanamide (47). This compound was prepared from (*S*)-2-((*tert*-butoxycarbonyl)amino)-2-methylbutanoic acid **M** (aa = (S)-$C(CH_3)CH_2CH_3$) as for compound **44** using chloropyrimidine **Q** (Z = CH) and 5-chloro-1*H*-pyrrolo[2,3-*b*]pyridine **50b** (X = CCl) to provide 5.1 mg of **47** as a white solid. ^{1}H NMR (300 MHz, DMSO-d6) δ 10.07 (s, 1H), 8.83 (d, 1H), 8.26 (d, 1H), 8.22 (d, 1H), 8.13 (d, 1H), 7.20 (m, 1H), 6.38 (d, 1H), 6.00 (s, 1H), 3.88 (m, 1H), 3.77 (m, 1H), 1.95 (m, 2H),

1.57 (s, 3H), 0.91 (t, 3H) CD3CN. LCMS $[M + H]^+ = 427.4$; rt = 1.8 min (10-90% CH_3CN-water with 0.1% TFA). HRMS $[M + H]^+$ calculated for (C18H18ClF3N6O + H^+): 427.12554, found: 427.12399 with a deviation of only 3.65 ppm.

(*R*)-2-((2-(1*H*-pyrrolo[2,3-*b*]pyridin-3-yl)pyrimidin-4-yl)amino)-2,3-dimethyl-*N*-(2,2,2-trifluoroethyl)butanamide (48). This compound was prepared from (*R*)-2-((*tert*-butoxycarbonyl)amino)-2,3-dimethylbutanoic acid **M** (aa = (R)-$C(CH_3)CH(CH_3)_2$)) as for compound **44** using chloropyrimidine **Q** (Z = CH) and 1*H*-pyrrolo[2,3-*b*]pyridine **50a** (X = H) to provide 4.8 g of **48** as a white solid. ^{1}H NMR (300 MHz, DMSO-d6) δ 9.89 (s, 1H), 8.79 (d, 1H), 8.27 (m, 1H), 8.19 (d, 1H), 8.10 (d, 1H), 7.18 (m, 2H), 6.49 (d, 1H), 5.80 (s, 1H), 3.97 (m, 1H), 3.59 (m, 1H), 1.53 (s, 3H), 1.02 (dd, 6H) CD3CN. LCMS $[M + H]^+ = 405.5$; rt = 1.72 min (10-90% CH_3CN-water with 0.1% TFA). HRMS $[M + H]^+$ calculated for (C19H21F3N6O + H^+): 407.18017, found: 407.17916 with a deviation of only 2.48 ppm.

(*R*)-2-((4-(1*H*-pyrrolo[2,3-*b*]pyridin-3-yl)-1,3,5-triazin-2-yl)amino)-2-methyl-*N*-(2,2,2-trifluoroethyl)butanamide (49). This compound was prepared from (*R*)-2-((*tert*-butoxycarbonyl)amino)-2-methylbutanoic acid **M** (aa = (R)-$C(CH_3)CH_2CH_3$) as for compound **44** using 2,4-dichloro-1,3,5-triazine **Q** (Z = N) and 1*H*-pyrrolo[2,3-*b*]pyridine **50a** (X = H) to provide 5.1 g of **49** as a white solid. ^{1}H NMR (500 MHz, CD_3OD) δ 9.14 (m, 0.25H), 8.95 (d, J = 6.7 Hz, 0.66H), 8.59 - 8.41 (m, 3.64 H), 7.45 (m, 1H), 3.84 (m, 2H), 2.21 - 2.18 (m, 1H), 2.05 - 2.02 (m, 1H), 1.67 (m, 3H), 0.97 (t, J = 7.3 Hz, 3H). LCMS $[M + H]^+ = 394.1$; rt = 2.16 min (10-90% CH_3CN-water with 0.1% TFA). HRMS $[M + H]^+$ calculated for (C17H18F3N7O + H^+): 394.15976, found: 394.15858 with a deviation of only 3.02 ppm.

Acknowledgements

The authors would like to thank David Lauffer and Alex Aronov for identifying early hits from the 1*H*-pyrrolo[2,3-*b*]pyridine class with JAK3 potency, Kenny Bonnano and Jacque Zwahlen for protein expression and cloning, respectively, Dean Boyall, Simon Everitt and Haley Binch for providing analogs from their previous kinase programs and Bill Markland for help in determining the minimal significant ratios. Also, the authors wish to thanks Ralph Stearns for helpful discussion and suggestions and Michael Clark, Janek Szychowski, Constantin Yannopoulos, and Louis Vaillancourt for proofreading the manuscript.

References

[1]Darnell, J. E. J.; Kerr, I. M.; Stark, G. R. Jak-STAT pathways and transcriptional activation in response to IFNs and other extracellular signaling proteins. *Science* **1994**, *264*, 1415–1421.

[2] Ghoreschi, K.; Laurence, A.; O'Shea, J. J. Janus kinases in immune cell signaling. *Immunol. Rev.* **2009**, *228*, 273–287.

[3] Johnston, J. A.; Bacon, C. M.; Riedy, M. C.; O'Shea, J. J. Signaling by IL-2 and related cytokines: JAKs, STATs and relationship to immunodeficiency. *J. Leukocyte Biol.* **1996**, *60*, 441–452.

[4] Oakes, S. A.; Candotti, F.; Johnston, J. A.; Chen, Y. Q.; Ryan, J. J.; Taylor, N.; Liu, X.; Henninghausen, L.; Notarangelo, L. D.; Paul, W. E.; Blaese, R. M.; O'Shea, J. J. Signaling via IL-2 and IL-4 in JAK3-deficient severe combined immunodeficiency lymphocytes: JAK3-dependent and independent pathways. *Immunity* **1996**, *5*, 605–615.

[5] Chen, M.; Cheng, A.; Chen, Y. Q.; Hymel, A.; Hanson, E. P.; Kimmel, L.; Minami, Y.; Taniguchi, T.; Changelian, P. S.; O'Shea, J. J. The amino terminus of JAK3 is necessary and sufficient for binding to the common gamma chain and confers the ability to transmit interleukin 2-mediated signals. *Proc. Natl. Acad. Sci. U.S.A.* **1997**, *94*, 6910–6915.

[6] Hofmann, S. R.; Ettinger, R.; Zhou, Y. J.; Gadina, M.; Lipsky, P.; Siegel, R.; Candotti, F.; O'Shea, J. J. Cytokines and their role in lymphoid development, differentiation and homeostasis. *Curr. Opin. Allergy Clin. Immunol.* **2002**, *2*, 495–506.

[7] Rochman, Y.; Spolski, R.; Leonard, W. J. New insights into the regulation of T cells by γ c family cytokines. *Nature Rev. Immunol.* **2009**, *9*, 480–490.

[8] Macchi, P.; Villa, A.; Giliani, S.; Sacco, M. G.; Frattini, A.; Porta, F.; Ugazio, A. G.; Johnston, J. A.; Candotti, F.; O'Shea, J. J. Mutations of Jak-3 gene in patients with autosomal severe combined immune deficiency (SCID). *Nature* **1995**, *377*, 65–68.

[9] Noguchi, M.; Rosenblatt, H. M.; Filipovich, A. H.; Adelstein, S.; Modi, W. S.; McBride, O. W.; Leonard, W. J. Interleukin-2 receptor gamma chain mutation results in X-linked severe combined immunodeficiency in humans. *Cell* **1993**, *73*, 147–157.

[10] Russell, S. M.; Tayebi, N.; Nakajima, H.; Riedy, M. C.; Roberts, J. L.; Aman, M. J.; Migone, T. S.; Noguchi, M.; Markert, M. L.; Buckley, R. H.; O'Shea, J. J.; Leonard, W. J. Mutation of Jak3 in a patient with SCID: essential role of Jak3 in lymphoid development. *Science* **1995**, *270*, 797–800.

[11] Pesu, M.; Candotti, F.; Husa, M.; Hofmann, S. R.; Notarangelo, L. D.; O'Shea, J. J. Jak3, severe combined immunodeficiency, and a new class of immunosuppressive drugs. *Immunol. Rev.* **2005**, *203*, 127–142.

[12] Changelian, P. S.; Flanagan, M. E.; Ball, D. J.; Kent, C. R.; Magnuson, K. S.; Martin, W. H.; Rizzuti, B. J.; Sawyer, P. S.; Perry, B. D.; Brissette, W. H.; McCurdy, S. P.; Kudlacz, E. M.; Conklyn, M. J.; Elliott, E. A.; Koslov, E. R.; Fisher, M. B.; Strelevitz, T. J.; Yoon, K.; Whipple, D. A.; Sun, J.; Munchhof, M. J.; Doty, J. L.; Casavant, J. M.; Blumenkopf, T. A.; Hines, M.; Brown, M. F.; Lillie, B. M.; Subramanyam, C.; Shang-Poa, C.; Milici, A. J.; Beckius, G. E.; Moyer, J. D.; Su, C.; Woodworth, T. G.; Gaweco, A. S.; Beals, C. R.; Littman, B. H.; Fisher, D. A.; Smith, J. F.; Zagouras, P.; Magna, H. A.; Saltarelli, M. J.; Johnson, K. S.; Nelms, L. F.; Des Etages, S. G.; Hayes, L. S.; Kawabata, T. T.; Finco-Kent, D.; Baker, D. L.; Larson, M.; Si, M. S.; Paniagua, R.; Higgins, J.; Holm, B.; Reitz, B.; Zhou, Y. J.; Morris, R. E.; O'Shea, J. J.; Borie, D. C. Prevention of organ allograft rejection by a specific Janus kinase 3 inhibitor. *Science* **2003**, *302*, 875–878.

[13] Kremer, J. M.; Bloom, B. J.; Breedveld, F. C.; Coombs, J. H.; Fletcher, M. P.; Gruben, D.; Krishnaswami, S.; Burgos-Vargas, R.; Wilkinson, B.; Zerbini, C. A.; Zwillich, S. H. The safety and efficacy of a JAK inhibitor in patients with active rheumatoid arthritis: Results of a double-blind, placebo-controlled phase IIa trial of three dosage levels of CP-690,550 versus placebo. *Arthritis Rheum.* **2009**, *60*, 1895–1905.

[14] Ghoreschi, K.; Laurence, A.; O'Shea, J. J. Selectivity and therapeutic inhibition of kinases: to be or not to be? *Nat. Immunol.* **2009**, *10*, 356–360.

[15] Cox L.; Cools J. JAK3 specific kinase inhibitors: when specificity is not enough. *Chem. Biol.* **2011,** *18*, 277–278.

[16] Fleischmann, R.; Cutolo, M.; Genovese, M. C.; Lee, E. B.; Kanik, K. S.; Sadis, S.; Connell, C. A.; Gruben, D.; Krishnaswami, S.; Wallenstein, G.; Wilkinson, B. E.l; Zwillich, S. H. Phase IIb dose-ranging study of the oral JAK inhibitor Tofacitinib (CP-690,550) or adalimumab monotherapy versus placebo in patients with active rheumatoid arthritis with an inadequate response to disease-modifying antirheumatic drugs. *Arthritis Rheum.* **2012**, *64*, 617–629.

[17] Thoma, G.; Nuninger, F.; Falchetto, R.; Hermes, E.; Tavares, G. A.; Vangrevelinghe, E.; Zerwes, H.-G. Identification of a potent Janus kinase 3 inhibitor with high selectivity within the Janus kinase family. *J. Med. Chem.* **2011**, *54*, 284–288.

[18] Lin, T. H.; Hegen, M.; Quadros, E.; Nickerson-Nutter, C. L.; Appell, K. C.; Cole, A. G.; Shao, Y.; Tam, S.; Ohlmeyer, M.; Wang, B.; Goodwin, D. G.; Kimble, E. F.; Quintero, J.; Gao, M.; Symanowicz, P.; Wrocklage, C.; Lussier, J.; Schelling, S. H.; Hewet, A. G.; Xuan, D.; Krykbaev, R.; Togias, J.; Xu, X.; Harrison, R.; Mansour, T.; Collins, M.; Clark, J. D.; Webb, M. L.; Seidl, K. J. Selective functional inhibition of JAK-3 is sufficient for efficacy in collagen-induced arthritis in mice. *Arthritis Rheum.* **2010**, *62*, 2283–2293.

[19] Soth, M.; Hermann, J. C.; Yee, C.; Alam, M.; Barnett, J. W.; Berry, P.; Browner, M. F.; Frank, K.; Frauchiger, S.; Harris, S.; He, Y.; Hekmat-Nejad, M.; Hendricks, T.; Henningsen, R.; Hilgenkamp, R.; Ho, H.; Hoffman, A.; Hsu, P. Y.; Hu, D. Q.; Itano, A.; Jaime-Figueroa, S.; Jahangir, A.; Jin, S.; Kuglstatter, A.; Kutach, A. K.; Liao, C.; Lynch, S.; Menke, J.; Niu, L.; Patel, V.; Railkar, A.; Roy, D.; Shao, A.; Shaw, D.; Steiner, S.; Sun, Y.; Tan, S. L.; Wang, S.; Vu, M. D. 3-Amido Pyrrolopyrazine JAK

Kinase Inhibitors: Development of a JAK3 vs JAK1 Selective Inhibitor and Evaluation in Cellular and in Vivo Models. *J. Med. Chem.* **2013**, *56*, 345–356.

[20] Clark, J. D.; Flanagan, M. E.; Telliez, J.-B. Discovery and Development of Janus Kinase (JAK) Inhibitors for Inflammatory Diseases. *J. Med. Chem.*, **2014**, *57*, 5023–5038 and references therein.

[21] Pesu, M.; Laurence, A.; Kishore, N.; Zwillich, S. H.; Chan, G.; O'Shea, J. J. Therapeutic targeting of Janus kinases. *Immunol. Rev.* **2008**, *223* 132–142

[22] Kontzias, A.; Kotlyar, A.; Laurence, A.; Changelian, P.; O'Shea, J. J. Jakinibs: a new class of kinase inhibitors in cancer and autoimmune disease. *Curr. Opin. Pharmacol.* **2012**, *12*, 464–470.

[23] Flanagan, M. E.; Blumenkopf, T. A.; Brissette, W. H.; Brown, M. F.; Casavant, J. M.; Shang-Poa, C.; Doty, J. L.; Elliott, E. A.; Fisher, M. B.; Hines, M.; Kent, C.; Kudlacz, E. M.; Lillie, B. M.; Magnuson, K. S.; McCurdy, S. P.; Munchhof, M. J.; Perry, B. D.; Sawyer, P. S.; Strelevitz, T. J.; Subramanyam, C.; Sun, J.; Whipple, D. A.; Changelian, P. S.Discovery of CP-690,550: a potent and selective Janus kinase (JAK) inhibitor for the treatment of autoimmune diseases and organ transplant rejection. *J. Med. Chem.* **2010**, 53, 8468– 8484

[24] (a) Mesa, R. A. Ruxolitinib, a selective JAK1 and JAK2 inhibitor for the treatment of myeloproliferative neoplasms and psoriasis. *IDrugs : the investigational drugs journal* **2010**, *13*, 394–403. (b) Mesa, R. A.; Yasothan, U.; Kirkpatrick, P. Ruxolitinib. *Nature Reviews Drug Discovery* **2012**, *11*, 103–4 and references therein.

[25] (a) Smolen, J. S.; Schlichting, D. E.; Sterling, K. L.; Keystone, E.; Taylor, P.; Genovese, M. C.; Johnson, L.; Rodriguez, J. C. R.; Lee, C. H.; Gaich, C. L.12-and 24-week patient reported outcomes from a phase 2b dose-ranging study of baricitinib, an oral Janus kinase 1/Janus kinase 2 inhibitor, in combination with traditional disease-modifying antirheumatic drugs in patients with rheumatoid arthritis. *Arthritis Rheum.* **2012**, *64*, S214– S220.; (b) Genovese, M. C.; Keystone, E.; Taylor, P.; Drescher, E.; Berclaz, P.-Y.; Lee, C. H.; Schlichting, D. E.; Beattie, S. D.; Fidelus-Gort, R. K.; Luchi, M. E.; Macias, W.24-week results of a blinded phase 2b dose-ranging study of baricitinib, an oral Janus kinase 1/Janus kinase 2 inhibitor, in combination with traditional disease modifying antirheumatic drugs in patients with rheumatoid arthritis. *Arthritis Rheum.* **2012**, 64, S1049– S1050.

[26] Van Rompaey, L.; Galien, R.; Van der Aar, E., M.; Clement-Lacroix, P.; Nelles, L.; Smets, B.; Lepescheux, L.; Cristophe, T.; Conrath, K.; Vandeghinste, N.; Vayssiere, B.; De Vos, S.; Fletcher, S.; Brys, R.; Van't Klooster, G.; Feyen, J.; Menet, C. Preclinical characterization of GLPG0634, a selective inhibitor of JAK1 for the treatment of inflammatory diseases. *J. Immunol*. **2013**, *191*, 3568-3577.

[27] Fleischmann, R. M.; Damjanov, N. S.; Kivitz, A. J.; Legedza, A.; Hoock, T. C.; Kinnman, N.; A Randomized Double-Blind, Placebo-Controlled, Twelve-Week, Dose-Ranging Study of Decernotinib, an Oral JAK-3 Inhibitor, as Monotherapy in Patients With Rheumatoid Arthritis. *Arthritis Rheum.* **2015**, *67*, 334-343.

[28] Genovese, M. C; Van Vollenhoven, R. F.; Zhang, Y.; Kinnman, N. VX-509 (Decernotinib), an Oral Selective Janus Kinase 3 Inhibitor, in Combination With Methotrexate in Patients With Rheumatoid Arthritis *Arthritis Rheum. In Preparation*

[29] Clark J. D.; Flanagan M. E.; Telliez, J.-B. Discovery and Development of Janus Kinase (JAK) Inhibitors for Inflammatory Diseases. *J. Med. Chem.* **2014**, *57*, 5023–5038.

[30] Thoma, G.; Druckes, P.; Zerwes, H.-G. Selective inhibitors of the Janus kinase Jak3-Are they effective? *Bioorg. Med. Chem. Letters* **2014**, *24*, 4617-4621.

[31] Mahajan, S.: Hogan. J. K; Schlyakter, D.; Oh, L.; Salituro, F. G.; Farmer, L; Hoock, T. C. VX-509 (Decernotinib) is a Potent and Selective Janus Kinase 3 Inhibitor that Attenuates Inflammation in Animal Models of Autoimmune Disease. *J. Pharmacol. Exp. Ther.* **2015**, *353*, 405-414.

[32] (a) Ledeboer, M. W.; Pierce, A. C.; Duffy, J. P.; Gao, H.; Messersmith, D.; Salituro, F. G.; Nanthakumar, S.; Come, J.; Zuccola, H. J.; Swenson, L.; Shlyakter, D.; Mahajan, S.; Hoock, T.; Fan, B.; Tsai, W.-J.; Kolaczkowski, E.; Carrier, S.; Hogan, J. K.; Zessis, R.; Pazhanisamy, S.; Bennani, Y. L. 2-Aminopyrazolo[1,5-a]pyrimidines as potent and selective inhibitors of JAK2. *Bioorg. Med. Chem. Lett.* **2009**, *19*, 6529–6533; (b) Wang, T.; Duffy, J. P.; Wang, J.; Halas, S.; Salituro, F. G.; Pierce, A. C.; Zuccola, H. J.; Black, J. R.; Hogan, J. K.; Jepson, S.; Shlyakter, D.; Mahajan, S.; Gu, Y.; Hoock, T.; Wood, M.; Brinley, F. F.; Frantz, J. D.; Dauffenbach, L. M.; Germann, U. A.; Fan, B.; Namchuk, M.; Bennani, Y. L.; Ledeboer, M. W.Janus Kinase 2 Inhibitors. Synthesis and Characterization of a Novel Polycyclic Azaindole. *J. Med. Chem.* **2009**, *52*, 7938–7941.

[33] The MSR (minimum significant ratio) was determined for each of the enzyme assays: JAK3 (2.5), JAK2 (3.3), AURA (1.3), FLT3 (2.5), SYK (1.5). This number was retrospectively derived from historical data in which the assay had been run at least twice using a data set that included from 14 to >20 individual compounds. A meaningful difference in Ki between compounds is given by the MSR e.g. in the JAK2 assay compounds must differ by at least 3.3 fold to be considered to have different potencies.

[34] Pierce, A. C.; Zuccola H. J. etal manuscript in preparation

[35] For reviews on Jak2 inhibitors in potential treatment of myeloproliferative disorders, see: (a) Atallah, E.; Verstovsek, S. Prospect of JAK2 inhibitor therapy in myeloproliferative neoplasms. *Exp. Rev. Anticancer Ther.* **2009**, *9*, 663–670.; (b) Pardanani, A. *Leukemia* **2008**, *22*, P23; (c) Skoda, R. C. Can we control JAK? *Blood* **2008**, *111*, 5419–5420.; (d) Morgan, K. J.; Gilliland, D. G. A role for JAK2 mutations in myeloproliferative diseases. *Annu. Rev. Med.* **2008**, *59*, 213–222.; (e) Sayyah, J.; Sayeski, P. P. Jak2 inhibitors: rationale and role as therapeutic agents in hematologic malignancies. *Curr. Oncol. Rep.* **2009**, *11*, 117–124.

[36] (a) Saharinen, P.; Silvennoinen, O. The Pseudokinase Domain Is Required for Suppression of Basal Activity of Jak2 and Jak3 Tyrosine Kinases and for Cytokine-inducible Activation of Signal Transduction. *J. Biol. Chem.* **2002**, *277*, 47954-47963; (b) Chen, M.; Cheng A., Candotti F.; Zhou Y-J.;

Hymel A.; Fasth, A.; Notarangelo, L. D.; and O'Shea, J. J. Complex effects of naturally occurring mutations in the JAK3 pseudokinase domain: evidence for interactions between the kinase and pseudokinase domains. *J. Mol. Cell. Biol.* **2000**, *20*, 947-956.

[37] Griffith, J.; Black, J.; Faerman, C.; Swenson, L.; Wynn, M.; Lu, F.; Lippke, J.; Saxena, K.; The structural basis for autoinhibition of FLT3 by the juxtamembrane domain. *Mol Cell.* **2004**, *13*, 169-178.

[38] Harrington, E. A.; Bebbington, D.; Moore, J.; Rasmussen, R. K.; Ajose-Adeogun, A. O.; Nakayama, T.; Graham, J. A.; Demur, C.; Hercend, T.; Diu-Hercend, A.; Su, M.; Golec, J. M.; Miller, K. M. VX-680, a potent and selective small-molecule inhibitor of the Aurora kinases, suppresses tumor growth in vivo. *Nat. Med.* **2004**, *10*, 262–267.

[39] For full details regarding JAK2 and JAK3 K_i determinations refer to Supporting Information and the following references: (a) Fox, T.; Coll, J. T.; Ford, P. J.; Germann, U. A.; Porter, M. D.; Pazhanisamy, S.; Fleming, M. A.; Galullo, V.; Su, M.-S.; Wilson, K. P.A single amino acid substitution makes ERK2 susceptible to pyridinyl imidazole inhibitors of p38 MAP kinase. *Protein Sci.* **1998**, 7, 2249– 2255. (b) (b) Morrison, J. F.; Stone, S. R.Approaches to the study and analysis of the inhibition of enzymes by slow- and tight-binding inhibitors. *Comments Mol. Cell. Biophys.* **1985**, 2, 347– 368.

[40] Vonrhein, C.; Flensburg, C.; Keller, P.; Sharff, A.; Smart, O.; Paciorek, W.; Womack, T.; Bricogne, G., Data processing and analysis with the autoPROC toolbox. *Acta crystallographica. Section D, Biological crystallography* **2011**, *67* (Pt 4), 293-302.

[41] Bricogne, G.; Blanc, E.; Brandl, M.; C., F.; Keller, P.; Paciorek, W.; P., R.; Sharff, A.; Smart, O. S.; Vonrhein, C.; Womack, T. *BUSTER*, 2.11.4; Global Phasing Ltd.: Cambridge, United Kingdom, 2011.

[42] Emsley, P.; Cowtan, K., Coot: model-building tools for molecular graphics. *Acta crystallographica. Section D, Biological crystallography* **2004**, *60* (Pt 12 Pt 1), 2126-32.

Revised Figures

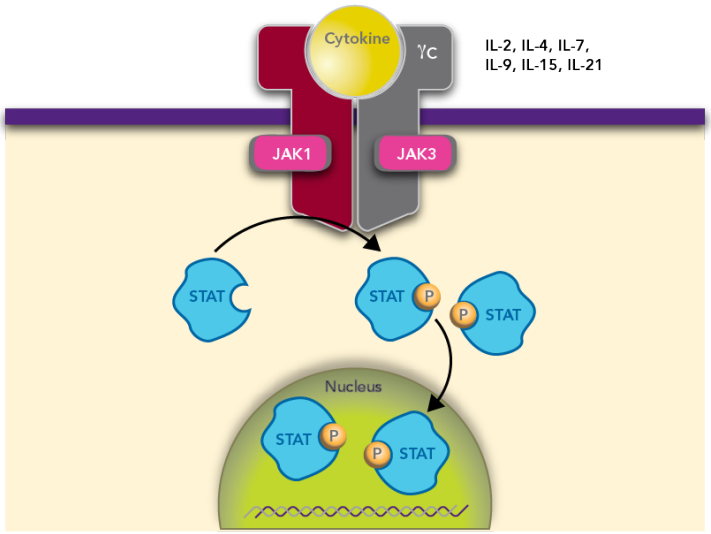

Figure 1. JAK-STAT signaling

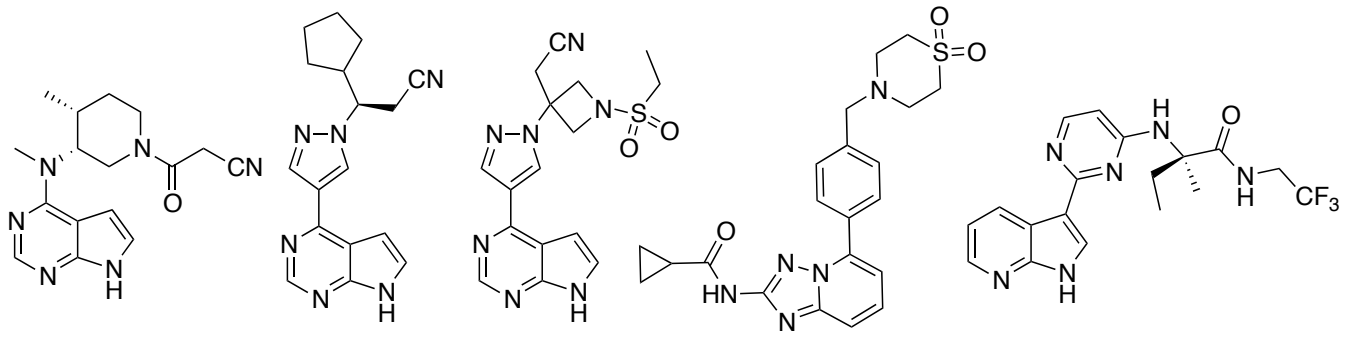

Tofacitinib **Ruxolitinib** **Baricitinib** **Filgotinib** **Decernotinib (VX-509)**

Figure 2. Selected Clinically Approved or Experimental JAK inhibitors

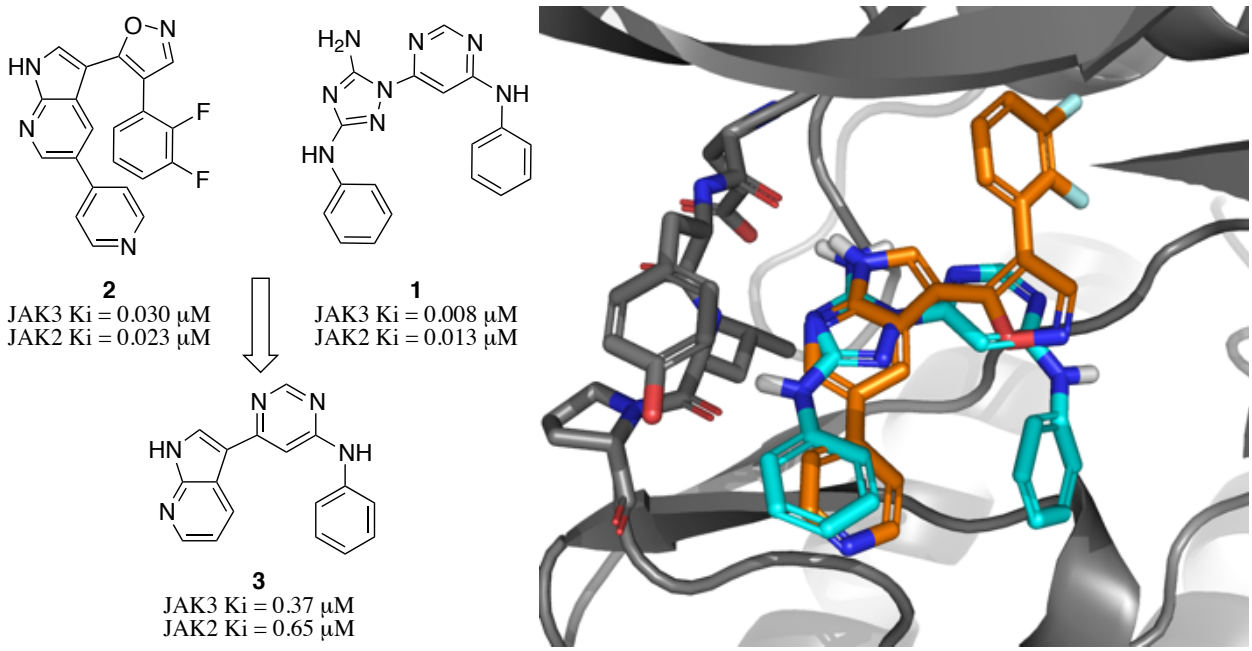

Figure 3. Compounds **1** and **2** overlaid in the JAK2 structure. Superposition created by overlaying the hinge regions of the ERK2 and JAK2 crystal structures

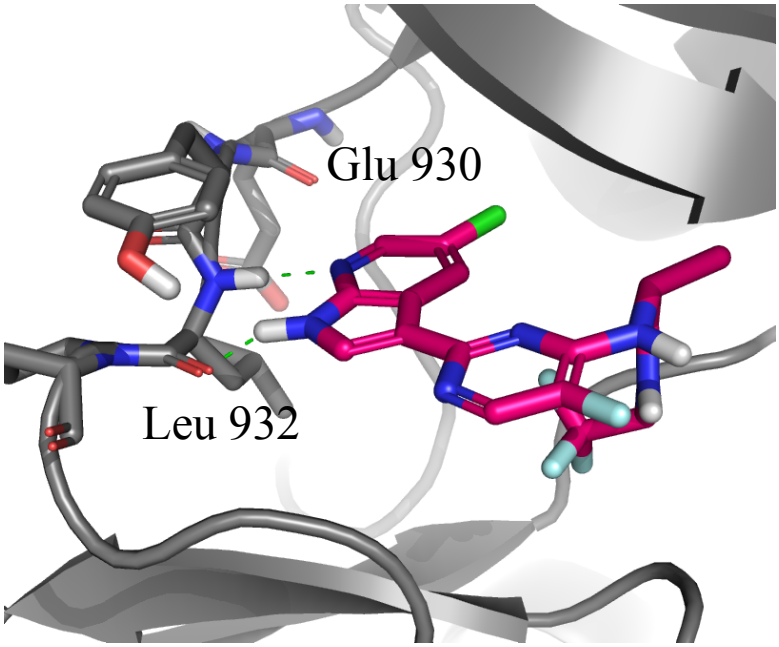

Figure 4. Crystal structure co-complex of **22** in JAK2. Hinge hydrogen bonds to Leu 932 highlighted in green.

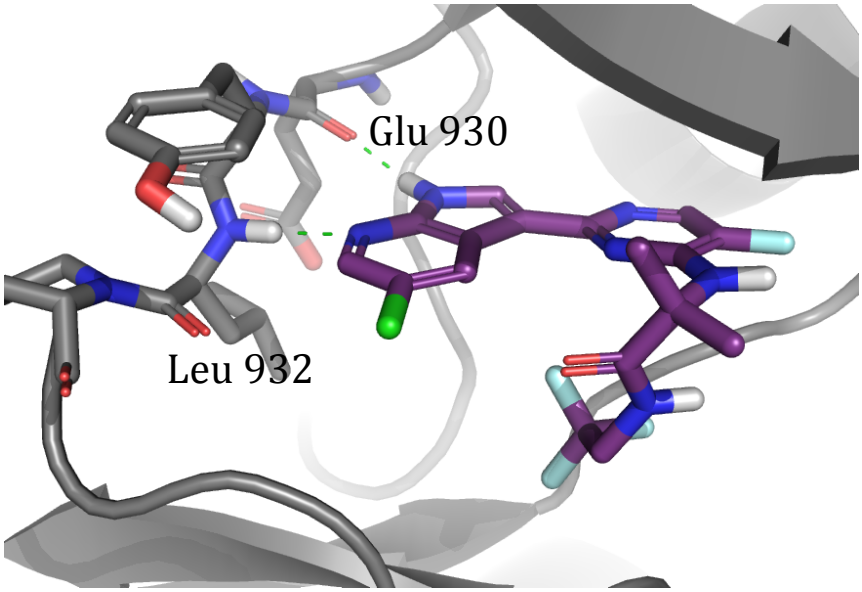

Figure 5. Crystal structure of **44** in JAK2. Hinge hydrogen bonds to Leu 932 and Glu 930 highlighted in green.

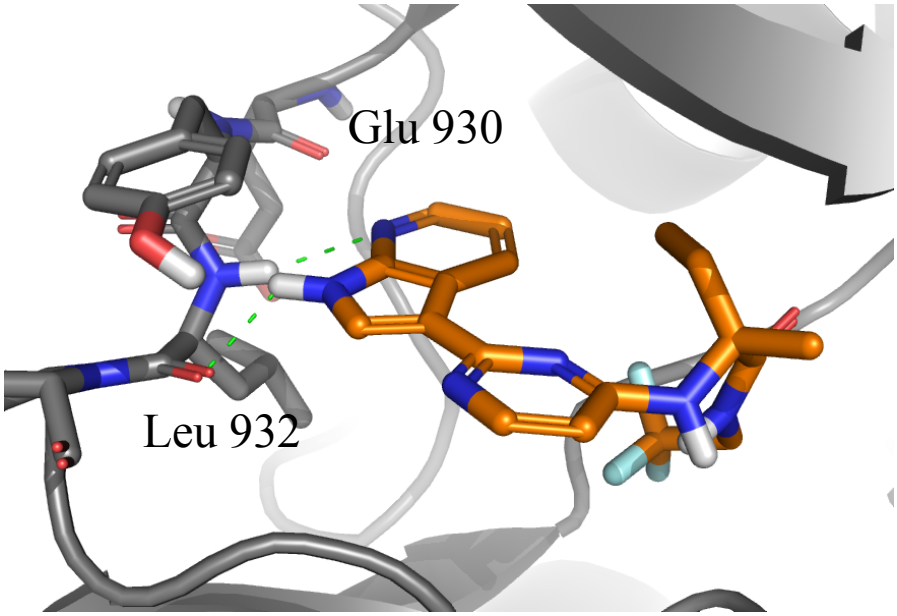

Figure 6. Crystal structure of **VX-509** in JAK2. Hinge hydrogen bonds to Leu 932 highlighted in green.

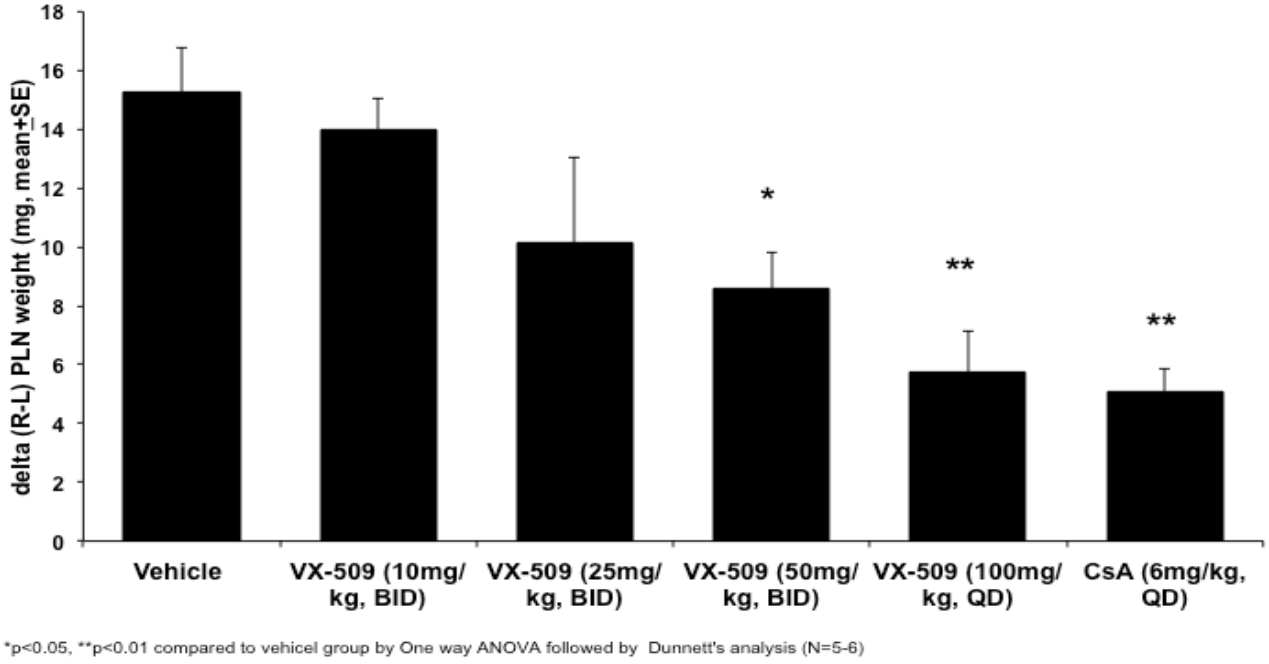

*p<0.05, **p<0.01 compared to vehicel group by One way ANOVA followed by Dunnett's analysis (N=5-6)

Figure 7. Dose dependent inhibition of popletial lymph node (PLN) hyperplasia by **VX-509** in Rat HvG Model.

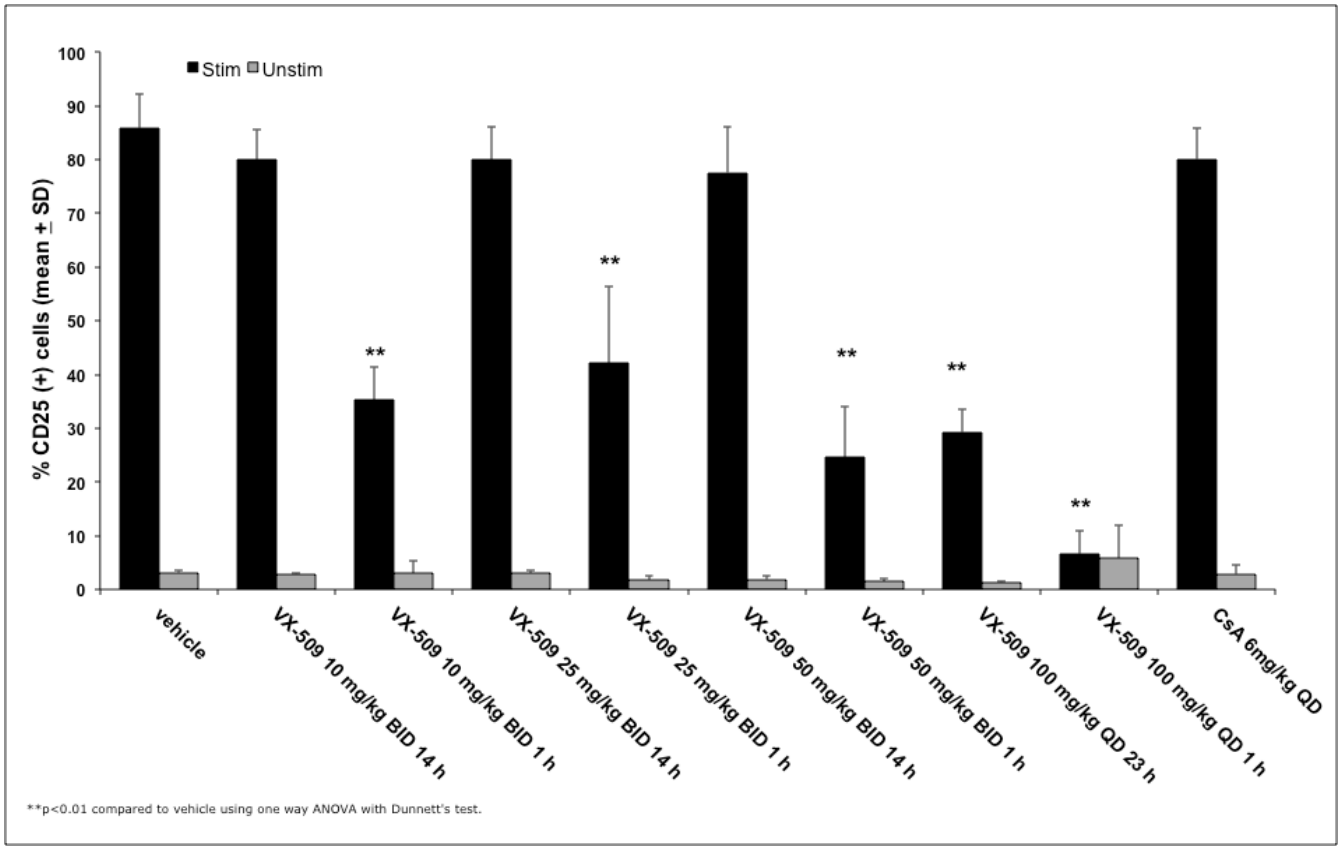

Figure 8. Dose dependent decrease in ex vivo stimulated biomarker CD25 by **VX-509** in Rat HvG model.

Tables revised

Table 1. Central Core Ring Variations

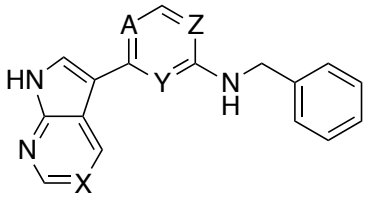

Compound	X	A	Y	Z	JAK3 Ki (μM)	JAK2 Ki (μM)	SYK Ki (μM)	FLT3 Ki (μM)	AURA Ki (μM)	HT-2-IL2 IC50 (μM)
4	CH	N	CH	N	0.014	0.035	2.9	< 0.06	> 0.8	9.85
5	CH	CH	N	N	0.096	0.11	> 3.33	< 0.06	0.38	> 20
6	CH	N	N	CH	0.38	0.35	> 3.33	0.7	0.8	N.A.
7	CCl	N	CH	N	0.003	0.006	0.2	< 0.06	0.062	5.4
8	CCl	CH	N	N	0.043	0.033	> 3.33	< 0.06	0.02	> 20
9	CCl	CH	N	CH	0.055	0.07	> 3.33	0.09	0.049	> 20
10	CCl	CH	CH	CH	0.15	0.22	1.9	0.078	N.A.	N.A.

Table 2. Side Chain Variations

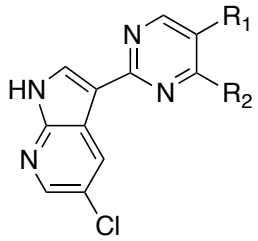

Compound	R1	R2	JAK3 Ki (μM)	JAK2 Ki (μM)	SYK Ki (μM)	FLT3 Ki (μM)	AURA Ki (μM)	HT-2-IL2 IC50 (μM)
11	F		0.005	0.005	0.39	0.33	0.030	> 20
12	F		0.011	0.012	0.43	0.05	N.A	N.A.
13	F	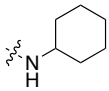	0.016	0.023	1.1	0.078	0.007	N.A.
14	H	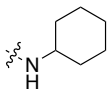	0.022	0.022	0.67	0.29	N.A.	N.A.
15	F	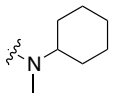	0.14	0.22	> 4	0.08	N.A.	N.A.
16	F	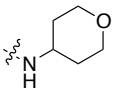	0.004	0.009	0.15	0.009	0.023	> 20
17	F	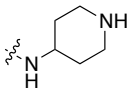	0.029	0.045	0.108	0.006	0.086	N.A.
18	F	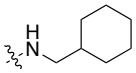	0.068	0.077	3.2	0.19	0.004	N.A.
19	F	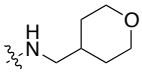	0.005	0.011	0.2	0.032	0.019	> 20
20	F	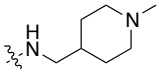	0.14	N.A.	3.6	0.045	0.27	N.A
21	H	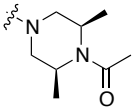	0.006	0.008	1.1	0.032	0.13	2.1

Table 3. 5-Substituted 1*H*-pyrrolo[2,3-*b*]pyridine with Aminoacid Side Chain Variations*

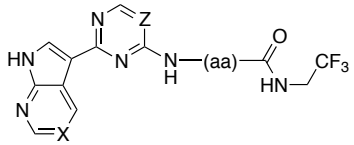

Cmpd	X	Z	(aa)	JAK3 Ki (μM)	JAK2 Ki (μM)	HT-2-IL2 IC50 (μM)	TF-1 GM-CSF IC50 (μM)	FLT3 Ki (μM)	AURA IC50 (μM)	RLM %
22	CCl	CF	(S)-Ala	0.002	0.007	0.074	2.67	0.55	0.004	95
23	CCl	CH	Gly	0.001	0.005	0.16	2.9	0.29	0.007	75
24	CCl	CF	(S)-Nva	0.002	0.023	0.75	3.6	1.3	< 0.025	65
25	CCl	CH	(S)-Ser	0.006	0.037	1.5	20	0.093	0.05	n/a
26	CCl	CH	(S)-SerOMe	0.013	0.069	8.3	n/a	0.49	0.26	n/a
27	CCl	CH	(S)-Met	0.04	0.03	2.9	n/a	0.39	0.02	n/a
28	CCl	CF	(S)-Pro	0.009	0.026	2.5	11	1.603	0.024	63
29	CCl	CF	(S)-aminobutanoic acid	0.045	0.12	11.4	n/a	0.31	0.15	n/a
30	CCl	CF	(R)-Ala	0.002	0.011	1.3	>20	>4	0.063	n/a
31	CCl	CH	(R)-Ala	0.001	0.005	0.11	14.3	0.61	0.027	96
32	CCl	CH	(R)-Nva	0.002	0.01	0.22	2.1	0.41	0.23	47
33	CCl	CH	(R)-Propargyl glycine	0.002	0.011	0.51	5.1	0.37	0.032	44
34	CCl	CH	(R)-Val	0.002	0.001	0.11	2.93	0.56	0.16	78
35	CCl	CH	(R)-Leu	0.004	0.023	1.7	10.3	1.5	0.405	n/a
36	CCl	CH	(R)-Phe	0.006	0.058	2.8	> 20	1.6	< 0.025	n/a
37	CCl	CF	(R)-His	0.018	0.081	2.6	2.3	1	0.15	n/a
38	CF	CF	(S)-Ala	0.007	0.042	5.5	n/a	>3.7	0.049	n/a
39	CH	CF	(S)-Ala	0.031	0.15	6.1	n/a	>4.0	0.21	n/a
40	COMe	CF	(S)-Ala	0.006	0.034	1.5	2.2	0.48	0.033	91
41	COMe	CF	(R)-Ala	0.007	0.038	1.3	n/a	0.61	0.21	79
42	N	CF	(R)-Ala	0.019	0.33	>20	n/a	>4.0	>0.8	n/a
43	CCl	CH		0.001	0.001	0.058	0.41	0.18	0.10	30
44	CCl	CF		0.001	0.002	0.081	0.96	0.325	0.082	88
45	CCl	CH		0.003	0.002	0.081	0.65	0.2	0.62	52
46	N	CH		0.003	0.006	0.52	3	1.3	> 0.8	100
VX-509	CH	CH		0.002	0.013	0.099	2.59	1.04	> 0.8	70
47	CCl	CH		0.002	0.028	0.9	7.9	0.29	0.070	n/a
48	CH	CH		0.003	0.004	0.072	1.65	0.54	> 0.8	63
49	CH	N		0.003	0.024	0.33	3.7	1.39	0.49	97

Table 4. Enzyme (K_i nM ± SD, n), Cell-Based Potency (IC_{50} nM ± SD, n) & Selectivity (ratio)

Assay	JAK isoform Involved	**VX-509**	**44**	**34**	**43**	**45**	tofacitinib
JAK3	JAK3	2 ± 0.7, 5	1 ± 0.07, 10	1 ± 0.09, 5	1 ± 0.3, 10	3 ± 2, 3	0.5 ± 0.07, 7
JAK1	JAK1	11 ± 0, 1	3 ± 0, 1	N.A.	2 ± 0, 1	N.A.	3 ± 0.4, 2
JAK2	JAK2	13 ± 0, 4	2 ± 0.5, 12	4 ± 009, 6	1 ± 0.5, 12	2 ± 1, 5	1 ± 0.9, 5
TYK2	TYK2	11 ± 2, 2	10 ± 0, 1	N.A.	11 ± 0, 1	N.A.	11 ± 0, 1
HT-2/IL-2/P-STAT5	JAK3/1	99 ± 50, 4	90 ± 30, 10	112 ± 70, 5	58 ± 40, 5	81 ± 70, 2	30 ± 20, 72
TF-1/GMCSF/P-STAT5	JAK2	2600 ± 1664, 4	1060 ± 600, 9	2927 ± 1350, 7	409 ± 142, 6	651 ± 13, 2	190 ± 137, 35
Mouse 2-Way MLR	JAK3/1	170 ± 100, 4	160 ± 110, 3	280, 1	170 ± 70, 2	N.A.	60, 1
1º Human IL-2 T-cell Blast	JAK3/1	240 ± 180, 2	N.A.	N.A.	N.A.	N.A.	130 ± 28, 2
Human CFU-E 3 U/ml EPO	JAK2	7700 ± 6100, 2	6100 ± 3400, 2	5400 ± 2000, 2	2500 ± 2200, 2	N.A.	380 ± 160, 10
Human CFU-E 0.3 U/ml EPO	JAK2	5300 ± 740, 2	3600 ± 1200, 2	3000 ± 1000, 2	1700 ± 325, 2	N.A.	320 ± 150, 10
HeLa IFN-a STAT2	JAK1/ TYK2	11900 ± 3650, 3	>20000, 1	N. A.	N.A.	N.A.	2800 ± 2000, 11
CFU-E / MLR (3 U/ml EPO)		45.3	38.1	22.1	10.6	N.A.	6.7
CFU-E / MLR (0.3 U/ml EPO)		31.3	22.5	14.2	7.6	N.A.	5.7
TF-1/HT-2 ratio		26	12	26	7	8	6

Table 5. Pharmacokinetic parameter determinations in Sprague-Dawley rats (single IV bolus dose)

Compound	Dose (mg/kg)	DN-AUC_{inf} [a] (hr*μg/ml)	CL (mL/min/kg)	$T_{1/2}$ (h)	V_{dss} (L/kg)
34	1.0	0.46	36.2	2.6	6.1
44	1.9	1.76	9.45	2.2	1.5
43	2.0	0.42	39.7	1.2	1.3
45	1.7	0.60	41.1	4.6	4.1
VX-509	0.98	0.74	24.3	5.57	4.98

[a]The AUC_{INF} values are normalized to a 1 mg/kg dose

Table 6. Mean $T_{1/2}$ and Predicted Hepatic Clearance for **VX-509** at an Initial Concentration of 1 μM in Liver Microsomes After Incubation at 37°C

Species	Mean $T_{1/2}$ (SD) and Mean Predicted Hepatic Clearances (SD)	
	$T_{1/2}$ (min)	Predicted Hepatic Clearance (mL/min/kg)
Mouse	19 ± 7.9	69 ± 6.4
Rat	21 ± 1.6	38 ± 0.9
Dog	34 ± 2.4	24 ± 0.4
Monkey	7 ± 0.4	38 ± 0.3
Human	19 ± 1.2	17 ± 0.2

Table 7. Mean $T_{1/2}$ and Predicted Hepatic Clearance for **VX-509** at an Initial Concentration of 1 μM in Liver S9 After Incubation at 37°C

Species	Mean $T_{1/2}$ (SD) and Mean Predicted Hepatic Clearances (SD)	
	$T_{1/2}$ (min)	Predicted Hepatic Clearance (mL/min/kg)
Mouse	9 ± 1.01	78 ± 1.2
Rat	21 ± 1.6	37 ± 0.9
Dog	36 ± 3.4	23 ± 0.6
Monkey	6 ± 0.3	39 ± 0.09
Human	20 ± 5.4	17 ± 0.9

Table 8. Mean Pharmacokinetic Parameters for **VX-509**

A) Single IV bolus dose

Species	Dose (mg/kg)	DN-AUC_{inf}[a] (hr*μg/ml)	CL (ml/min/kg)	V_{dss} (L/kg)	$T_{1/2}$ (hr)
Rat	0.98	0.74	24.3	4.98	5.57
Dog	0.88	4.06	4.17	0.39	1.58
Monkey	0.88	0.79	21.7	1.65	1.28

[a]The AUC_{INF} values are normalized to a 1 mg/kg dose

B) Single oral dose

Species	Dose (mg/kg)	DN-AUC_{inf}[a] (hr*μg/ml)	C_{max} (μg/mg)	T_{max} (hr)	$T_{1/2}$ (hr)	F %
Rat	10.7	6.75	1.73	1.50	5.87	91.8
Dog	9.65	44.6	7.46	1.00	5.82	100

[a]The AUC_{INF} values are normalized to a 10 mg/kg dose

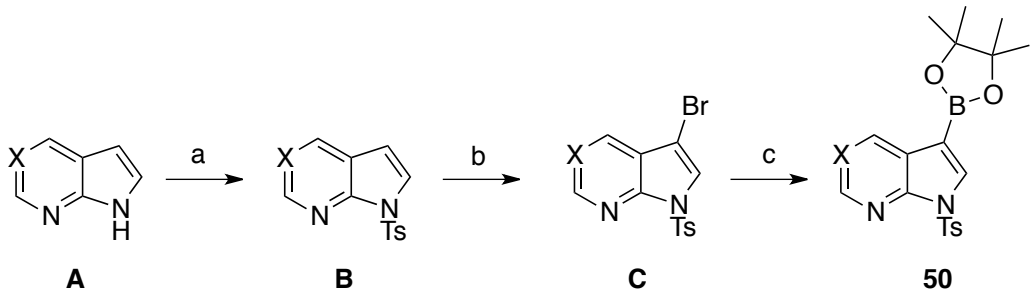

A **B** **C** **50**

a: X = CH, **b:** X = CCl, **c:** x = CF, **d:** X = $COCH_3$, or **e**: X = N

Scheme 1. Conditions: a) NaH, TsCl, THF; b) Br_2, CH_2Cl_2; c) bis(pinacolato)diboron, $Pd(PPh_3)_4$, KOAc, 1,4-dioxane.

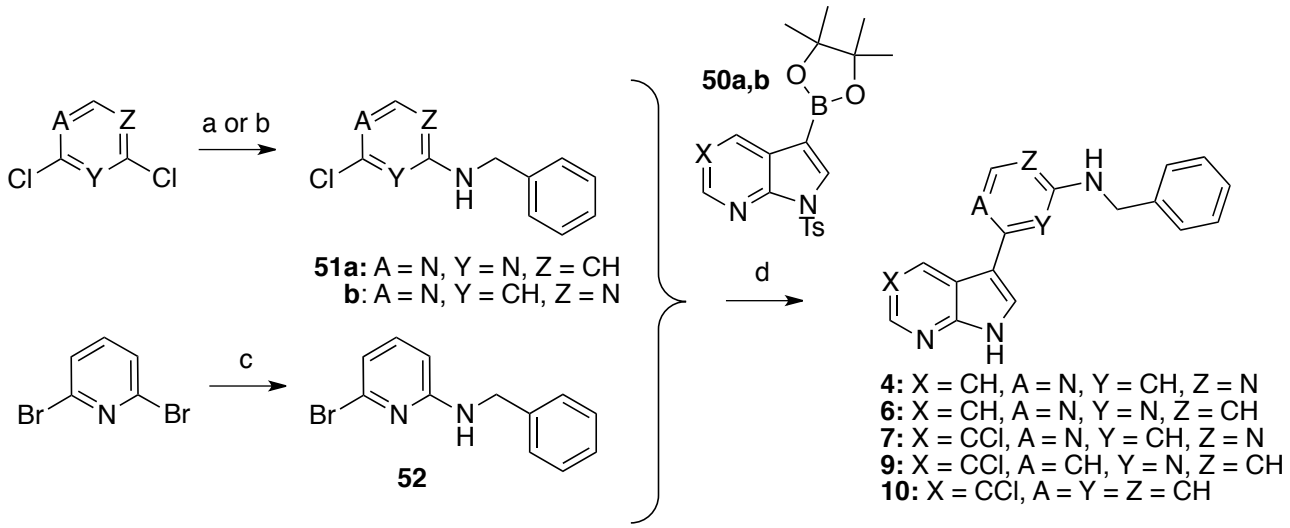

Scheme 2a. Conditions: a) $PhCH_2NH_2$, DIPEA, THF, reflux, 1-2h or IPA, 90 °C, (54-79%); b) $PhCH_2NH_2$, neat, (79%); c) $PhCH_2NH_2$, 150 °C (μW) (40-55%) d) i: $Pd(PPh_3)_4$, DME, 2 M Na_2CO_3, reflux ii: NaO*t*Bu, 130-160 °C, 10-20 min (μW) (25-89%)

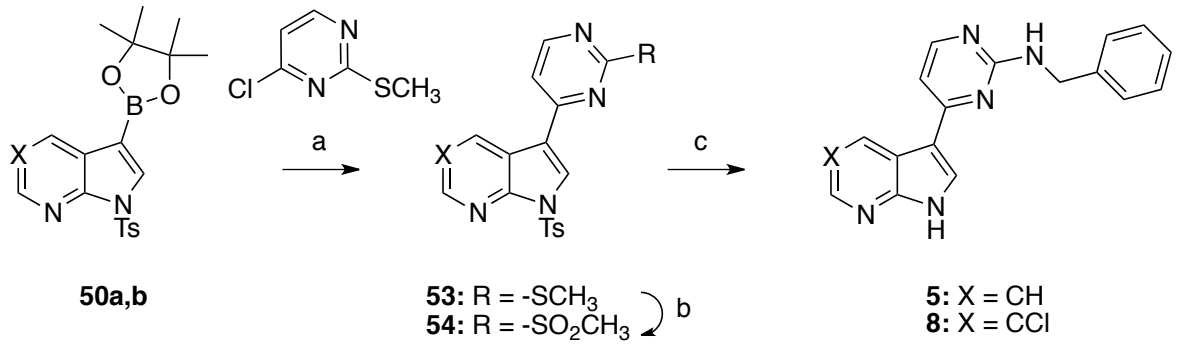

Scheme 2b. Conditions: a) $Pd(PPh_3)_4$, DME, 2M Na_2CO_3, reflux (51%; X = CCl); b) Oxone, CH_3OH-H_2O (1:1) (32%; X = CCl); c) i: $PhCH_2NH_2$, EtOH, reflux, 16 h (94%; X = CCl), ii: 3N NaOH, CH_3OH (75%; X = CCl) or NaO*t*Bu, 130-160 °C, 10-20 min (μW)

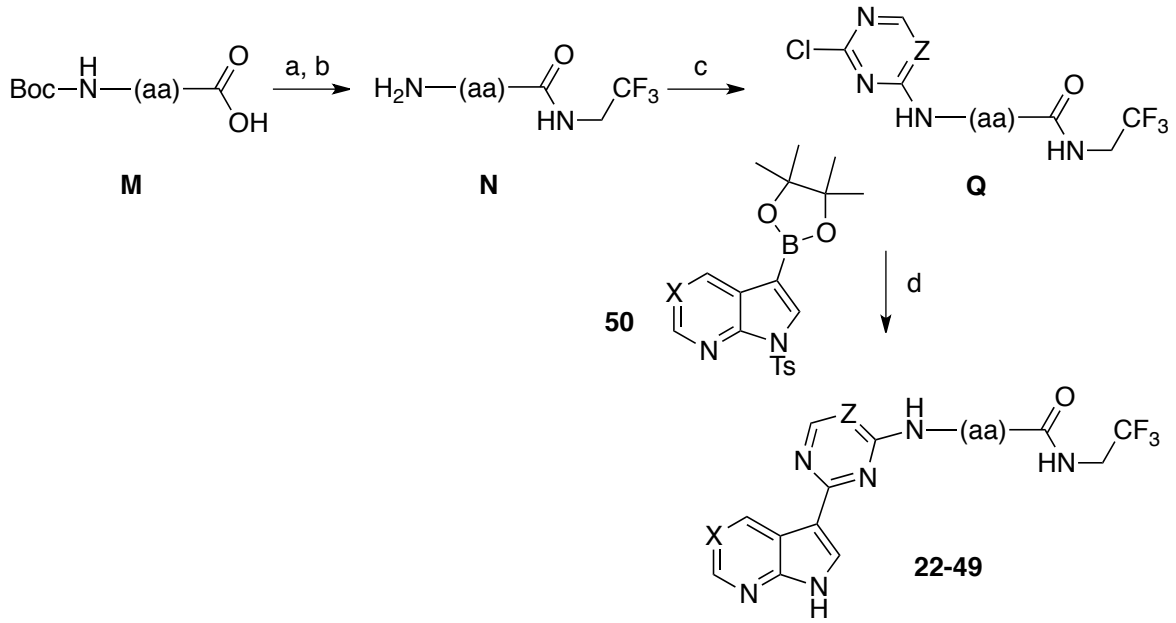

Scheme 3. a) HATU or EDC, HOBt, DIEA, DMF, $CF_3CH_2NH_2$-HCl, rt (60-92%); b) 1:1 TFA- CH_2Cl_2 or 2 M HCl, Et_2O-CH_3OH (quant.); c) DIEA, IPA or THF (29-80%); d) *i*) **50a-e**, 2 M Na_2CO_3, $Pd(PPh_3)_4$, DME, 150 °C, 10 min. (μW) or reflux; 16h; ii) LiOH, THF, H_2O, rt or CH_3OH, 25% $NaOCH_3$ in CH_3OH, 60 °C,1h (30-65% 2-steps)

Table of Content Graphic